Delft University of Technology

Sustainability of Deep Sea Mining Transport Plans

Important note
To cite this publication, please use the final published version (if applicable).
Please check the document version above.

Sustainability of Deep Sea Mining Transport Plans

Wenbin Ma

Delft University of Technology

Sustainability of Deep Sea Mining Transport Plans

Proefschrift

ter verkrijging van de graad van doctor

aan de Technische Universiteit Delft,

op gezag van de Rector Magnificus Prof. dr.ir. T.H.J.J. van der Hagen,

voorzitter van het College voor Promoties,

in het openbaar te verdedigen op maandag 3 juni 2019 om 10:00 uur

door

Wenbin MA

Master of Science in Ship and Ocean Structure Design and Manufacturing,

Wuhan University of Technology, Wuhan, China

geboren te Tengzhou, Shandong, China

To my families

Preface

I have to say it is an excellent experience working at Delft University of Technology with many passionate and inspirative colleagues. I have a lot of people to thank for their great help and favour during my PhD studies.

Firstly, I would like to express my sincere thanks to my promotors Prof. Cees van Rhee and Dingena Schott. Prof. Cees van Rhee, as an expert in the field of dredging and offshore engineering, showed his solid and valuable engineering expertise during our discussions. His cheerful personality is also a model for me to learn. Dingena Schott, as an expert in the field of machine-cargo interface, biomass material handling and logistic energy transition, gave me a lot significant guiding comments and suggestions for my research and daily life. Without your diligent guidances, I could not be able to obtain so many meaningful results. Your research spirit and attitude also inspires me for my future career. Additionally, I would also like to thank Prof. Gabriel Lodewijks who supervised me at the beginning of my PhD research. I am really impressed by your humor, kindness, and research experience.

Then, I would like to thank my kindly colleagues and friends in the Netherlands such as Linxiao, Qingsong, Lindert, Johan, Frans, and so many of you. I am appreciate and happy that you accompanied me during my PhD research period and gave me a lot helps.

The last but not the least, I would like to thank my families. You gave me the courage and motivation to move forward continuously. Thanks to my wife Ying and my lovely son Youran. I am proud of you.

Wenbin Ma

Delft, May, 2018

Contents

Chapter 1

Introduction

1.1 Introduction

With the significant worldwide increase of mineral resource consumption, in the future the terrestrial mining would not be able to supply enough mineral resources to fulfill the demand (McLellan et al., 2016). In 1965, the concept of deep sea mining (DSM) was proposed by Jorn L Mero's book *The Mineral Resources of the Sea*, which depicts a large amount of deposits of many kinds of expensive and rare mineral resources in the ocean. Since then, DSM is considered as one of the most promising and viable ways to solve the world mineral resource shortage (Chung and Tsurusaki, 1994; Chung, 1985).
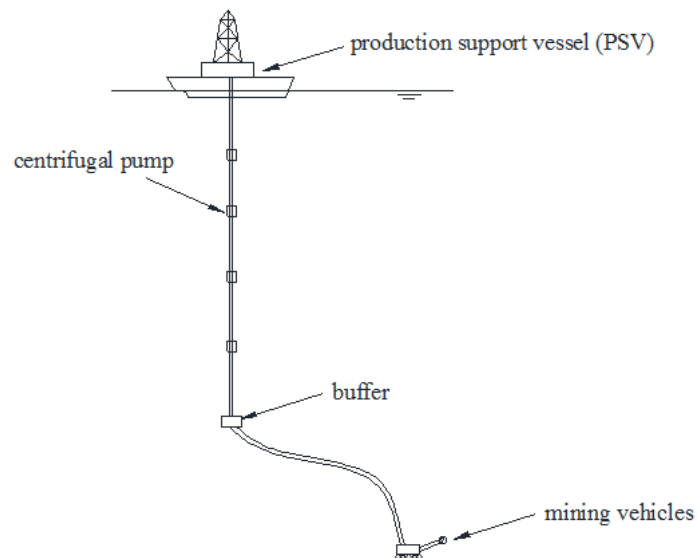
Figure 1.1: A typical DSM system with a ship-pipe-miner system (Ma et al., 2017a).

The DSM activity could be defined as a mineral retrieval process, which takes place majorly in the ocean and transports different kinds of minerals from the seafloor to the ocean surface (Chung and Tsurusaki, 1994; Chung, 1985). A typical DSM system, which is described as a ship-pipe-miner system, is shown in Figure 1.1 (Ma et al., 2017a). The integrated ship-pipe-

miner system consists of several mining vehicles working on the seafloor, a vertical lifting pipe system, and a production support vessel (PSV) working on the ocean surface for the preliminary mineral processing and temporary mineral storage.

The working areas of DSM are often located at the active places on the seafloor, such as the hydrothermal vents with a large specie biomass and biodiversity (Reed et al., 2015). In addition, the DSM depth often depends on the mining mineral locations. Figure 1.2 depicts the location depth of different kinds of mineral resources in the ocean (Ma et al., 2017b). Considering the mineral resource locating depth range in Figure 1.2, the mining depth researched in this thesis is set ranging roughly from 800 m to 6000 m.
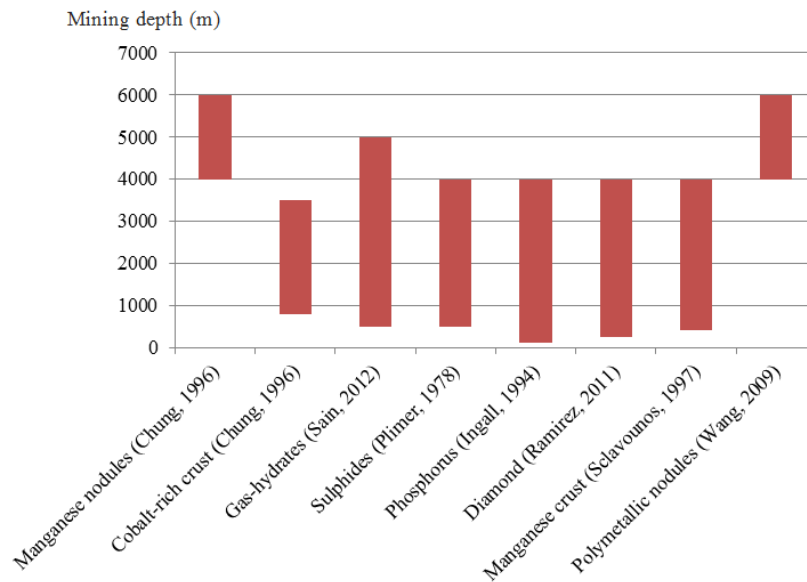
Figure 1.2: Minerals locating depth (Ma et al., 2017b).

Although the DSM industry could be easily influenced by the worldwide mineral market (Hoagland et al., 2010), which means the research and development (R&D) of DSM could be suppressed by the low mineral prices, its R&D process has not been interrupted completely. Especially, with the significant decrease of mineral resource storage on-land, more and more countries and international mining companies put more efforts and investments on the DSM research (ISA, 2018a).

However, since the start-up of DSM research, there is no commercial scale DSM project before and in progress. At present, the application of marine seabed mining is only limited in the coastal area because of the high initial investment and complex technical issues (Sweeney et al., 1974). The major barrier of the DSM industrialization is to judge the sustainability of a DSM transport plan (Birney et al., 2006; Copley et al., 2007). With the severity increase of mineral resources exhaustion (Hoagland et al., 2010; Sweeney et al., 1974; Birney et al., 2006; Copley et al., 2007), the design of an assessment system for judging the sustainability of a DSM transport plan seems to be necessary for the future development.

To design an assessment system for sustainable DSM transport plans, the influencing aspects of technological feasibility, economic profitability, and environmental impacts should be taken into consideration (Sharma, 2011).

From a technological perspective, in the DSM industry, Schulte (2013) analysed two typical lifting technologies by numerical calculations: (i) continuous line bucket lifting – mechanical lifting and (ii) hydraulic lifting with centrifugal pumps or air pumps. Different lifting technologies have their special features which could be applied in different DSM working conditions. The technological performances typically are evaluated by comparing the energy consumption, mineral production rate and geometry dimension of DSM facilities (Kice, 1986; Chung, 1996).

Except for the existing technological issues, the economic profitability of DSM project is another major consideration hindering its commercialization (Sharma, 2011). The challenges of economic profitability in DSM industry are of a high initial capital expenditure to purchase the PSV, seafloor mining vehicles, mineral transport vessels, and the mineral processing plants, and an expensive operation expenditure on the DSM activities, e.g., human resources fee, energy consumption cost and equipment maintenance fee (Birney et al., 2006; Kice, 1986).

The DSM industry is also a huge challenge for the environment (Ramirez-Llodra et al., 2011). The coming of the DSM era represents not only a leap development opportunity to the world economy, but also an urgent environment challenge which might lead to significant influences on the deep ocean water system, seafloor habitat, and species communities (Weaver et al., 2018).

As an emerging industry, there are many problems existing in its industrialization process. In this thesis, we only focus on the sustainability problem of DSM transport plans of manganese nodules mining projects. To the best of our knowledge, the major research gap for DSM activities is no prior research considering the technological feasibility, economic profitability, and environmental impacts all together when addressing its sustainability assessment problem.

1.2   Research aims and research questions

The thesis aim is to design an assessment system to evaluate the sustainability of DSM transport plans. The main question is formulated as follows:

How to evaluate the sustainability of DSM transport plans?

In order to answer the main question above, five key research questions are proposed as follows:

(1) Which factors influence the sustainability of DSM transport plan?

(2) How to select the proper transport technology for different DSM working depths?

(3) How to select a method to calculate the economic profitability of a DSM transport plan?

(4) How to develop a systematic calculation method for the DSM environmental impacts?

(5) How to evaluate and determine a sustainable DSM transport plan utilizing multi-criteria decision making method?

1.3   Methodologies

To address our major research questions, we start with literature review to understand the latest research status in depth and figure out the research gaps in DSM sustainability determination and assessment. Based on the literature review, there are individual researches on DSM technologies and related environmental impacts. However there is no systematic research integrating the DSM technological, economic, environmental impacts aspects together. During our research, the experimental data published in the literature are utilized to validate our numerical calculation results. In order to compare the technological feasibility of DSM transport plans, continuous line bucket lifting and hydraulic lifting system are compared and analysed focusing on the energy consumption lifting per tonnage mineral for specific cases. For the DSM economic research, a numerical calculation model is proposed focusing on the parameter of project capital expenditure, operation and maintenance expenditure, and profitability lifting per tonnage mineral. As to the DSM environmental impacts research, a systematic framework covering the sediment plume, tailings disposal, and species disturbances is proposed. Following the research framework, various kinds of DSM environmental impacts are calculated taking into consideration the interconnections. Finally, after analysing these influencing aspects, a suitable multi-criteria decision making (MCDM) method is selected to assess and determine the sustainability of DSM transport plans.

1.4   Outline of thesis

The structure of the thesis is presented as Figure 1.3.

Chapter 2 describes the basic knowledge and the influencing aspects of sustainable DSM transport plans.

Chapter 3 analyses the technological performances of two typical DSM lifting systems, i.e., continuous line bucket lifting and hydraulic lifting systems focusing on the energy consumption, lifting efficiency, and transport performance to identify the most suitable transport technology for different DSM working depths.

Chapter 4 analyses the modelling method of the economic profitability of a DSM transport plan, which takes the profitability lifting per tonnage minerals into consideration.

In **Chapter 5**, a systematic modelling framework of DSM environmental impact is proposed and analysed, which considers tailings disposal, sediment plume, and species disturbances.

Chapter 6 applies a MCDM method into the assessment system to determine a sustainable DSM transport plan taking into consideration the technological feasibility, economic profitability, and environmental impacts simultaneously.

Chapter 7 gives conclusions and recommendations.
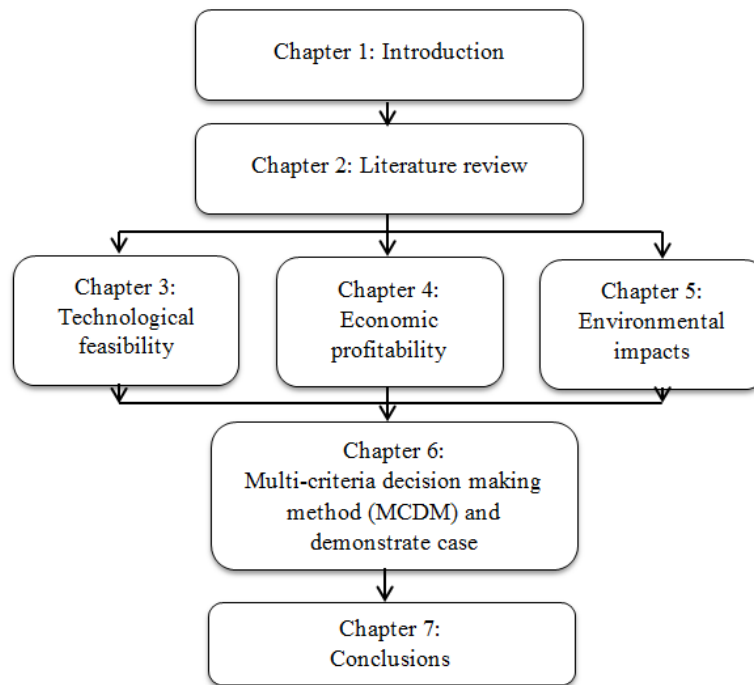
Figure 1.3: Thesis outline.

Chapter 2

Sustainability Review of Deep Sea Mining Transport Plans *

2.1. Introduction

With the increased consumption and gradual depletion of terrestrial mineral resources, deep sea mining (DSM) is attracting more and more attention from researchers addressing the world resource shortage problem (Hoagland et al., 2010). According to Jorn Mero (1965), the seabed has abundant storages of different kinds of expensive and rare mineral resources, which could supply the running of world economy for hundreds or even up to thousands of years. Despite the potential environmental impacts of DSM activities, its research and development (R&D) seems to be imperative (ISA, 2018a). A picture describing the broad distributions of mineral resources on the seabed around the world is shown in Figure 2.1 (Miller et al., 2018).
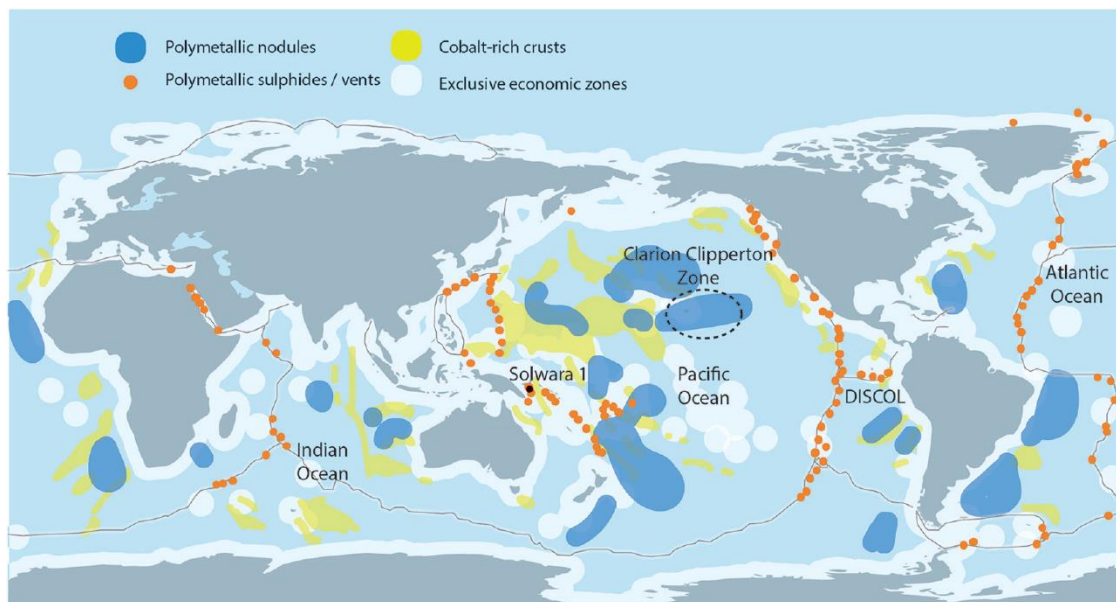
Figure 2.1: The three main marine minerals distribution around the world (Miller et al., 2018; Hein et al., 2013).

*This chapter is particially based on Ma et al. (2017b).

To most of DSM stakeholders, there is a consensus that has been recognized – if DSM companies would like to implement the industrial scale mining activities, its sustainability should be researched and must be analysed thoroughly (Sharma, 2011). The sustainability research of DSM transport plans is a complex and cross-disciplinary research topic, which is majorly related to several interconnected aspects including the technological feasibility, economic profitability and environmental impacts (Sharma, 2011).

A DSM project is schematically illustrated in figure 2.2. It describes the DSM environmental impacts including the sediment plume, direct habitat destroying, temperature increase and species disturbances. Taking sediment plumes as an example, it occurs in many different conditions, such as river estuaries (Wilber and Clarke, 2001; Shi, 2010) and benthic trawling fishery activities (O'Neill et al., 2013; Bradshaw et al., 2012). However, deep ocean, characterized by high pressure, cold temperature, e.g., roughly 4℃, absence of light, abundant nutrients, good water quality, e.g., free of pathogen and stable and low productivity, is a completely different environment with these above mentioned conditions, which seems to be more complex and vulnerable (Nakasone and Akeda, 1999). Therefore, for deep ocean sediment plume simulations, researchers could refer to the existing simulation and calculation methods and theories working in estuaries and fishery activities, but most importantly they also need to take into consideration the deep ocean special conditions, e.g., current condition and ecological vulnerability (Jankowski et al., 1996).
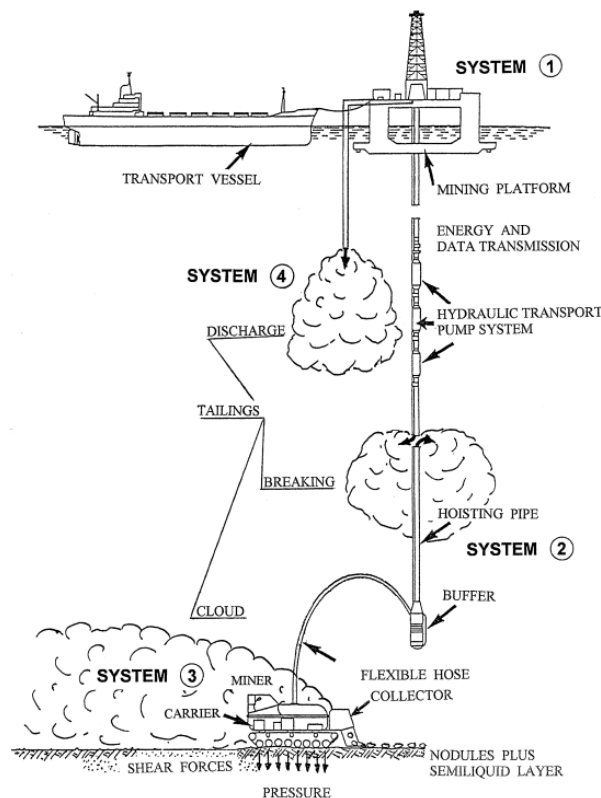
Figure 2.2: The schematic diagram of a DSM project (Oebius et al., 2001).

Technological feasibility and economic profitability are two other important aspects influencing the sustainability of DSM transport plans (Chung, 2003; Sharma, 2011; Chung

and Tsurusaki, 1994). For DSM activities, there are two typical kinds of technologies for mineral vertical transportation: continuous line bucket lifting (CLB) and hydraulic pipe lifting with centrifugal pumps and air pumps (Schulte, 2013). Different lifting technological systems would have different lifting efficiency, working reliability and technology maturity. The initial capital cost, operation and maintenance cost, and project investment recovery period could also have huge differences (Nyhart et al., 1978). Besides the vertical lifting technologies, Nautilus Minerals, a Canadian DSM company, developed and manufactured a series of seafloor working vehicles, e.g., auxiliary cutter (AC), bulk cutter (BC), and minerals collecting machine (CM), for DSM activities. Since 2017, Nautilus Minerals has also been busy with manufacturing the world first production support vessel (PSV) cooperating with Mawei Shipbuilding Ltd. in China (NAUTILUS Minerals, 2018a).

The above mentioned aspects, technological feasibility, economic profitability and environmental impact, are not independent, but interconnected with each other (Sharma, 2011). There exists a series of individual simulation and calculation methods for each of these influencing aspects. However, until now, there is no prior research taking into consideration the interconnections between them. The objective of this chapter is to analyse and discuss the factors influencing the achievement of DSM sustainable transport plans. The DSM transport plan is defined as the mineral transportation working plan, which includes the parameters of the capital cost, operation and maintenance cost, investment recovery period, mineral characteristics, working period, mineral production rate, generate sediment plume and species disturbances. This chapter is arranged as follows: the existing technological, economic and environmental impact researches are summarized and discussed in section 2. Section 3 analyses the existing researches and endeavours related to the sustainability of DSM transport plans and proposes the research gaps and implementing challenges to achieve a sustainable DSM transport plan. Then in section four, conclusions are given.

2.2. DSM technological, economic and environmental impact considerations

2.2.1. DSM technological research on vertical transport

The commercial coastal diamond and sand mining activities have been implemented for more than decades under a water depth smaller than 100 m (Pulfrich et al., 2003). The distribution depths of various kinds of deep ocean minerals could be up to 3000 – 6000 m (Ramirez-Llodra et al., 2011). The large operation water depth in DSM activities poses great challenges to the mining technology, minerals vertical lifting technology and tailings processing technology (Chung, 2003). The technology composition of a DSM project is complex and covers numerous aspects: seafloor mining technology including sediment cutting, minerals collecting, mineral separation, vertical lifting technology including hydraulic lifting and continuous line bucket lifting (see figure 2.3), but also mineral processing technology including the mineral grinding, separation and tailings disposal technologies. In this thesis, we focus on the vertical lifting technologies because of its technical challenges and large energy

consumption in DSM projects (Deepak et al., 2001; Chung and Tsurusaki, 1994; Masuda et al., 1971).
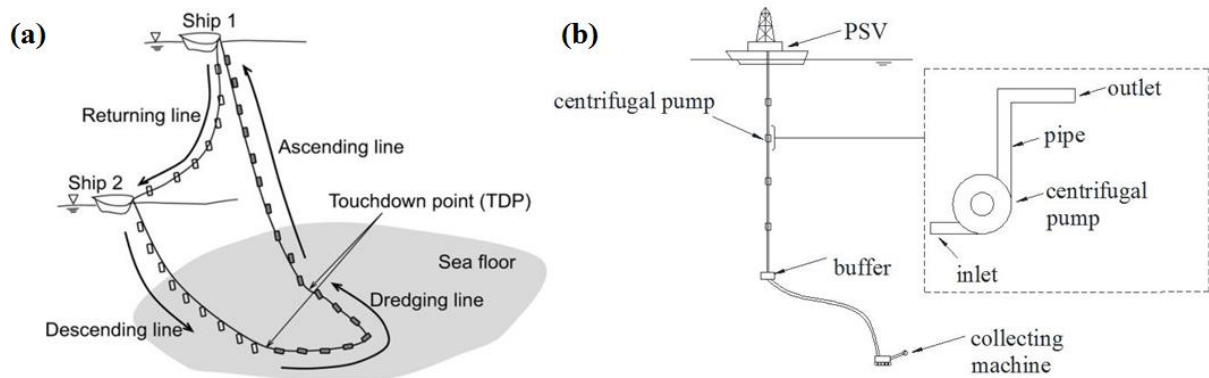
Figure 2.3: Two kinds of vertical lifting technologies in DSM activities. (a) continuous line bucket DSM system; (b) pipe lifting system with centrifugal pumps (Nishi, 2012).

Continuous line bucket lifting, as a kind of mechanical structure, was selected as the major by Japan Resources Association for DSM activity marine research taking into consideration its structure simplicity (Masuda et al., 1971; Masuda and Cruickshank, 1997). Research on continuous line bucket lifting was carried out mostly at the end of last century. With the rise of manufacturing technology and pumping technology, research on the hydraulic lifting system emerged at the beginning of the 21st century (Fan et al., 2013; Nam-Cheol et al., 2009; Xia et al., 1997; Hanafizadeh et al., 2011; Zou, 2007; Kassab et al., 2007; Yoon et al., 2000; Dare and Oturuhoyi, 2007; Vercruijsse et al., 2011; Gandhi et al., 2002; Vlasák et al., 2014; Leach et al., 2012). Additionally, many research on continuous line bucket lifting system and hydraulic lifting system are combined with small scale lab experiments (Vlasak and Chara, 2011; Nam-Cheol et al., 2009; Masuda, 1987; Xia et al., 1997; Hanafizadeh et al., 2011; Zou, 2007; Kassab et al., 2007; Yoon et al., 2000; Dare and Oturuhoyi, 2007; Gandhi et al., 2002; Vlasák et al., 2014) and in-situ tests (Fan et al., 2013; Masuda and Cruickshank, 1994; Masuda et al., 1971). As Leach et al. (2012) stated, '*Each technology has advantages and disadvantages but none can be considered to be technically unfeasible*', the importance is '*How to select a proper technology for a given DSM project*'.

2.2.2. DSM environmental impact researches

Due to the sharp decline of terrestrial mineral resources, many researchers believe that DSM industry would be a practical and feasible option to support the running of world economy. While, due to the vulnerability and unknownness of the deep ocean environment, researchers are also very worried about the caused environmental consequences (Ramirez-Llodra et al., 2015; Sharma, 2011; Oebius et al., 2001; Ramirez-Llodra et al., 2011; Glover and Smith, 2003; Fallon et al., 2002; Elberling et al., 2003).

Based on a systematic literature review, DSM environmental impacts are considered in many subjects covering:(i) tailings disposal (Ramirez-Llodra et al., 2015; Elberling et al., 2003; Edinger et al., 2007; McKinnon, 2002), (ii) sediment plume (Sharma et al., 2001; Jankowski

et al., 1996; Kineke et al., 2000; Thiel and Tiefsee-Umweltschutz, 2001), (iii) species disturbances (Glover and Smith, 2003; Sharma et al., 2001; Kineke et al., 2000; Van Dover, 2014; Van Dover et al., 2017; Thiel and Tiefsee-Umweltschutz, 2001; Schriever et al., 1997; Ingole et al., 2001; Borowski and Thiel, 1998; Miljutin et al., 2011), (iv) ecological restorations (Thiel, 1992; Miljutin et al., 2011; Van Dover et al., 2014), (v) heavy metal pollution (Elberling et al., 2003). In addition, most of these DSM environmental impact researches follow the research procedure of environment disturbing – monitoring – analysing (Fallon et al., 2002; Elberling et al., 2003; Edinger et al., 2007; Sharma et al., 2001; Kineke et al., 2000; Thiel and Tiefsee-Umweltschutz, 2001; Schriever et al., 1997; Ingole et al., 2001; Borowski and Thiel, 1998; Miljutin et al., 2011). Based on a workshop report by Collins et al. (2013), the DSM environmental impact assessment is a complex interdisciplinary topic, which should be established by all stakeholders of DSM activity in academic, commercial, governmental and non-governmental fields.

Although the news of commercial scale DSM implementation in Papua New Guinea (PNG) was announced by Nautilus minerals company, the R&D on DSM environmental impacts is still incomplete and uncomprehensive (Van Dover, 2014; Van Dover et al., 2017; Van Dover, 2011; Van Dover et al., 2014). Especially the marine species responses to sediment plume, the restoration of marine ecology after DSM activities, and the establishment of DSM environmental impact standard, there are remaining many research blanks requiring more efforts on them (Van Dover et al., 2017; Thiel, 1992; Miljutin et al., 2011; Van Dover et al., 2014; Whitney, 1977; Vrijenhoek, 2010). Most of previous studies focus on specific environmental impacts, while neglecting the interconnections between different aspects (Gideiri, 1984; Jankowski et al., 1996; Nakata et al., 1999; Oebius et al., 2001; Van Dover, 2011; Hoagland et al., 2010). For instance, sediment plume could be caused by the cutting and collecting activities, submarine tailings disposal and sediment leakage on the transport process, which might also present a threat to the marine species (Wilber and Clarke, 2001; Rodrigues et al., 2001; Trueblood and Ozturgut, 1997; Raghukumar et al., 2001; Turner and Millward, 2002; Lander et al., 2013).

2.2.3. DSM economic research

Compared to the technological and environmental impact researches, there are relatively less papers focusing on DSM economic profitability (Sharma, 2011; Mero, 1977; Nyhart et al., 1978; Hoagland, 1993). In 1977, Jorn Mero described, the manganese nodules average concentration should be in range of 5 - 20 kg/m^2 for an economic DSM feasible area. He described the composition of high grade sampled manganese nodule at North Pacific, which is critical to the price of gross minerals. These high grade manganese nodules are composed by 35% Mn, 2.3% Cu, 1.9% Ni, and 0.2% Co. He also summarized the important factors for a promising and profitable DSM project including nodule composition, nodule distribution density and size, continuity of the deposits, seafloor topography and the character of the associated sediment.

Nyhart et al. (1978) categorized the expenditures of DSM commercialization into '*research and development*', '*prospecting and exploration*', '*capital*', and '*operation expenses*'. Until

now, most of the researches still stay at the first two categories, and there is no substantial research involved in the capital expenditure. The capital expenditure, and operation and maintenance expenditure, could be further divided into three parts: mining, transport and processing. Taking an example of processing capital expenditure, it consists of cost on the equipment, utilities, plant sites and buildings. The operation and maintenance expenditure of a system generally covers the energy, labour, materials, fixed charges and miscellaneous items. As Nyhart et al. (1978) explained, the DSM economic analysis is closely related to time factor, economic factor, technological factor, policy factor, investment return factor and financial factor, see figure 2.4.
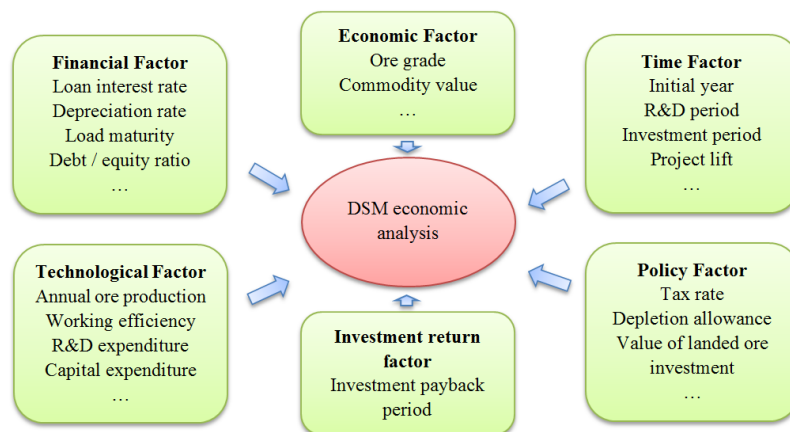
Figure 2.4: DSM economic analysis components adopted from Nyhart et al. (1978).

Hoagland (1993) analysed the DSM economic conditions focusing on the price trend of manganese nodules in both long-term and short-term perspectives. Based on the linear and quadratic price trend prediction, Hoagland (1993) presented a cost-benefit analysis, which indicates that '*the most optimistic expected data of commercialization resulting from these predictions is well into the 21st century*'. Based on the data from International Seabed Authority (ISA) and published papers, Sharma (2011) presented a basic estimation of DSM economic conditions. It supplies the ranges of gross income, production rate and generated tailings of a normal DSM project for the future research (Sharma, 2011). All in all, it is noticeable that researchers established the basic theoretical descriptions and estimation methods for DSM economic considerations (Sharma, 2011; Mero, 1977; Nyhart et al., 1978; Hoagland, 1993). Although researchers have noticed the importance of relationship between DSM economic analysis and other related aspects, e.g., technological factors, the related studies are limited at a very early stage.

2.3. Sustainability of DSM transport plans

2.3.1. Definition of a sustainable DSM transport plan

The definition and requirement of '*sustainability*' could be different at different application fields (Brown et al., 1987). A selection of '*sustainability*' definitions is as follows.

- Oxford English Dictionary explains the '*sustainable*' as '*capable of being upheld; maintainable*' (Brown et al., 1987);
- Ecosystem (biological) sustainability given by Tivy and O'Hare (1982) is given as '*management of a resource for maximum continuing production, consistent with the maintenance of a constantly renewable stock*'.
- Another kind of biological sustainability is summarized by Gatto (1995) as '*sustainable yield of resources that derive from the exploitation of populations and ecosystems*'.
- Gatto (1995) also summarized the economic sustainability as '*sustained economic development, without compromising the existing resources for future generations*'.
- Energy use sustainability is given as resources consumption not faster than they are created focusing on the '*exceeding carrying capacity*' by Gever et al. (1986).
- Social sustainability is given as '*an enduring one, self-reliant and less vulnerable to external forces*' (Brown, 1982).
- Environmental sustainability is generally regarded as the important subset of ecological sustainability given as '*a condition of balance, resilience, and interconnectedness that allows human society to satisfy its needs while neither exceeding the capacity of its supporting ecosystems to continue to regenerate the services necessary to meet those needs nor by our actions diminishing biological diversity*' by Morelli (2011).

The sustainability applied in this thesis on DSM transport plans is a comprehensive concept connecting the '*environmental sustainability*', '*economic sustainability*', '*biological sustainability*', '*energy use sustainability*', which would analyse its environmental and social impacts, economic profitability, production rate, working efficiency and social impacts. The sustainability research of DSM transport plan is to assess different DSM designs taking into consideration the technological, economic, environmental and social aspects simultaneously and find a compromise balance or an optimal balance between all influencing aspects.

2.3.2. Research gap in sustainability of DSM transport plan

Although there are many researches related to DSM, there are very few studies focusing on the sustainability of DSM transport plans (Sharma, 2011; Giurco and Cooper, 2012; Abramowski and Stoyanova, 2012; McLellan et al., 2013; Lambert, 2001; Wiltshire, 2017).

Lambert (2001) claimed the sustainability of mineral mining industry is a completely strategic issue and tried to explain this problem through conceptual thinking, sustainable development trend analysis, influencing factors comparison, e.g., economic consideration and tailings disposal. Van Bloois and Frumau (2009) also noted the important role of economic, social and environmental impacts on the sustainable DSM transport plan determination. Sharma (2011) proposed a basic case analysis trying to explain the sustainability problem of DSM transport plans and mentioned the important roles of economic, technical, technological and environmental considerations in DSM sustainable development. However, his research does not address the issues involved in DSM sustainable development in depth, and neither connects the exact utilized technology with the economic analysis and the following

environmental impacts. Giurco and Cooper (2012) proposed a theoretical framework - *Mineral Resources Landscape* as an expanded conceptualisation of mining industry sustainability emphasizing the importance of social, ecological, technological, economic and governance considerations. Abramowski and Stoyanova (2012) focused on the environmental sustainability of deep ocean polymetallic nodules mining activity explaining the maintenance of the deep ocean ecosystem and the natural resource base theoretically. McLellan et al. (2013) reviewed the sustainability of rare earth (RE) element mining industry in terms of technological, environmental, social and economic aspects. McLellan et al. (2013) also claimed '*there is no prior research that has addressed the wide sustainability impacts of RE across these multiple areas*'. Wiltshire (2017) explained the sustainable development as '*a goal that can be achieved in the handling of processing tailings of deep-sea manganese nodules and crusts*'.

Analysing these aforementioned literature focusing on DSM sustainable development, almost all these researches stay at the level of theoretical explaining, conceptualisation making and framework establishment. Even until now, there is no research addressing the sustainability of DSM transport plan across the areas of technological, environmental and economic considerations.

2.3.3. Challenges in the research of sustainability of DSM transport plan

When addressing the sustainability problem of DSM transport plan, there would be several foreseeable challenges in its realization process.

- Multi-criteria decision making application

To determine a sustainable DSM transport plan, the traditional cost-benefit method is not qualified because there are more (>3) interconnected and independent evaluating criteria (Majumder, 2015). Referring to the existing literature in similar research fields, it presents that multi-criteria decision method (MCDM) might be a good option to address this problem. Although MCDM method has not been applied in DSM activity before, it has been applied in many the other similar industrial fields addressing the project sustainability (Pohekar and Ramachandran, 2004; McDowall and Eames, 2007; Afgan and Carvalho, 2008; Jovanović et al., 2009). For instance, Pohekar and Ramachandran (2004) analysed the MCDM application in sustainable energy planning through a systematic literature review. McDowall and Eames (2007) analysed the sustainable hydrogen economy, a kind of energy utilization system, with MCDM method. Afgan and Carvalho (2008) carried out a sustainability assessment of a hybrid energy system. Jovanović et al. (2009) focused on the energy system sustainable development in Belgrade utilizing MCDM method. Then another important research question is raised here '*How to apply multi-criteria decision making method addressing the sustainability of DSM transport plans?*' As there are so many different kinds of MCDM methods, selecting which method to apply depends on the specific working conditions, such as the given data, expected data, application assumptions and scenarios.

- Realizing the numerical calculations of different influencing aspects of the sustainable DSM transport plans

For these major DSM sustainable influencing aspects, e.g., environmental impacts and technological considerations, there are series of individual analytical and simulation models for them respectively. For instance, the numerical calculation models of sediment plume, which is one of the most important parameters in DSM environmental impact consideration, consist of large scale model (Zielke et al., 1995), mesoscale regional model (Jankowski et al., 1996), and near-field model (Decrop et al., 2015). It is critical to select a proper numerical calculation model for our research, because these mentioned various simulation models have their special focuses, boundary conditions and fluid conditions (Decrop et al., 2015; Zielke et al., 1995; Jankowski et al., 1996).

- Including all stakeholders of DSM activities from academia, industry, technical consultants, project investors and environmentalists

When referring to other industrial and manufacturing sustainability, many researchers would like to address such kinds of issues from a global and strategic perspective, which means all related departments, systems and stakeholders, as more comprehensive as possible, would coordinate experts from varying backgrounds together (Jovanović et al., 2009; Pilavachi et al., 2009; Portney, 2013). In DSM sustainability research, a lot of researchers have also noticed the importance of cooperation and coordination between all stakeholders (Sharma, 2011; Collins et al., 2013). However, there is no manifest achievement of the cooperation between all DSM stakeholders. One reason might be research progresses of different DSM influencing aspects are not synchronized and the attentions of society are majorly focused on the most intuitive and obvious aspects, e.g., DSM environmental impacts.

2.4. Conclusions

Through a systematic literature review, the current R&D status on DSM technological, environmental and economic aspects have been analysed and discussed. Based on the related information collection, comparison and discussion on the sustainability of DSM transport plans, it is noticeable that almost all research stays at the level of theoretical explaining, conceptualisation making and framework establishment. Until now, there is no research addressing the sustainability problem of DSM transport plan across these multiple areas of technological, environmental and economic considerations. In addition, several foreseeable challenges in the research of sustainability of DSM transport plans, e.g., MCDM method application and cooperation between experts from varying backgrounds, are also introduced and explained for guiding the future research.

Chapter 3

Technological Feasibility Analysis of DSM Vertical Lifting Systems*

Based on the literature review results in chapter 2, the influencing aspects of the sustainable DSM transport plans consist of the technological feasibility, economic profitability, and environmental impacts.. This chapter focuses on the technological performance calculations of two typical DSM lifting systems: continuous line bucket lifting (CLB) and pipe hydraulic lifting (PLS) systems. In this chapter, section 3.1 gives an introduction of these two lifting systems. Section 3.2 presents the numerical analysis of CLB and PLS working principles. In section 3.3, the technological performances of CLB and PLS systems are analysed and discussed. Finally, the conclusions are presented in section 3.4.

3.1. Introduction

In the deep sea mining (DSM) industry, two typical lifting technologies are most widely focused and developed: the continuous line bucket lifting system (CLB) equipped with the towing buckets and the hydraulic pipe lifting system (PLS) equipped with self-maneuverable mining vehicles including the auxiliary cut vehicle (AC), bulk cut vehicle (BC) and mineral collecting vehicle (CM) (Amos and Roels, 1977). The PLS technology in DSM activity majorly consists of the pneumatic lifting and the centrifugal pump lifting systems. The hydraulic lifting method is utilized normally in DSM industry due to its simple working principle and high degree of mechanization. Compared to the centrifugal pump lifting system, the pneumatic lifting consumes much more energy and needs a relatively larger pipe diameter (Kice, 1986). Besides, the minerals mixture flow moved by pneumatic lifting method has a great influence on the movement of the vertical pipeline system (Chung, 1996). Therefore, the PLS lifting method analysed in this paper focuses on the centrifugal pump lifting method.

The CLB lifting method employs a line attached with the specifically designed buckets to lift the minerals from the seabed to the production support vessel (PSV) (Eckert, 1974). The CLB lifting system used to sweep the seabed, as a farmer plowing process, to collect the minerals (Morgan et al., 1999). Although the simple CLB mining systems has a theoretical high transport efficiency of approximately 87% (Glasby, 2002), the realistic mining efficiency is

limited by several technical issues, such as the mineral collecting process and the buckets movement operation under the water. So the CLB system utilized recently is an innovated version of the original one. A controller coordinating the movement of the mineral collecting vehicle and the bucket system is added into the CLB system design to improve the collecting efficiency of the minerals at the seafloor in Figure 3.1.

In the hydraulic lifting process research, researchers emphasize on the lifting pipe dimensions, the properties of the mineral particles (regular or irregular, shape, volumetric concentration of the mineral solid). The schematic diagram of the PLS lifting system utilizing the centrifugal pump lifting is shown in Figure 3.2. For the DSM industry, in addition to an evaluation of the lifting principle of the CLB and the PLS lifting methods, its economic analysis is also quite necessary (Kotlinski et al., 2008). Although the DSM industry is influenced by the international mineral resources market, its research and development in so many countries shows an overall upward trend (Bath, 1989). So is it necessary to establish an explicit comparison system for the normal utilized DSM lifting methods.
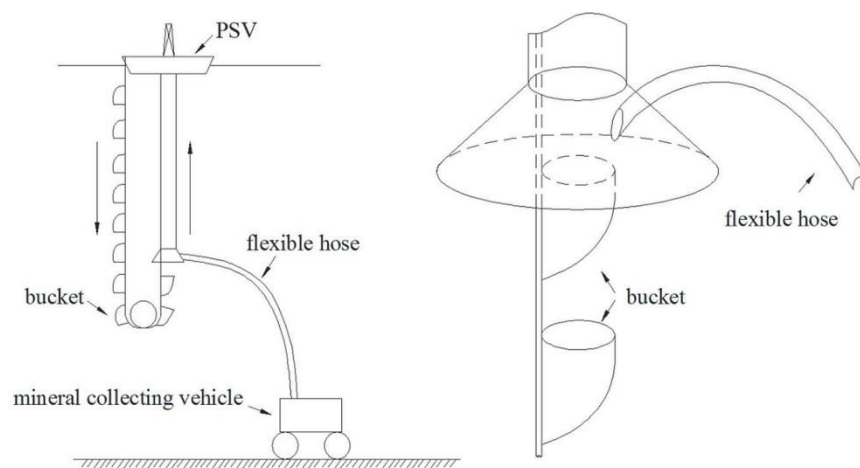
Figure 3.1: A new innovated CLB system.
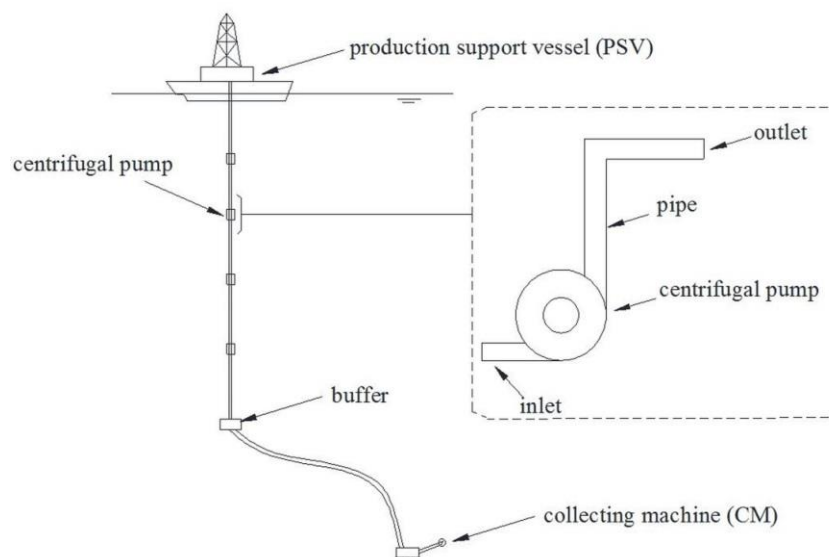
Figure 3.2: The schematic diagram of the deep sea mining PLS system.

This chapter compares the CLB and PLS lifting systems considering the lifting efficiency and the energy consumption. The objective of this chapter is to select the appropriate lifting method for DSM projects depending on its different focus on the technology. The researchers and the engineers can then refer to the comparison results to implement their experiments or the in-situ field tests. The chapter is arranged as follows. The second section is the numerical analysis of CLB and PLS working principles. In the third section, the technological performances of CLB and PLS systems are analysed and discussed. Finally, in section four, conclusions of the conducted research are given.

3.2. Numerical analysis of CLB and PLS working principles

3.2.1. Numerical modelling of CLB system

The CLB system considered in this chapter is shown in Fig. 1. The working process can be divided into ascending process and descending process. The upper side of the buckets line links with the winch. The bottom side of the buckets line links with a fixed pulley (Schulte, 2013). The following assumptions of the CLB modelling are made (Schulte, 2013):

- The buckets line is continuous;
- There is no mineral leakage in the lifting process (buckets with cover);
- The transient velocities on the line are the same;

The CLB forces relationship of the ascending process and the descending process is described as follows (Schulte, 2013).

$$\begin{cases} ascending \quad process: \quad F_{r\_a} = F_{wi} + F_{b\_a} - F_{g\_a} - F_{d\_a} \\ descending \quad process: \quad F_{r\_d} = F_{g\_d} - F_{b\_d} - F_{d\_d} \end{cases} \quad (3.1)$$

where F_{wi} is the winch force, [N]; F_r is the resultant force, [N]; F_b is the buoyancy force, [N]; F_g is the gravitational force, [N]; F_d is the drag force, [N]; Subscript a represents the ascending process; Subscript d represents the descending process.

The gravity of the CLB system can be calculated with Eq. 3.2.

$$\begin{cases} ascending \quad process: \quad F_{g\_a} = n \cdot \left(n_f \cdot l^2 \cdot t_b \cdot \rho_b + l^3 \cdot \gamma \cdot \rho_s \right) \cdot g + n_{wr} \cdot H \cdot m_{\_c} \\ descending \quad process: \quad F_{g\_d} = n_f \cdot n \cdot l^2 \cdot t_b \cdot \rho_b \cdot g + n_{wr} \cdot H \cdot m_{\_c} \end{cases} \quad (3.2)$$

where n_f is the number of faces of the buckets, which is set to be 5; n is the buckets number in each side under the water; l is the side length of the cubic bucket, [m]; n_{wr} is the number of cables, which is set to be 3; t_b is the thickness of the bucket wall, [m]; γ is the bucket filling ratio, [-]; $m_{\_c}$ is the mass of the cable, which is set to be 14.7 kg/m length; ρ_b, ρ_s are the

density of the bucket and the mineral respectively, which are set to be 7650 kg/m^3 and 3750 kg/m^3; H is the mining depth, [m].

The buoyancy forces can be calculated with Eq. 3.3.

$$\begin{cases} ascending \quad process: \quad F_{b\_a} = n \cdot \rho_l \cdot \left(n_f \cdot l^2 \cdot t_b + l^3 \cdot \gamma \right) \cdot g + n_{wr} \cdot \rho_l \cdot \pi \cdot r_c^2 \cdot H \cdot g \\ descending \quad process: \quad F_{b\_d} = n_f \cdot n \cdot l^2 \cdot t_b \cdot \rho_l \cdot g + n_{wr} \cdot \rho_l \cdot \pi \cdot r_c^2 \cdot H \cdot g \end{cases} \tag{3.3}$$

where r_c is the radius of the cable, [m]; ρ_l is the liquid density, [kg/m^3].

The drag forces can be calculated with Eq. 3.4.

$$F_{d\_a} = F_{d\_d} = C_{d\_v} \cdot \frac{1}{2} \cdot \rho_l \cdot l^2 \cdot v_c^2 + 4 \cdot C_{d\_h} \cdot \frac{1}{2} \cdot \rho_l \cdot l^2 \cdot v_c^2 \tag{3.4}$$

where C_{d_v} is the drag coefficient for the plate perpendicular to the flow, [-]; C_{d_h} is the drag coefficient for the plate parallel to the flow, [-]; v_c is the CLB moving velocity, [m/s]. The negative sign represents that the vector parameters of F_{d_a}, F_{d_d} have the opposite directions.

The CLB system can also be analysed through an overall force analysis method. To the total CLB system, the gravity force and the buoyancy force belong to the system internal forces. The winch force, the drag force belong to the system external force, see Eq. 3.5.

$$m_{\_CLB} \cdot \frac{dv_c}{dt} = F_{wi} - F_{d\_a} - F_{d\_d} - F'_{g\_m} \tag{3.5}$$

where $m_{\_CLB}$ is the mass of the total CLB system, which consists of the buckets mass, the wire rope mass, and the mineral mass, [kg]; F'_{g_m} is the gravity force of the minerals in the ascending process.

Depending on the power consumption of the CLB system, the energy consumption lifting per tonnage mineral and the corresponding efficiency could be calculated as follows:

$$\begin{cases} E_{c\_u} = Q_s \cdot g \cdot H \cdot (1 - \dfrac{\rho_l}{\rho_s}) + Q_s \cdot g \cdot h \\ E_{c\_t} = 3600 \cdot P \\ \eta_c = \dfrac{E_{c\_u}}{E_{c\_t}} \\ E_{ton} = \dfrac{E_{c\_t}}{Q_s} \end{cases} \tag{3.6}$$

where E_{c_u} is the useful energy consumption, [J/h]; E_{c_t} is the total energy consumption, [J/h]; Q_s is the solid mineral production rate, [ton/h]; P is the power of winch lifting system [W]; η_c is the CLB system efficiency, [-]; E_{ton} is the energy consumption lifting per tonnage mineral, [J/ton] or [kWh/ton].

3.2.2. PLS modelling

The PLS lifting method utilizes the pressure difference supplied by the centrifugal pumps to lift the minerals slurry mixtures (Shook and Bartosik, 1994). The importance of the PLS method is to calculate the required pressure in the system with Eq. 3.7 (Schulte, 2013).

$$
\begin{aligned}
P_r = (\xi_f + \xi_H(H)) \cdot \frac{1}{2} \cdot (\rho_l \cdot C_l \cdot v_l^2 + \rho_s \cdot C_s \cdot v_s^2) + \frac{1}{2} \cdot \frac{H}{D_i}\left(\lambda_l \cdot \rho_l \cdot C_l \cdot v_l^2 + \lambda_s \cdot \rho_s \cdot C_s \cdot v_s^2\right) + \\
H \cdot g \cdot (\rho_m - \rho_l)
\end{aligned}
\tag{3.7}
$$

where P_r is the required pressure to lift the mixture minerals from the seabed to the PSV, [Pa]; ξ_f is the inlet and the acceleration coefficient, [-]; ξ_H is the valve coefficient, [-]; λ_l, λ_s are the liquid and the solid particles friction coefficient respectively, [-]; D_i is the rigid pipe diameter, [m]; H is the mining depth, [m]; ρ_m is the slurry mixture density, [kg/m^3]; C_l, C_s are the volume concentration of the liquid and the solid respectively, [-]; v_l, v_s are the liquid velocity and the solid particle velocity respectively, [m/s].

The relationship between the mixture velocity, the mineral solid velocity and liquid velocity can be calculated with Eq. 3.8 (Van Wijk, 2014).

$$
\begin{cases}
v_s = v_l - v_{sl} \\
v_s = v_m - v_{sl} \cdot (1 - C_s) \\
v_{sl} = 10^{-d_s/D_i} \cdot v_{st} \cdot (1 - C_s)^{n'-1}
\end{cases}
\tag{3.8}
$$

where v_s, v_l, v_m are the solid velocity, the liquid velocity and the mixture velocity respectively, [m/s]; v_{sl} is the slip velocity, [m/s]; d_s is the particle diameter, [m]; n' is the calculation index relating with the particle Reynolds number; v_{st} is the particle settling velocity determined by the particle size, [m/s].

The particle settling velocity is calculated depending on its diameter with Eq. 3.9 (Van Rijn, 1984).

$$
\begin{cases}
v_{st} = \dfrac{1}{18}\dfrac{(\rho_s / \rho_l - 1) \cdot g \cdot d_s^2}{\upsilon'} & d_s < 0.1mm \\[2ex]
v_{st} = 10\dfrac{\upsilon'}{d_s}\left(\sqrt{1 + \dfrac{0.01 \cdot (\rho_s / \rho_l - 1) \cdot d_s^3 \cdot g}{\upsilon'^2}} - 1\right) & 0.1mm < d_s < 1mm \\[2ex]
v_{st} = 1.1\sqrt{(\rho_s / \rho_l - 1) \cdot d_s \cdot g} & d_s > 1mm
\end{cases}
\tag{3.9}
$$

where υ' is the kinematic viscosity, [m^2/s]. The kinematic viscosity is determined by the liquid density and the dynamic viscosity.

The energy consumption lifting per tonnage mineral and the efficiency for the PLS system can be calculated as follows.

$$\begin{cases} E_{p\_u} = \left(1 - \dfrac{\rho_l}{\rho_s}\right) \cdot Q_s \cdot g \cdot H \\[2mm] E_{p\_t} = \dfrac{v_m \cdot A_p \cdot P_r}{\eta_h \cdot (a_w)^{N_p}} \\[2mm] \eta_r = \dfrac{E_{p\_u}}{E_{p\_t}} \\[2mm] E_{ton} = \dfrac{E_{p\_t}}{Q_s} \end{cases} \qquad (3.10)$$

where N_p is the number of the centrifugal pumps, [-]; a_w is the work ability factor, [-]; A_p is the transverse area of the rigid pipe, [m^2]; η_h is the hydraulic efficiency; E_{p_u} is the useful energy consumption, [J/h]; E_{p_t} is the total energy consumption, [J/h]; η_r is the PLS system efficiency, [-].

3.3. Technological performance analysis of CLB and PLS systems

In this section, the technological performances of the CLB and the PLS transport methods are compared with each other. The research focuses on two important transport parameters: the transport efficiency and the solid mineral production rate.

For the CLB lifting system, the winch force should be determined firstly depending on the following parameters: the cable moving velocity, bucket geometry, and the bucket distribution conditions. Therefore, it is necessary to figure out the relationship between the winch force and the CLB cable velocity. The CLB cable velocity is set ranging from 0 m/s to 3 m/s (Masuda et al., 1971; Brink and Chung, 1981). Combining Eq. 3.1 to Eq. 3.5, the relationship of the CLB cable velocity and the winch force can be calculated through solving a differential equation, see Eq. 3.11.

$$v_c = \frac{\sqrt{F_{wi} - C}}{\sqrt{A}} \cdot \frac{1 - e^{-\frac{2 \cdot \sqrt{A} \cdot \sqrt{F_{wi} - C}}{B} t}}{1 + e^{-\frac{2 \cdot \sqrt{A} \cdot \sqrt{F_{wi} - C}}{B} t}} \qquad \left(F_{wi} \geq C\right) \qquad (3.11)$$

In Eq. 3.11, A, B and C are depicted as follows:

$$\begin{cases} A = \left(C_{d\_v} \cdot \dfrac{1}{2} \cdot \rho_l \cdot l^2 + 4 \cdot C_{d\_h} \cdot \dfrac{1}{2} \cdot \rho_l \cdot l^2\right) \cdot 2 \cdot H / (l + l') \\[2mm] B = \begin{bmatrix} n_a \cdot \left(l^3 \cdot \gamma \cdot \rho_s + 2 \cdot n_f \cdot l^2 \cdot t_b \cdot \rho_b\right) + \\ 2 \cdot n_f \cdot l^2 \cdot t_b \cdot (\rho_b - \rho_l) \cdot n + l^3 \cdot \gamma \cdot (\rho_s - \rho_l) \cdot n + n_{wr} \cdot H \cdot m_{\_c} \end{bmatrix} \\[2mm] C = l^3 \cdot \gamma \cdot (\rho_s - \rho_l) \cdot g \cdot n + n_a \cdot l^3 \cdot \gamma \cdot \rho_s \cdot g \end{cases} \qquad (3.12)$$

The system transport efficiency represents the energy utilization degree and the energy capital expenditure. The solid mineral production rate represents the economic gross profits. The optimal transport plan can be regarded as the optimal level combinations of the transport efficiency and the solid mineral production rate to achieve lowest energy consumption per tonnage of the minerals when considering the technological performances.

Case – Technological performance analysis

After the numerical modelling of the CLB and the PLS lifting methods, the energy consumption and the lifting efficiency can be calculated following Eq. 3.6 and Eq. 3.10. In this case, it is necessary to guarantee that both transport systems have the same solid mineral production rate.

At the beginning of the technological performance analysis of the CLB and the PLS transport systems, it is necessary to find out the optimal transport plan depending on its optimal function, i.e., the energy consumption per tonnage mineral. For instance, the supplied winch force and the mining depth are set to be 860 kN and 800 m respectively. The maximum transport efficiency and the maximum solid mineral production rate are calculated to be 97.39 % and 1.29×10^3 ton/h. The corresponding solid mineral production rate and the transport efficiency for the maximum transport efficiency and the maximum solid mineral production rate are 54.27 ton/h and 55 % respectively. The optimal transport plan in technological analysis part is determined by the lowest energy consumption per tonnage mineral. Figure 3.3 depicts the relationship of the energy consumption per tonnage mineral versus the mining depth of the CLB transport systems. Figure 3.4 depicts the relationship of the energy consumption per tonnage mineral versus the mining depth of the PLS transport systems.
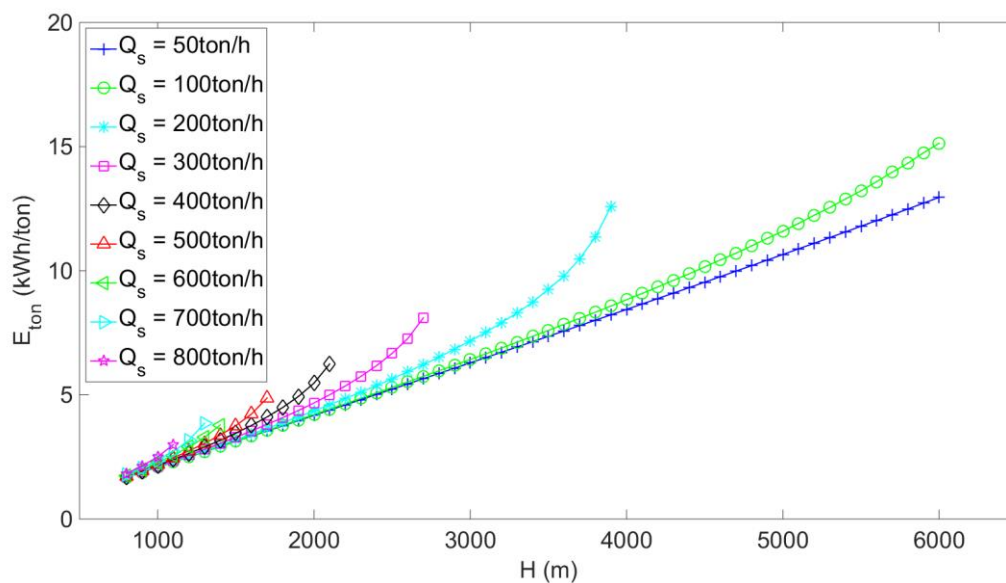
Figure 3.3: The energy consumption per tonnage mineral versus the mining depth of the CLB system.
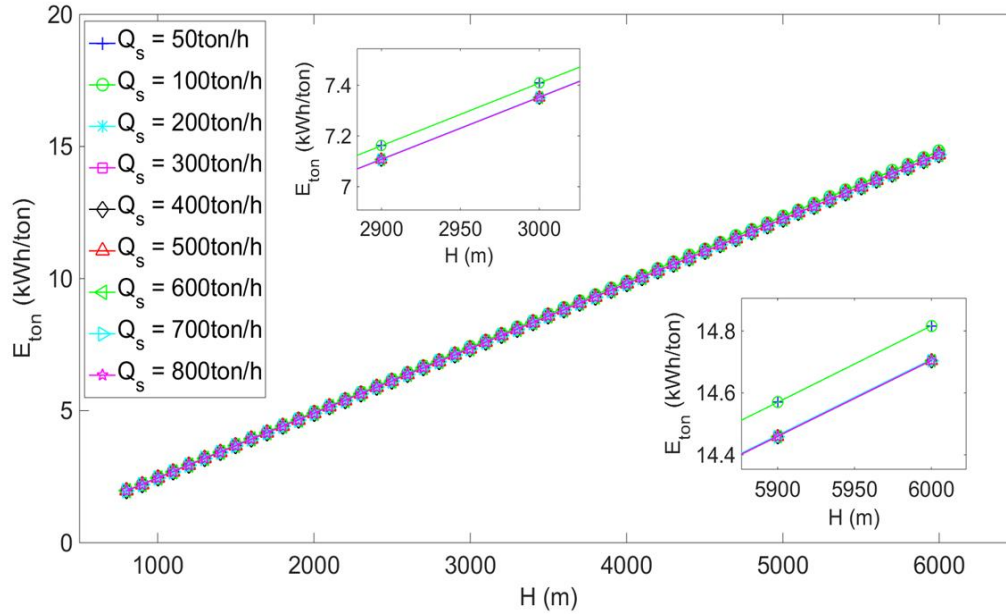
Figure 3.4: The energy consumption per tonnage mineral versus the mining depth of PLS systems.

Analysing Fig. 3.3, with the constant winch force for the CLB system, the energy consumption per tonnage mineral changes with the mining depth and the selected solid mineral production rate. For the CLB and the PLS transport systems, the energy consumption per tonnage mineral increases with the increasing of the mining depth because of the significant increasing of the useful energy consumption to lift the minerals. Comparing the relationship of the energy consumption per tonnage mineral of the CLB and the PLS systems in Fig. 3.3 and Fig. 3.4, it is obvious that different solid mineral production rates have more significant influences on the CLB system than on the PLS system. For instance, when the solid mineral production rate is bigger than 800 ton/h, the CLB system cannot be applied on the DSM projects deeper than 1000 m. That is because, for the CLB system, the system application range is greatly limited by the maximum winch force. Additionally, the selection of the DSM transport method can be changeable depending on its different mining depth and the purpose solid mineral production rate. For instance, when the purpose solid mineral production rate is 50 ton/h, the CLB system is better than the PLS system of the depth ranging from 800 m to 6000 m. When the solid mineral production rate is 200 ton/h, the PLS system is better than the CLB system of the depth deeper than 3500 m. The critical depth, where the PLS system is better than the CLB system, totally disappears when the solid mineral production rate is set to be 600 ton/h. The PLS system locates at a more conspicuous favourable position than the CLB system, when the solid mineral is bigger than 800 ton/h. Just only when the mining depth is quite small, e.g., 800 m, the CLB system can obtain a similar technological performances as the PLS system.
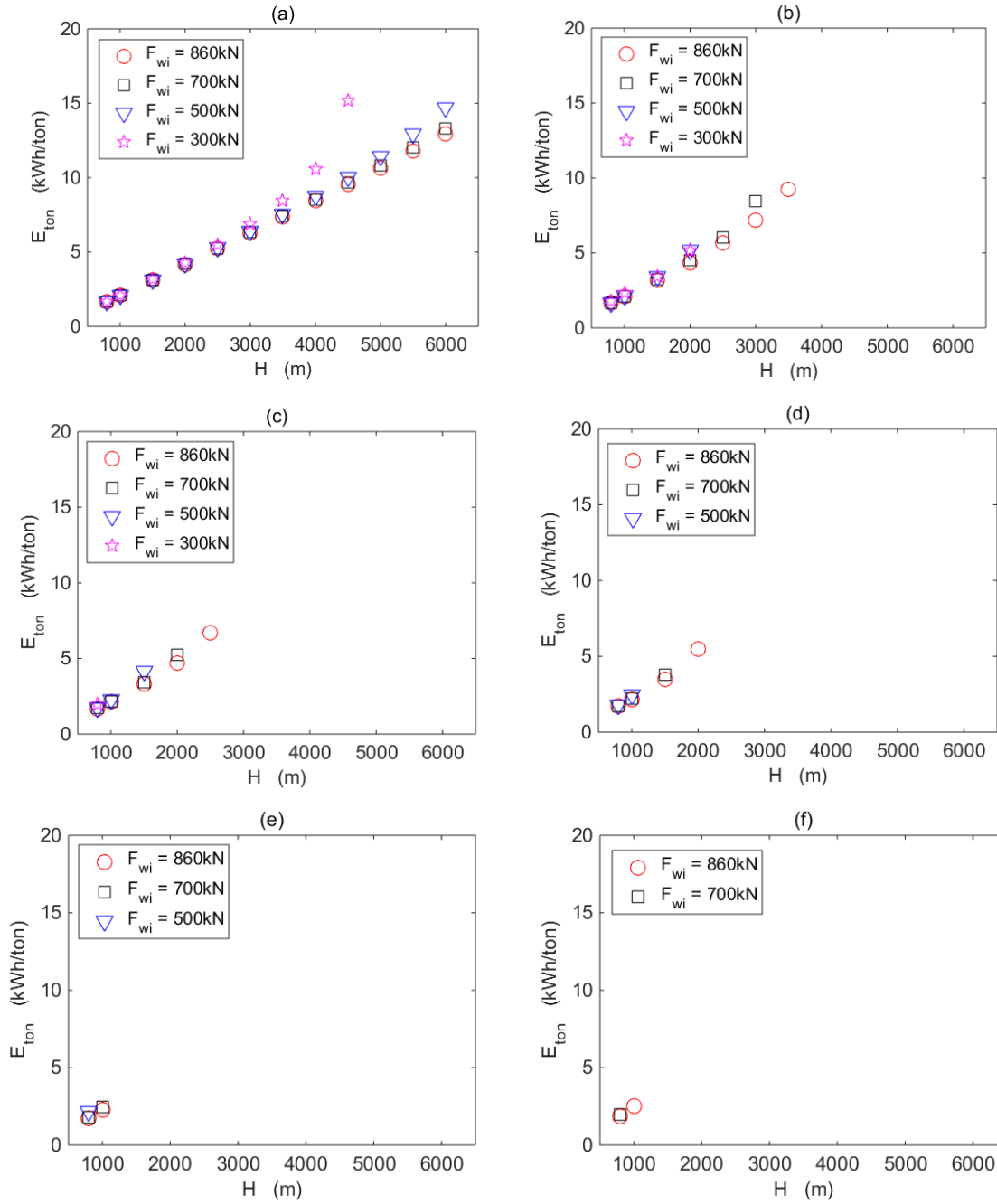
Figure 3.5. Energy Consumption per Tonnage Mineral versus the Mining Depth and the Solid Mineral Production Rate. Note: figure (a), (b), (c), (d), (e), (f) represent the solid mineral production rate at 50 ton/h, 200 ton/h, 300 ton/h, 400 ton/h, 600 ton/h, and 800 ton/h respectively.

It is obvious that the maximum solid mineral production rate and the mining depth of the CLB system are greatly influenced by the supplied winch force. Fig. 5 depicts the energy consumption per tonnage mineral versus the mining depth and the solid mineral production rate at different winch forces. Comparing Fig. 3.5 (a) to Fig. 3.5 (f), the higher winch force can be applied in a deeper depth of the DSM project with the same solid mineral production rate. Additionally, when the mining depth is small, i.e., smaller than 4000 m in Fig. 3.5 (a) and (b), with the same mining depth and the solid mineral production rate, the energy

consumption per tonnage mineral will not be influenced too much by the different winch forces. That is because when the mining depth and the solid mineral production rate are small, the used winch force and the optimal transport efficiency are similar to each other. Whereas, with the increasing of the mining depth, the CLB system with a higher winch force can obtain a higher transport efficiency to decrease the energy consumption per tonnage mineral. Therefore, in the application of the CLB system, the winch force should be selected big enough considering the technological performances and the engineering safety. Furthermore, analysing the Fig. 3.5 (a) and Fig. 3.5 (b), the energy consumption per tonnage mineral curve has a sudden increase, when the mining depth is closer to its maximum DSM depth. The dramatically decreasing of the transport efficiency and the significantly increasing of the useful energy consumption derived from the increasing mining depth lead to this phenomenon. The phenomenon is more apparent for the CLB system with a lower winch force. For instance, when the solid mineral production rate is 50 ton/h, the CLB system transport efficiencies at 100m and 4500 m are 96.86 % and 58.82 % respectively with the same solid mineral production rate, i.e., 50 ton/h, and winch force, i.e., 300 kN, see Fig. 3.5 (a).

3.4. Conclusions

In this chapter the CLB and the PLS lifting methods were compared. The conclusions derived can be summarized as follows:

Through the technological performances analysis, the mining depth and the solid mineral production rate of the PLS system have a wider application range compared with the CLB system. Furthermore, when the purpose solid mineral production rate is low, the CLB system performance is better or similar with the PLS system. Whereas, the performance of the CLB system disappears quickly with an increasing solid mineral production rate. The PLS system performs better than the CLB system, when the solid mineral production rate is larger than 800 ton/h. If the solid mineral production rate is larger than 800 ton/h, the CLB system can obtain a similar technological performance as the PLS system, only when the mining depth is small, e.g., 800 m.

Chapter 4

Profitability Analysis of Airlifting in Deep Sea Mining Systems*

Based on the literature review in chapter 2, the influencing aspects of sustainable DSM transport plan consist of the technological feasibility, economic profitability, and environmental impacts. After the analysis of technological performance of DSM transport plans in chapter 3, the economic profitability and environmental impacts research is still missing.. To evaluate the sustainability of DSM transport plans, the profitability analysis is taken into consideration in this chapter. This chapter emphasizes on the profitability analysis of airlifting in deep sea mining systems. In this chapter, section 4.1 gives an introduction of the research status of the current economic profitability analysis of DSM transport plans. Section 4.2 presents the theoretical models of airlifting momentum, airlifting energy consumption and profitability of airlifting utilized in DSM systems. In the section 4.3, the validations of the numerical calculation method and calculation results of the solid production rate, airlifting energy consumption lifting per tonnage mineral, and profitability per tonnage of mineral are analysed and discussed. Finally, in section 4.4 conclusions of the conducted research are given.

4.1. Introduction

In the DSM industry, airlifting is one of the most widely researched technologies equipped with the corresponding facilities, e.g., collecting machine (CM) (Amos and Roels, 1977). Airlifting uses compressed gas to lift the liquid-gas or solid-liquid-gas multiphase flow (Pougatch and Salcudean, 2008). It is also used in other industries, such as in chemical industry to transport toxic substances and sewage treatment plants (Kassab et al., 2007). Although the airlifting transport in DSM has been researched for a long time, until now there is no corresponding commercial scaled DSM project in progress. Technological feasibility and profitability analyses are two of the major considerations for its industrialization (Birney et al., 2006).

---

*This chapter is based on Ma et al. (2017d).

A lot of experimental and theoretical analyses of airlifting technology utilized in the DSM industry started in the 70s of last century, which was triggered by the discovery of vast amounts of manganese nodules on the seabed of depth ranging from 4000 to 6000 m (Hatta et al., 1998). Yoshinaga and Sato (1996) proposed a numerical modeling method of the airlifting pump depending on momentum equation analysis, which was validated by a vertical pipe lifting system with height of 6.74 m and diameter of 26 and 40 mm, respectively. In Yoshinaga and Sato's research, the flux rates of solid and gas are given parameters to calculate the liquid flux rate, which does not agree with the realistic working condition. Actually, the gas flux rate is the given parameter and the flux rates of solid and liquid are calculated parameters. Additionally, Yoshinaga and Sato's model is created for uniform particles size distribution. Kassab et al. (2007) innovated Yoshinaga and Sato's model by taking the relationship between the liquid and gas flux rates into consideration, which was validated by a vertical pipe lifting system with height of 3.75 m and diameter of 25.4 mm. In the numerical calculation model proposed by Yoshinaga and Sato, the compressibility of gas is neglected because of the small-scaled experiments. Hatta et al. (1998) proposed an airlifting numerical model depending on the solid-liquid mass conservation equations, two momentum equations, and an equation for the solid-liquid volumetric fractions. Additionally, Hatta et al. (1999) analyzed a special kind of pipe with an abrupt diameter enlargement. Hatta et al. (1998, 1999) utilized the multifluid method to predict the performances of airlifting pumps, which can be used to calculate the gas flux rate up to 45 m/s. However, Hatta et al. (1998, 1999) admitted that it is quite difficult to establish the transitional situation of the multiphase flow in a pipe system. Margaris and Papanikas (1997) proposed an airlifting numerical method by analyzing the fundamental conservation equations of flow continuity and momentum. Hong et al. (2005) analyzed pipe inclination effects of airlifting water pump by experiments. They investigated the airlifting performance as a function of the variation of inclination angles. Nam-Cheol et al. (2009) studied the airlifting pump with air jet nozzle analyzing its performance influenced by submerged depth, lifting head, and gas flux rate. Researches of both Hong et al. and Nam-Cheol et al. focused on the experiments and did not consider the corresponding theoretical explanation and analysis for their experimental data. Fan et al. (2013) researched airlifting pump performances utilized in an artificial upwelling. Almost all of these theoretical and experimental investigations are far away from the industrial scaled working conditions of DSM. These realistic conditions need to be considered concerning the scale effects between the up-scaled model and its industrial scaled prototype. Additionally, no research has considered all related parameters that can influence the airlifting performances in DSM projects.

Based on the literature review, airlifting technological consideration in DSM industry focuses on the transport performances influenced by the submergence ratio which is defined as the ratio between submergence and the total length of the pipe, mining depth, pipe diameter, gas flux rate, and particle diameter (Hatta, 1998&1999; Yoshinaga and Sato, 1996; Margaris and Papanikas, 1997; Hong et al., 2005; Nam-Cheol et al., 2009; Fan et al., 2013). For the technological analysis of vertical transport in DSM industry, energy consumption lifting per tonnage of mineral and solid production rate were introduced by Ma et al. (2017). These parameters will also be introduced for the technological analysis of airlifting in this chapter.

Additionally, profitability is another influencing factor for airlifting technology utilized in DSM, which is mainly reflected by a high initial capital expenditure to purchase the related facilities and high operating cost on these facilities, e.g., production support vessel (PSV), seafloor vehicles, transshipment vessels, mineral processing plants, and even the tailings treatment facilities in a later stage (Birney et al., 2006; Ma et al., 2017a). For the profitable analysis of airlifting technology utilized in DSM, profitability lifting per tonnage of mineral is researched in this chapter. The numerical calculation method used in this chapter is based on the original models of Yoshinaga and Sato, and Kassab et al., and considers the compressibility of the gas, which is important because of the large mining depth in engineering conditions. Additionally, the numerical calculation method considers the complete parameters, which consists of the submergence ratio, mining depth, pipe diameter, particle diameter, and gas flux rate.

The objective of this chapter is to assess the technological feasibility and profitability in terms of solid production rate, energy consumption per tonnage of mineral, and profitability per tonnage of mineral. The effects of submergence ratio, pipe diameter, particle diameter, mining depth, and gas flux rate are investigated. This chapter in combination with paper written by Ma et al. (2017) can be used as a reference to select a proper transport plan for DSM projects. The chapter is arranged as follows. The second section is the theoretical analysis including theoretical models of airlifting momentum, airlifting energy consumption per tonnage of minerals, and profitability of airlifting utilized in DSM systems. In the third section, the validations of the numerical calculation method and calculation results of the solid production rate, airlifting energy consumption per tonnage of minerals, and profitability per tonnage of mineral are analyzed and discussed. Finally, in section four conclusions of the conducted research are given.

4.2. Theoretical Analysis

4.2.1. Airlifting Momentum Modelling

The schematic diagram of airlifting is shown in Figure 4.1 (Yoshinaga and Sato, 1996). The airlifting pipe system consists of a solid-liquid two-phase flow happened between gas inlet and seabed, and a solid-liquid-gas three-phase flow happened between pipe outlet and gas inlet as shown in Figure 4.1. In Figure 4.1, the letters of E, I, O represent two-phase flow entrance, gas inlet, and outlet of mineral mixtures.

Figure 4.1: The schematic diagram of an airlifting system (Yoshinaga and Sato, 1996).

The momentum equation for airlifting can be written as Eq. 4.1 (Kassab et al., 2007; Yoshinaga and Sato, 1996).

$$A\left\{J_l\rho_l v_{l,E} + \sum_{i=1}^{n} J_s(i)\rho_s(i)v_{s,E}(i)\right\} - A\left\{J_{g,o}\rho_{g,o}v_{g,o} + J_l\rho_l v_l + \sum_{i=1}^{n} J_s(i)\rho_s(i)v_s(i)\right\}$$

$$-\pi D_i \int_E^I \tau_{ls}dz - \pi D_i \int_I^O \tau_3 dz - A\int_E^I \left\{\rho_l C_{l,2} + \sum_{i=1}^{n}\rho_s(i)C_{s,2}(i)\right\}gdz \qquad (4.1)$$

$$-A\int_I^O \left\{\rho_g C_{g,3} + \rho_l C_{l,3} + \sum_{i=1}^{n}\rho_s(i)C_{s,3}(i)\right\}gdz + A\left\{\rho_l g(L_2 + L_3)\right\} = 0$$

in which A is the pipe cross sectional area [m^2], J is the volumetric flux [m/s], ρ is the density [kg/m^3], v is the velocity [m/s], the subscripts of s, l, g represent solid particle, liquid, and gas respectively, τ is the shear stress [N/m^2], D_i is the pipe diameter [m], C is the volume concentration, 2, 3 represent two-phase flow and three-phase flow respectively, i represents the type of different particles.

For the solid-liquid two-phase flow, solid and liquid are regarded as incompressible. For the solid-liquid-gas three-phase flow, as density and flux rate of gas are easily influenced by surrounding pressure, Yoshinaga and Sato proposed to divide the up-riser pipe into N elements (Yoshinaga and Sato, 1996). The third term of Eq. 4.1 is written as Eq. 4.2 (Kassab et al., 2007; Yoshinaga and Sato, 1996).

$$\pi D_i \int_E^I \tau_{ls}dz = A\left\{\frac{\Delta P_{f.ls}}{\Delta z}L_2 + \Delta P_E\right\} \qquad (4.2)$$

in which $\Delta P_{f.ls} / \Delta z$ is the friction pressure gradient in solid-liquid flow [Pa/m], ΔP_E is the pressure decrease at the entrance position [Pa].

The fourth term in Eq. 4.1 can be rewritten as Eq. 4.3 (Dedegil, 1987).

$$\pi D_i \int_E^I \tau_3 dz = A \left\{ \sum_{k=1}^{N} \frac{\Delta P_{f.3}(k)}{\Delta z(k)} \Delta z(k) + \Delta P_I \right\}$$

(4.3)

in which $\Delta P_{f.3}(k) / \Delta z(k)$ is the friction pressure gradient in solid-liquid-gas flow [Pa/m], ΔP_I is the pressure decrease at the gas inlet position [Pa].

In the airlifting numerical calculation process, the velocity relationship of solid particles needs to be considered. For three-phase flow, the velocity of particles can be calculated as Eq. 4.4 (Sato and Yoshinaga, 1991).

$$v_s(i) = c \frac{m}{\rho_A} + v_{sw}(i)$$

(4.4)

in which c is the distribution coefficient, m is the mass flux of the three-phase flow $\left[\text{kg/m}^2 \cdot \text{s} \right]$, ρ_A is the apparent density of the three-phase mixture [kg/m^3], v_{sw} is the wall affected settling velocity in a three-phase flow [m/s].

For solid-liquid two-phase flow, the volume concentration of solid, liquid can be calculated through solving Eq. 4.5 (Schulte, 2013).

$$C_l^2 + \left(\frac{-v_{sl} - J_l - J_s}{v_{sl}} \right) C_l + \frac{J_l}{v_{sl}} = 0$$

(4.5)

in which v_{sl} is the slip velocity, which is related to the particle diameter, pipe diameter, settling velocity, and solid volume concentration [m/s].

The volume concentration of the gas can be calculated as Eq. 4.6 (Yoshinaga and Sato, 1996).

$$C_g = \left[1 + 0.4 \frac{\rho_g}{\rho_{ls,3}} \left(\frac{m}{\rho_g J_g} - 1 \right) + 0.6 \frac{\rho_g}{\rho_{ls,3}} \left(\frac{m}{\rho_g J_g} - 1 \right) \left\{ \frac{\frac{\rho_{ls,3}}{\rho_g} + 0.4 \left(\frac{m}{\rho_g J_g} - 1 \right)}{1 + 0.4 \left(\frac{m}{\rho_g J_g} - 1 \right)} \right\}^{0.5} \right]^{-1}$$

(4.6)

in which $\rho_{ls,3}$ is the mean density of the slurry [kg/m^3].

Compared to the original model of Yoshinaga and Sato, the significant difference of gas density and flux rate, which are caused by the large mining depth in engineering conditions, are taken into consideration, see Eq. 4.7 (Schulte, 2013).

$$\begin{cases} J_{g\_z} = \dfrac{J_{g\_0} \cdot P_0}{P_z} \\[3mm] \rho_{g\_z} = \dfrac{\rho_{g\_0} \cdot P_z}{P_0} \end{cases} \tag{4.7}$$

in which P_0 is the initial gas pressure [Pa], P_z is the gas pressure at the vertical position of z [Pa], ρ_{g_0} is the initial gas density [kg/m^3], ρ_{g_z} is the gas density at the vertical position of z [kg/m^3].

Based on Eq. 4.1 to Eq. 4.7, the airlifting process in the vertical pipe system can be calculated. After the establishment of airlifting numerical model, the next section will focus on the energy consumption calculation.

4.2.2. Energy Consumption per tonnage of mineral Modelling

The energy consumption of airlifting system is closely related to the compressor's expansion type, which is defined as an isothermal expansion in this chapter (Fan et al., 2013). The airlifting efficiency can be calculated as Eq. 4.8 (Schulte, 2013; Reinemann, 1987).

$$\eta_a = (1 - \frac{\rho_l}{\rho_s}) \frac{E_u}{E_t} \tag{4.8}$$

in which E_u is the useful energy consumption of the airlifting system [J], E_t is the total energy consumption of the airlifting system [J].

The useful energy consumption of the airlifting system is defined as the anti-gravitational energy consumption of lifting mineral solids from seabed to pipe outlet. It can be calculated as Eq. 4.9 (Schulte, 2013; Reinemann, 1987; Fan et al., 2013).

$$E_u = \rho_s \cdot A \cdot J_s \cdot g \cdot (L_2 + L_1) \tag{4.9}$$

in which L_1 and L_2 are lengths of different segments of the vertical pipe [m], see Figure 4.1.

The total energy consumption of the airlifting system is the isothermal energy consumption of the compressor. It can be calculated as Eq. 4.10 (Schulte, 2013; Reinemann, 1987; Fan et al., 2013).

$$E_t = J_{g\_atm} \cdot A \cdot ln \frac{P_I}{P_{atm}} \tag{4.10}$$

in which J_{g_atm} is the gas flux under atmospheric pressure [m/s], P_I is the pressure at the inlet [Pa], P_{atm} is the atmospheric pressure [Pa].

Additionally, the energy consumption per tonnage of minerals is also an important parameter, which can be calculated as Eq. 4.11 (Ma et al., 2017a).

$$E_{ton} = \frac{E_t}{Q_s} \qquad (4.11)$$

in which Q_s is the mineral solids production rate [ton].

4.2.3. Profitability per tonnage of mineral Modelling

The profitability analysis of airlifting utilized in DSM systems focuses on the difference between gross income and total expenditure derived from minerals. The total expenditure of an airlifting system is divided into capital expenditure (CAPEX) and operational expenditure (OPEX) (Ma et al., 2017a; Sharma, 2011).

$$M_t = M_c + M_o \qquad (4.12)$$

in which M represents the cost [$], c, o represent the initial capital expenditure and operation expenditure.

The M_c and M_0 in Eq. 4.12 can be calculated as Eq. 4. 13 (Norgate et al., 2007; Ma et al., 2017a).

$$\begin{cases} M_c = M_{c\_m} + M_{c\_t} + M_{c\_p} \\ M_o = M_{o\_m} + M_{o\_t} + M_{o\_p} \end{cases} \qquad (4.13)$$

in which m, t, p represent the mining system, transport system, and processing plant respectively. The initial capital expenditure of the mining system is spent on different kinds of seafloor vehicles.

The pipe system of airlifting technology in DSM projects consists of a major up-riser pipe and an auxiliary air-injection pipe, which is required to calculate initial capital cost of pipe systems (Ma et al., 2017a).

$$\begin{cases} n_r = \dfrac{(L_1 + L_2)}{l_{pr}} \\ n_I = \dfrac{L_1}{l_{pI}} \end{cases} \qquad (4.14)$$

in which n_r and n_I are the up-riser and air-injection pipe elements number, l_{pr} and l_{pI} are the pipe element length of the up-riser pipe and air-injection pipe respectively [m]. Therefore, the initial capital cost of the transport system can be calculated as Eq. 4.15 (Ma et al., 2017a).

$$M_{c\_t} = M_{sv} + \pi \cdot \rho_p \cdot M_{m\_p} \cdot (1 + \varepsilon_1) \cdot \left\{ l_{pr} \cdot \left(r_{r\_1}^2 - r_{r\_2}^2 \right) \cdot n_r + l_{pI} \cdot \left(r_{I\_1}^2 - r_{I\_2}^2 \right) \cdot n_I \right\} + M_{\_ot} \quad (4.15)$$

in which M_{sv} is the initial capital cost on the shipping vessel including production support vessel and trans-shipment vessels [$], M_{m_p} is the manufacturing cost of the pipeline system [$], ρ_p is the material density of the pipe [kg/m^3], ε_1 is the pipe manufacturing price factor

which means the added value of materials, r is the radius of pipelines [m], 1, 2 represent the external and internal radius of pipelines [m], $M_{\_ot}$ is the other transport cost [$].

The operation expenditure of the mining system, transport system, and processing system can be calculated as Eq. 4.16 (Ma et al., 2017a).

$$\begin{cases} M_{o\_m} = M_{m\_ma} + M_{m\_pe} \\ M_{o\_t} = M_{t\_ma} + M_{t\_pe} \\ M_{o\_p} = M_{p\_la} + M_{p\_ma} + M_{p\_pe} \end{cases} \tag{4.16}$$

in which ma, pe, and la represent the maintenance, power and energy consumption, and labor expenditures.

The M_{p_la} in Eq. 4.16 can be calculated as Eq. 4.17.

$$M_{p\_la} = \sum_{j=1}^{N} \sum_{i=1}^{n_s} W_i \cdot (1+a)^N \tag{4.17}$$

in which W_i is the salary for the staff i [$/year], n_s is the staff number, N is the mining period [year], a is the inflation rate.

The maintenance, power, and energy consumption expenditures can be calculated as Eq. 4.18.

$$\begin{cases} M_{j\_ma} = \sum_{i=1}^{N} 24 \cdot s \cdot Q_s \cdot K_{j\_k} \cdot (1+a)^N \\ M_{j\_pe} = \sum_{i=1}^{N} 24 \cdot s \cdot E_k \cdot R \cdot (1+a)^N \end{cases} \tag{4.18}$$

in which j represents the mining system, transport system, and the processing system respectively, K is the maintenance fee every year [$/ton], R is the power and energy consumption price [$/kWh], E_k is the energy consumption [kWh/h], s is the mean working days per year.

The income derived from minerals can be calculated as Eq. 4.19 (Ma et al., 2017a).

$$M_{in} = \sum_{i=1}^{N} \left(24 \cdot s \cdot Q_s \cdot M_{i,mm} \cdot (1+a)^N \right) \tag{4.19}$$

in which $M_{i,mm}$ is the mineral ore price which is set to be 95 $/ton.

The profitability per tonnage of mineral can be calculated as Eq. 4. 20 (Ma et al., 2017a).

$$M_{ton} = \frac{M_{be}}{\sum_{i=1}^{N}(24 \cdot s \cdot Q_s)} = \frac{M_{in} - M_t + M_{re}}{\sum_{i=1}^{N}(24 \cdot s \cdot Q_s)} \tag{4.20}$$

in which M_{be} is the pure benefit of DSM project [$], M_{re} is the residual value [$].

4.3. Results and Discussions

4.3.1. Validations

- Model Validated by Experimental Data of Yoshinaga and Sato

The numerical calculation model of Eq. 4.1 to Eq. 4.7 proposed by Yoshinaga and Sato (1996) is used in this section. Additionally, the experimental data found in Yoshinaga and Sato's paper can be used as the validation data. In Yoshinaga and Sato's experiment (1996), spherical and uniform particles are used, as follows: C1-Sp-06, which density and diameter are 2540 kg/m^3 and 6.1 mm respectively, C1-Sp-10, which density and diameter are 2540 kg/m^3 and 9.9 mm respectively, and C2-Sp-06, which density and diameter are 3630 kg/m^3 and 9.5 mm respectively. In Figure 4.2, nine types of airlifting conditions are shown with solid flux rate ranging from 0.014 to 0.095 m/s. Axis x represents the experimental data of liquid flux rate from 0 to 1 m/s. Axis y represents the calculation data of liquid flux rate from 0 to 1 m/s. The closer the data points are to the diagonal, the more accurate the calculation results. The majority of data points are located in the area within 10% deviation of the diagonal, which indicates that the model is sufficiently accurate.
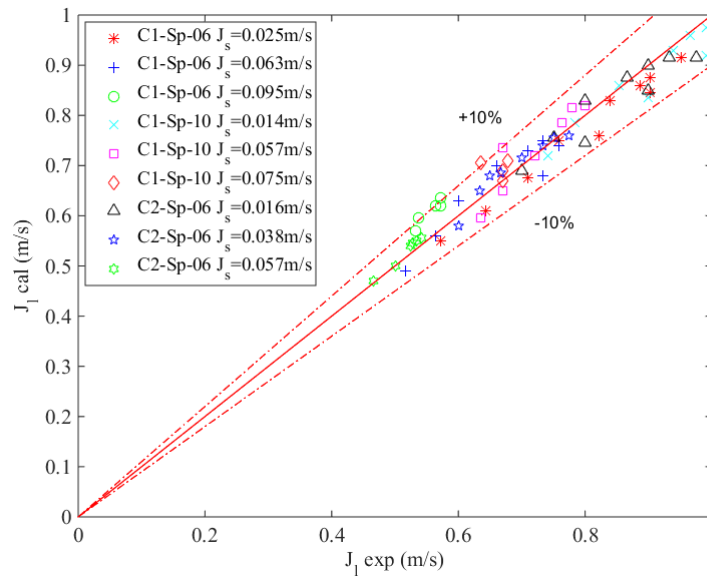
Figure 4.2: Validation results by experimental data from Yoshinaga and Sato.

- Model Validated by Experimental Data of Kassab et al.

In Yoshinaga and Sato's model of simulating a solid-liquid-gas airlifting system, the flux rates of gas and solid are designated as a pair of original values. Then based on momentum balance equation, the flux rate of liquid is determined (Yoshinaga and Sato, 1996). Kassab et al. (2007) utilize the Stenning and Martin equation, see Eq. 4.21, combining with momentum method to solve the flux rates of solid and liquid directly from gas flux rate (Stenning and Martin, 1968).

$$\frac{L_3}{L_1} - \frac{1}{1+\left(V_g / (s_l \cdot V_l)\right)} = \frac{J_l^2}{2g \cdot L_1}\left[\left(K_c+1\right)+\left(K_c+2\right)\frac{V_g}{V_l}\right] \tag{4.21}$$

in which V_g, V_l are the volume flow rate of gas and liquid [m^3/s], s_l is the slip factor, K_c is the friction factor.

The s_l in Eq. 4.21 can be calculated with Eq. 4.22 (Griffith, 1964).

$$s_l = 1.2 + 0.2\frac{V_g}{V_l} + \frac{0.35 \cdot \sqrt{g \cdot D_i}}{J_l} \tag{4.22}$$

The K_c in Eq. 4.21 can be calculated with Eq. 4.23 (Stenning and Martin, 1968).

$$K_c = \frac{4 \cdot f \cdot L_1}{D_i} \tag{4.23}$$

in which f is the friction coefficient calculated by Colebrook-White equation, which can be calculated as Eq. 4. 24 (Navarro et al., 2017).

$$f = 0.25 \cdot \left[log\left(\frac{\varepsilon / D_i}{3.7} + \frac{5.74}{Re^{0.9}}\right)\right]^{-2} \tag{4.24}$$

in which ε is the pipe wall roughness [m], Re is the liquid Reynolds number.

Based on Eq. 4.21 to Eq. 4.24, the innovated numerical method of airlifting by Kassab et al. is validated in Figure 4.3. Kassab et al. investigated airlifting performances influenced by submergence ratio and particle diameter (Kassab et al., 2007). In Figure 4.3, particle diameters of 4.75, 7.10, and 9.50 mm, and submergence ratio of 0.50, 0.72, and 0.78, are calculated. Alike the validation principle described in Figure 4.2, the closer the data points to the diagonal, the more accurate the calculation results are. As most of data points are located in the area within 10% deviation of the diagonal, the calculation system used in this chapter is sufficiently accurate.
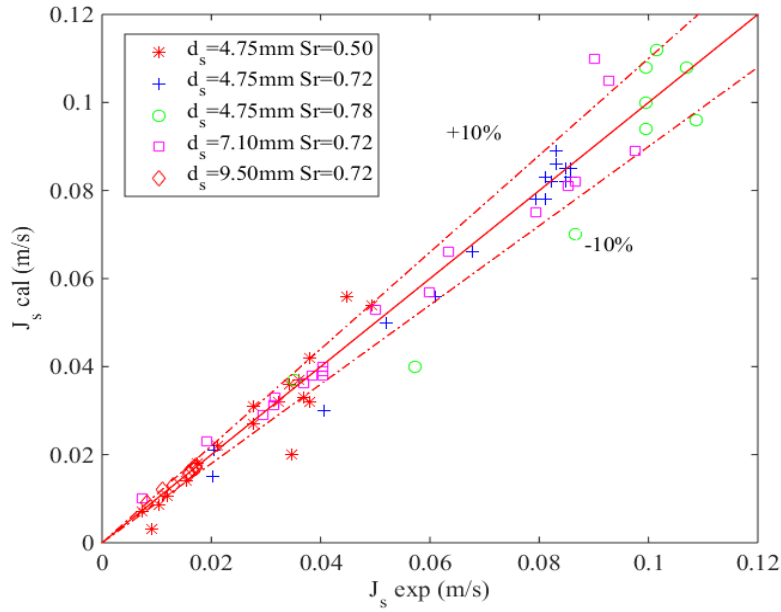
Figure 4.3: Validation results by experimental data from Kassab et al.

- Scale Effect

Scale effect arises due to differences between an up-scaled model and its industrial scaled prototype, which leads to some deviations between the simulation results (Heller, 2011). The scale ratio between the general up-scaled model and industrial scaled prototype of airlifting model in DSM projects can be up to 500~600, which is much larger than that in normal mechanical and hydraulic simulations (Kassab et al., 2007; Yoshinaga and Sato, 1996; Hoagland et al., 2010). Additionally, most parameters of the experimental and theoretical airlifting modeling researches are smaller than the industrial scaled airlifting parameters in DSM projects (Kassab et al., 2007; Yoshinaga and Sato, 1996). The most frequently used method to compensate scale effect is to distort model geometry by giving up exact geometric similarities or change the related parameter appropriately, e.g., model roughness (Heller, 2011). In this section, flow regime conditions both in the experiments of Yoshinaga and Sato and Kassab et al., and the following large-scale calculation case are taken into consideration. Because of the lack of theoretical research on solid-liquid-gas three-phase flow regimes in a vertical pipe system, the flow regime of gas-liquid flow in a vertical pipe system is used. In the airlifting vertical pipe system, there exist five different type flow regimes including bubble, slug, froth, annular, and finely dispersed bubbles depending on the velocity and geometry of the lifting components (Schulte, 2013; Taitel et al., 1980). This thought has already been used by the other researchers in the DSM field (Doyle and Halkyard, 2007). The flow regime transitions are calculated as Eq. 4.25-4.29 (Schulte, 2013; Taitel et al., 1980).

$$J_l = 3.0 \cdot J_g - 1.15 \cdot \left[\sigma \cdot g \cdot \left(\rho_l - \rho_g \right) / \rho_l^2 \right]^{0.25} \tag{4.25}$$

$$J_l + J_g = 4.0 \cdot \left\{ \left[D_i^{0.429} \cdot \left(\frac{\sigma}{\rho_l} \right)^{0.089} / J_l^{0.072} \right] \cdot \left[g \cdot \left(\rho_l - \rho_g \right) / \rho_l \right]^{0.446} \right\} \tag{4.26}$$

$$J_g = J_l \tag{4.27}$$

$$J_g = -J_l + \alpha_{sf} \cdot \sqrt{g \cdot D_i} \tag{4.28}$$

$$J_g \cdot \rho_g^{0.5} = 3.1 \cdot \left[\sigma \cdot g \cdot \left(\rho_l - \rho_g \right) \right]^{0.25} \tag{4.29}$$

in which σ is the surface tension of the liquid [N/m^2], α_{sf} is a factor which is influenced by the airlifting geometries. Eq. 4. 25 depicts the regime transition from bubble to slug flow. The following Eq. 4. 26 - 4.29 are corresponding to bubbly to dispersed bubbly flow, froth to dispersed bubbly flow, slug to froth flow, and froth to annular flow. Figure 4.4 depicts the calculation results of the flow regime.
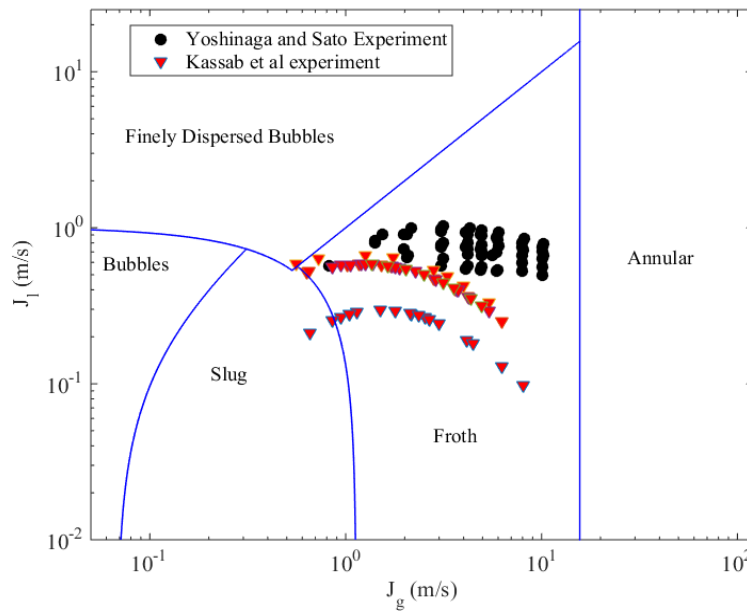
Figure 4.4: Flow regime figure combining the experimental results of Yoshinaga and Sato (1996) and Kassab et al. (2007).

Analyzing Figure 4.4, most of the flow regimes in Yoshinaga and Sato, and Kassab's experiments are froth flows, which is limited by the small-scaled gas flux rate. However, for the case studies in this chapter, as the gas flux rates change from 30 to 180 m/s, all the flow regimes in the following calculation system are annular flows. Therefore, besides the scale effects between the up-scaled model and an industrial scaled prototype of airlifting model, flow pattern differences between the experimental tests and the industrial working conditions should also be taken into consideration in the future. Additionally, the larger gas flux rate would also lead to a fast moving velocity of solid mineral ores, which might be a security risk and has a great influence on the abrasion of transport pipelines.

4.3.2. Solid Production Rate Analysis

Solid production rate is an important parameter in DSM, which determines the gross income directly; see Eq. 4.19. In this section, the relationships between solid production rate and

submergence ratio, mining depth, pipe diameter, particle diameter, and gas flux rate are researched. The parameter changing ranges of airlifting in DSM systems are given as Table 4. 1.

Table 4.1: The parameters of the airlifting system in DSM.

Parameters	S_r (-)	d_s (mm)	D_i (m)	Jg (m/s)	H (m)
Range	0.985–1.000	1.0–50.0	0.25–0.40	30–180	500–6000

Figure 4. 5 depicts the relationship between the solid production rate and submergence ratio at different mining depth and gas flux rate with pipe diameter of 0.40 m and particle diameter of 5.0 mm. Analyzing Figure 4. 5a to Figure 4. 5d, it is obvious that with the same gas flux rate the solid production rate of airlifting decreases with the increase of mining depth on the whole. Additionally, when the submergence ratio is set to be 1.000, 0.995, 0.990, and 0.985 respectively, there are not so many differences between these calculating conditions. Although with a small changing amplitude, by analyzing the data, it proves that larger submergence ratio may also represent larger solid production rate with the same gas flux rate. It can be explained as that a larger submergence ratio also means lifting a relative smaller vertical distance when the mining depth is the same. Therefore, an airlifting system can lift more minerals with a larger submergence ratio. As submergence ratio is an important parameter in airlifting system, the calculation here is conducted to have an insight of its influencing on industrial scaled DSM working conditions. However, taking into account the actual working conditions, the values of submergence ratio should not be too small, which range from 0.985 to 1.000. Furthermore, when the mining depth is set the same, a larger gas flux rate may not produce a larger solid production rate. For instance, in Figure 4. 5a when the mining depth is 500 and 1000 m respectively, the airlifting system with gas flux rate of 70 m/s and 90 m/s transports the maximum minerals of 497.9 and 428.0 ton/h respectively. However, a larger gas flux rate may always represent a larger range of applicable mining depth. For instance, in Figure 4. 5c, the maximum applicable mining depths of gas flux rate of 30, 50, 90 and 150 m/s are 1000, 2000, 3500 and 4500 m respectively. For the airlifting system with gas flux rate of 180 m/s at mining depth of 1000 m, there is a sudden decrease of solid production rate. It could be explained as that solid production rate is influenced by both the increased airlifting efficiency and the mining depth which have the conflict effect on the performances of airlifting system.
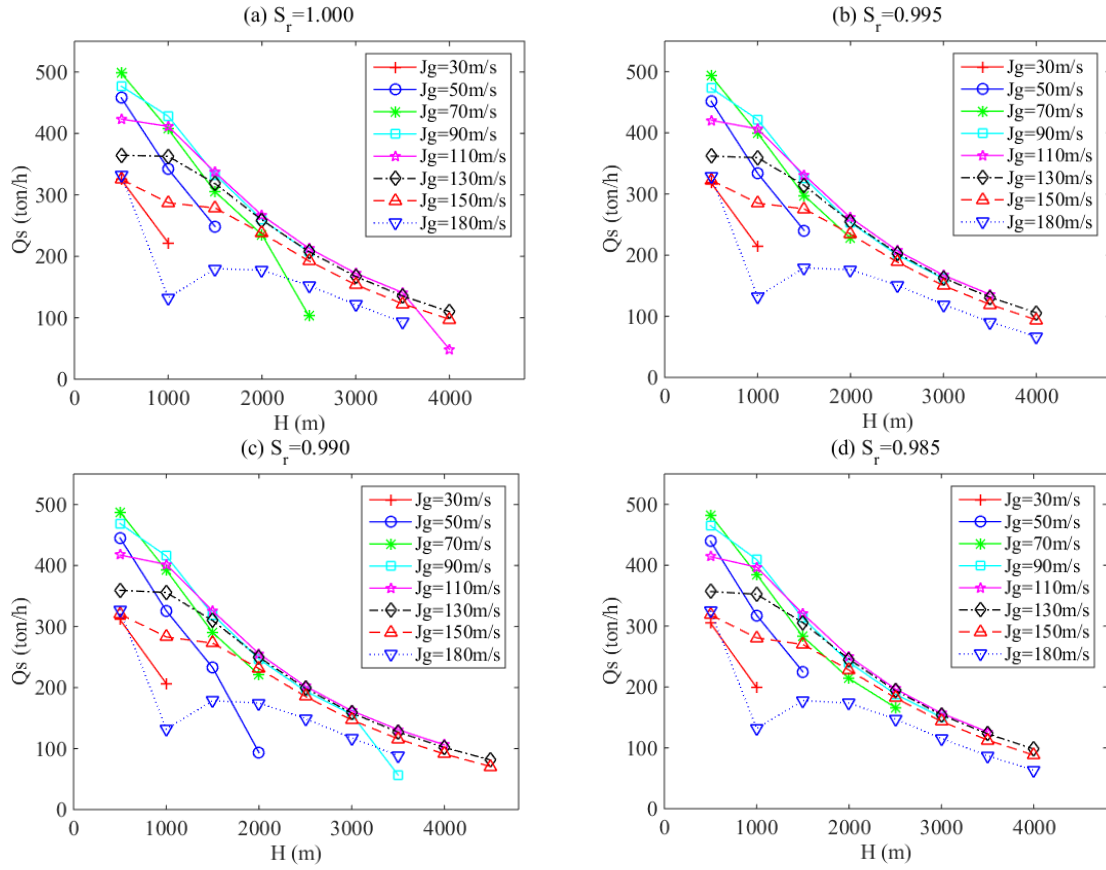
Figure 4.5: Figure of solid production rate Qs influenced by submergence ratio S_r at different mining depth H and gas flux rate Jg. The submergence ratio of figure 4. 5 (a), (b), (c), (d) are 1.000, 0.995, 0.990, 0.985 respectively.

Figure 4. 6 depicts the relationship between the solid production rate and pipe diameter at different mining depths and gas flux rate with the submergence ratio of 0.990 and particle diameter of 5.0 mm. Analyzing Figure 4. 6a to Figure 4. 6d, a larger pipe diameter can increase the solid production rate significantly. For instance, when the mining depth is 500 m and gas flux rate is 70 m/s, the solid production rate is 487.6 ton/h in Figure 4. 6a with a pipe diameter of 0.40 m and 143.8 ton/h in Figure 4. 6d with a pipe diameter of 0.25 m. Additionally, a larger pipe diameter may also represent a larger applicable mining depth with the same gas flux rate which means the pipe diameter plays as a bottleneck to the solid production rate and the applicable mining depth. For instance, considering solid production rate more than 50 ton/h and gas flux rate of 150 m/s, the maximum mining depth of airlifting system with a pipe diameter of 0.40 m is 4500 m, see Figure 4. 6a, which is much larger than 2500 m of an airlifting system with a pipe diameter of 0.30 m, see Figure 4. 6c. Furthermore, analyzing Figure 4. 6d, the airlifting system with gas flux rate of 180 m/s produces the largest solid production rate at the mining depth of 500 m. However, with the increase of pipe diameter, the airlifting system with gas flux rate of 70 m/s produces the largest solid production rate. It means that, for a special working condition of an airlifting system, the maximum solid production rate is determined by the mining depth, gas flux rate, and pipe diameter together.

Figure 4.6: Figure of solid production rate Qs influenced by pipe diameter D_i at different mining depth H and gas flux rate Jg. The pipe diameter of figure 4. 6 (a), (b), (c), (d) are 0.40m, 0.35m, 0.30m, 0.25m respectively.

Figure 4. 7 depicts the relationship between the solid production rate and particle diameter at different mining depth and gas flux rate with the submergence ratio of 0.990 and pipe diameter of 0.30 m. Analyzing Figure 4. 7a to Figure 4. 7d, airlifting small particles has a higher solid production rate comparing to the large particles as expected. For instance, in Figure 4. 7a, the solid production rate is 223.5 ton/h when the mining depth is 500 m and gas flux rate is 50 m/s. However, in Figure 4. 7d, with the same mining depth and gas flux rate, the solid production rate is only 148.8 ton/h, which means lifting small particles is much easier than lifting large particles. The significant difference may be because the drag forces and pressure losses of large particles in the transport process are larger than that of the small particles (Kassab et al., 2007; Kato et al., 1975). Additionally, the airlifting system with gas flux rate of 180 m/s is only applicable at the depth of 500 m when the pipe diameter is 0.30 m. It can be explained as that pipe diameter plays as a more significant bottleneck to the solid production rate comparing with the particle diameter, see Figures 4. 6c and 4. 7. Furthermore, there are different degrees of reductions of solid production rate at the mining depth of 500 m lifting 30 mm particles, see Figure 4. 7d, it means that the particle diameter plays as a bottleneck to the solid production rate when the gas flux rate is smaller than 130 m/s comparing with the airlifting system transport particles of 5 mm, see Figure 4. 7a.
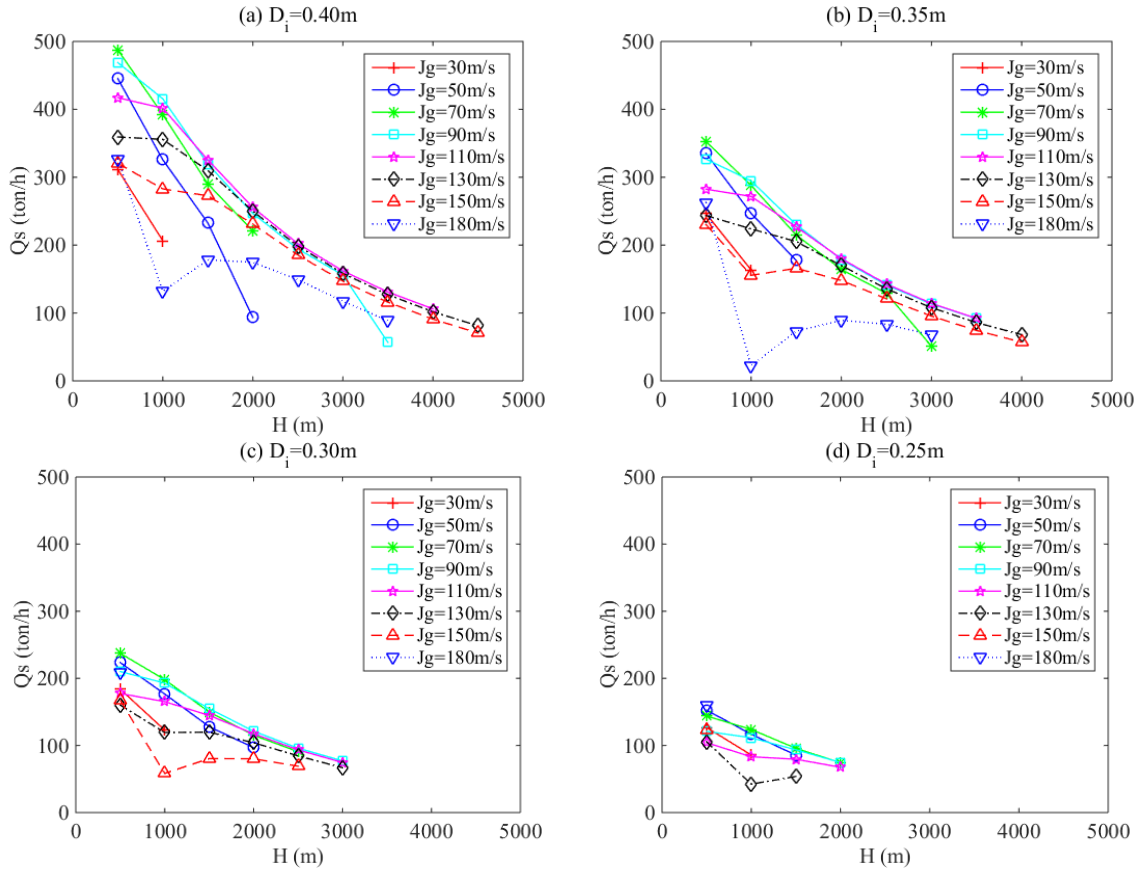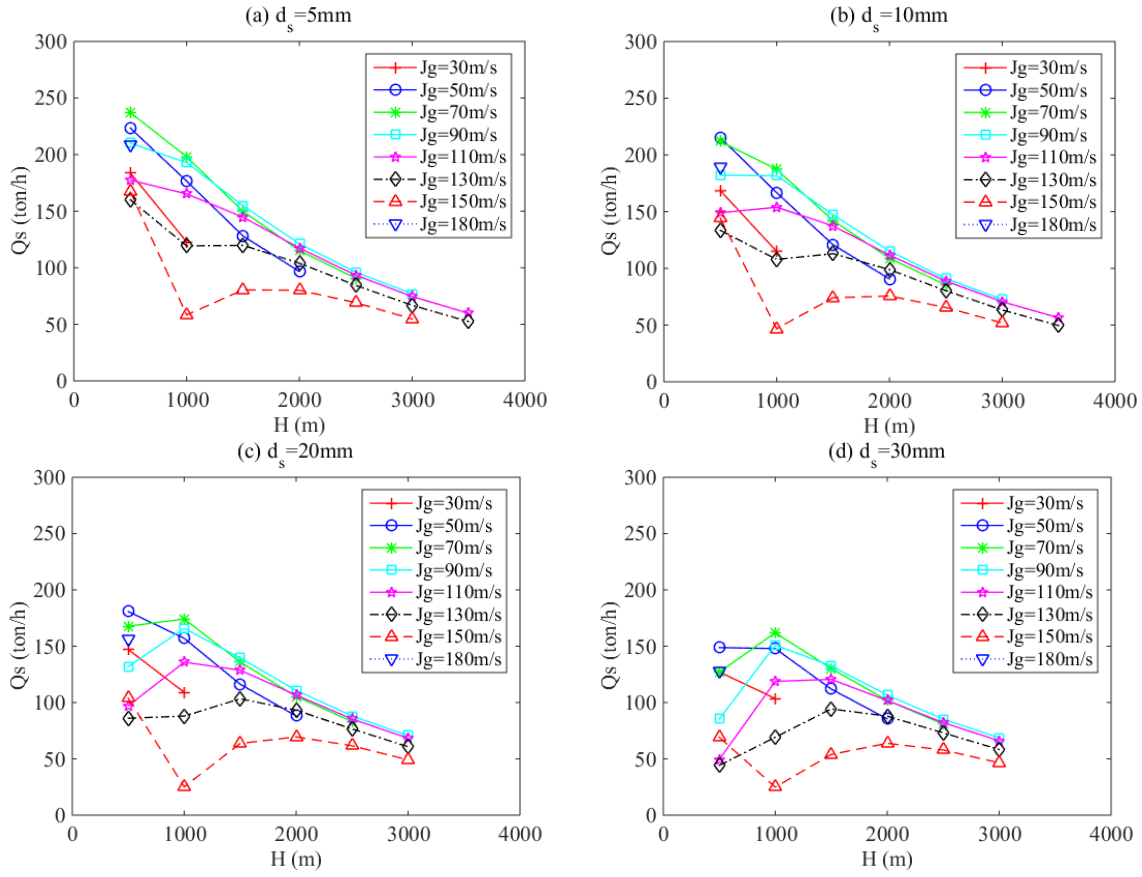
Figure 4.7: Figure of solid production rate Qs influenced by particle diameter d_s at different mining depth H and gas flux rate Jg. The particle diameter of figure 4.7 (a), (b), (c), (d) are 5mm, 10mm, 20mm, 30mm respectively.

4.3.3. Energy Consumption per tonnage of minerals Analysis

Only considering the total solid production rate is not enough to obtain an optimal transport plan, energy consumption per tonnage of mineral is also an important parameter which can influence the stakeholder's final decision. In this section, the relationships between energy consumption per tonnage of mineral and submergence ratio, pipe diameter, mining depth, particle diameter, and gas flux rate are presented.

Figure 4.8 depicts the relationship between the energy consumption per tonnage of mineral and submergence ratio at different mining depth and gas flux rate with pipe diameter of 0.40 m and particle diameter of 5.0 mm. Analyzing Figure 4.8a to Figure 4.8d, it is obvious that the energy consumption per tonnage of mineral increases with the increase of mining depth. Although airlifting efficiency increases with the mining depth (Schulte, 2013), it is notable that the higher efficiency cannot guarantee lower energy consumption per tonnage of mineral. In other words, airlifting with the same gas flux rate used on smaller mining depth has a better performance with a larger solid production rate and smaller energy consumption per tonnage of minerals. Additionally, as the values of submergence ratio is set within a small changing range from 0.985 to 1.000, there are not so many significant differences among Figure 4.8a to Figure 4.8d, which is also consistent with the results in Figure 4.5. By analyzing the data in

Figure 4.8, it is proved that larger submergence ratio may also represent slightly smaller energy consumption per tonnage of mineral. For instance, when the gas flux rate is 180 m/s and mining depth is 4000 m, the energy consumption per tonnage of mineral with the submergence ratio of 1.000 is 190.4 kWh/ton, see Figure 4.8a, which is smaller than that of 208.1 kWh/ton with the submergence ratio of 0.985, see Figure 4.8d. It can be explained as that a larger submergence ratio means a smaller lifting depth when the total mining depth is the same. Furthermore, compared to the airlifting system with gas flux rate smaller than 150 m/s, the airlifting system with gas flux rate of 180 m/s consumes much more energy consumption per tonnage of mineral. It means the flux rate of 180 m/s is too much large for the airlifting system with pipe diameter of 0.40 m and particle diameter of 5 mm.

Figure 4.8. Figure of energy consumption per tonnage of mineral *Eton* influenced by submergence ratio S_r at different mining depth H and gas flux rate Jg. The submergence ratio of figure 4.8 (a), (b), (c), (d) are 1.000, 0.995, 0.990, 0.985 respectively.

Figure 4.9 depicts the relationship between the energy consumption per tonnage of mineral and pipe diameter at different mining depth and gas flux rate with the submergence ratio of 0.990 and particle diameter of 5.0 mm. Analyzing Figure 4.9a to Figure 4.9d, it is notable that airlifting with a larger pipe diameter can be used for a deeper mining depth. For instance, when the gas flux rate is 150 m/s, the maximum airlifting depth with a 0.40 m pipe diameter is 4500 m, see Figure 4.9a, and 2500 m with a 0.30 m pipe diameter; see Figure 4.9c. This is because when the gas flux rate is large enough, pipe diameter has become the bottleneck of the airlifting applicable depth. For airlifting system with gas flux rate of 180 m/s, its energy

consumption lifting per tonnage of mineral is much larger than the airlifting system with smaller gas flux rate, see Figure 4.9a,b. Additionally, the curve of energy consumption per tonnage of mineral changing with the mining depth is also significantly different with the other changing curves. It may be caused by the complicated interactions between the airlifting efficiency and the mining depth. An airlifting system with too much large gas flux rate could represent a large percentage of energy waste. Furthermore, as the models mentioned in this chapter are validated by the small scaled mechanism with a lower gas flux rate, the model may be not applicable to the too much large gas flux rate completely. Comparing Figure 4.9a to Figure 4.9d, the airlifting system with gas flux rate of 30 m/s consumes the minimum energy consumption per tonnage of mineral. Therefore, the airlifting performance in terms of energy consumption per tonnage of mineral, see Figure 4.9, is not completely consistent with that in terms of solid production rate, see Figure 4.6.
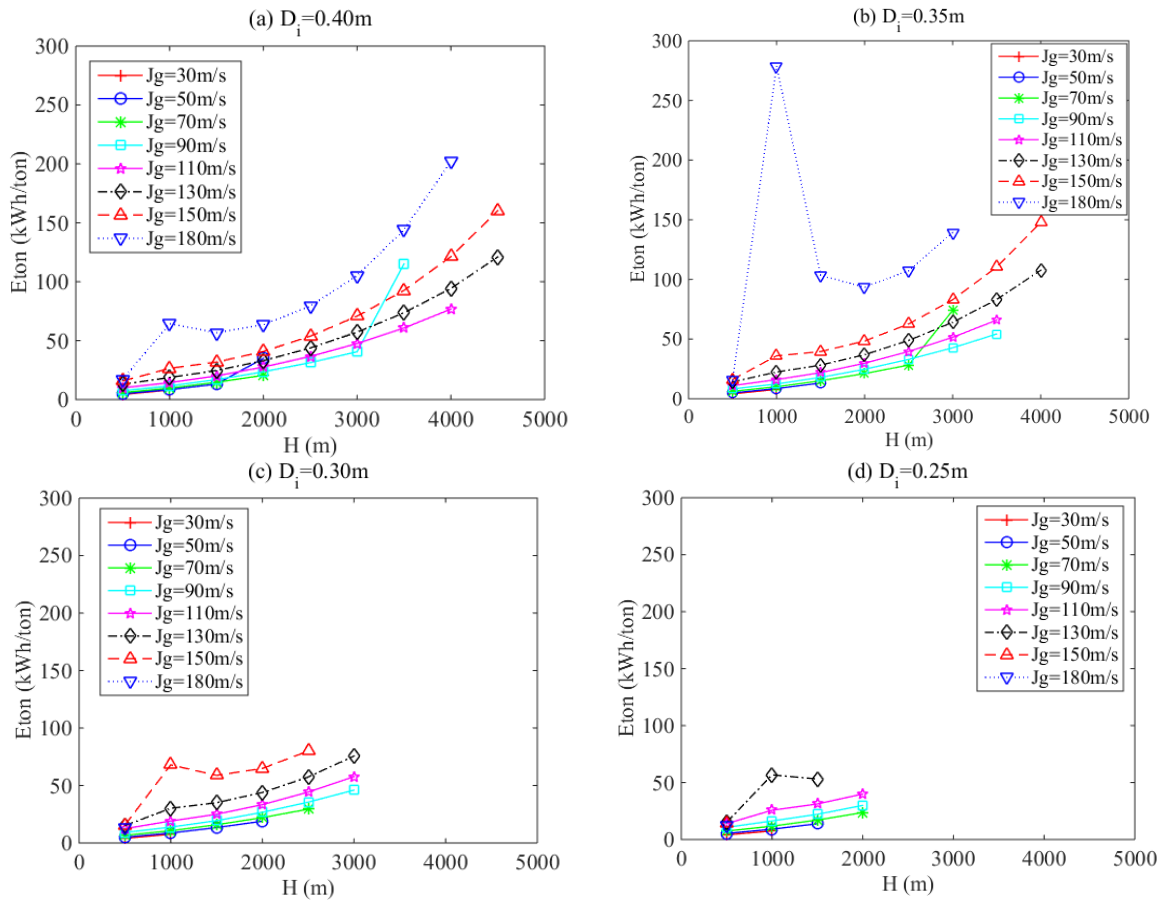
Figure 4.9: Figure of energy consumption per tonnage of mineral *Eton* influenced by pipe diameter D_i at different mining depth H and gas flux rate *Jg*. The pipe diameter of figure 4.9 (a), (b), (c), (d) are 0.40m, 0.35m, 0.30m, 0.25m respectively.

Figure 4.10 depicts the relationship between the energy consumption per tonnage of mineral and particle diameter at different mining depth and gas flux rate with the submergence ratio of 0.900 and pipe diameter of 0.30 m. Analyzing Figure 4.10a to Figure 4.10d, the curves of airlifting system with gas flux rate of 30, 50, 70 and 90 m/s are concentrated with the similar curve changing trend which are divergent when the gas flux rate is larger than 110 m/s.

Additionally, the airlifting system transporting of small particles has a more concentrated and consistent curve changing trend. It means particle diameter may play as a significant bottleneck to the energy consumption per tonnage of mineral for large gas flux rate. It maybe also represent that the model utilized in this chapter may be more suitable for fine particles and small gas flux rate which may also be used to explain the sudden increase of energy consumption per tonnage of mineral of gas flux rate at 150 m/s. Obviously, with the increase of mining depth, the energy consumption per tonnage of mineral is also increasing. Comparing Figures 4.7 and 4.10, it is shown that the airlifting system with gas flux rate of 150 m/s produces the minimum solid production rate and consumes the maximum energy consumption per tonnage of mineral. It means the gas flux rate of 150 m/s is not suitable to select as the airlifting parameter under the calculated working conditions.
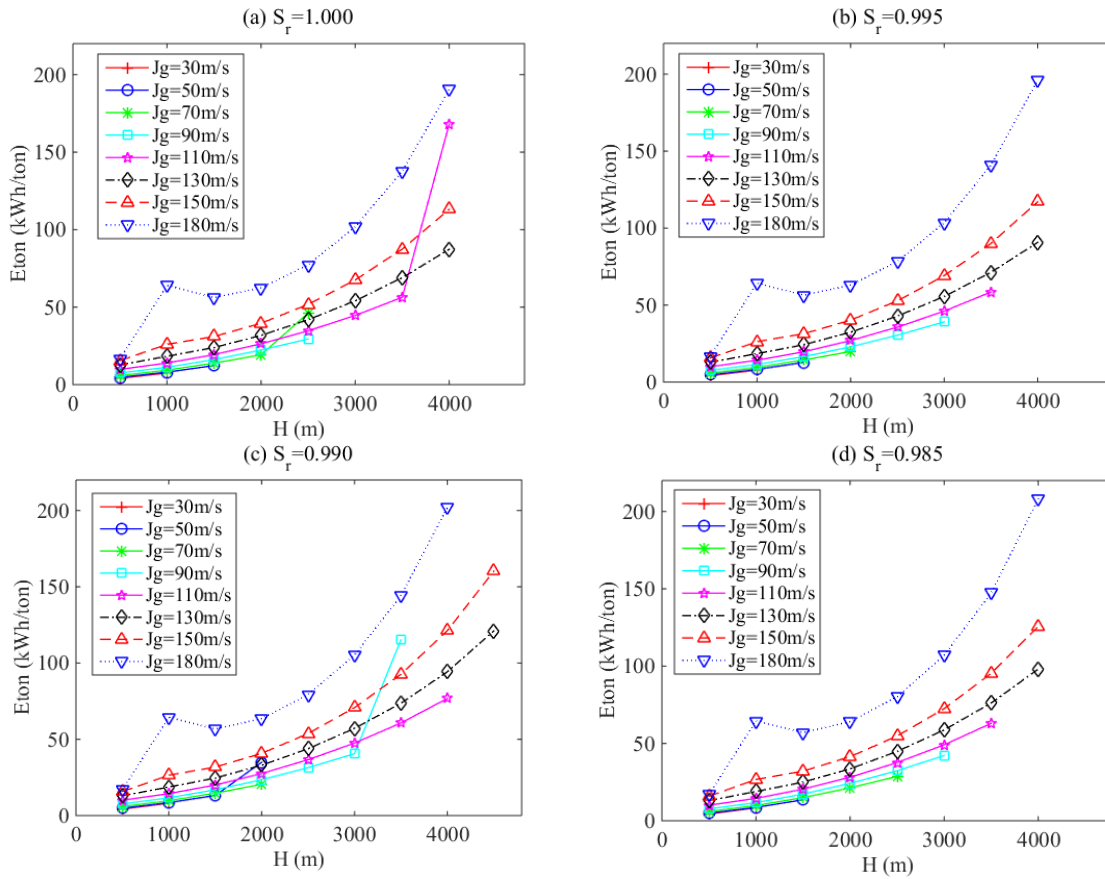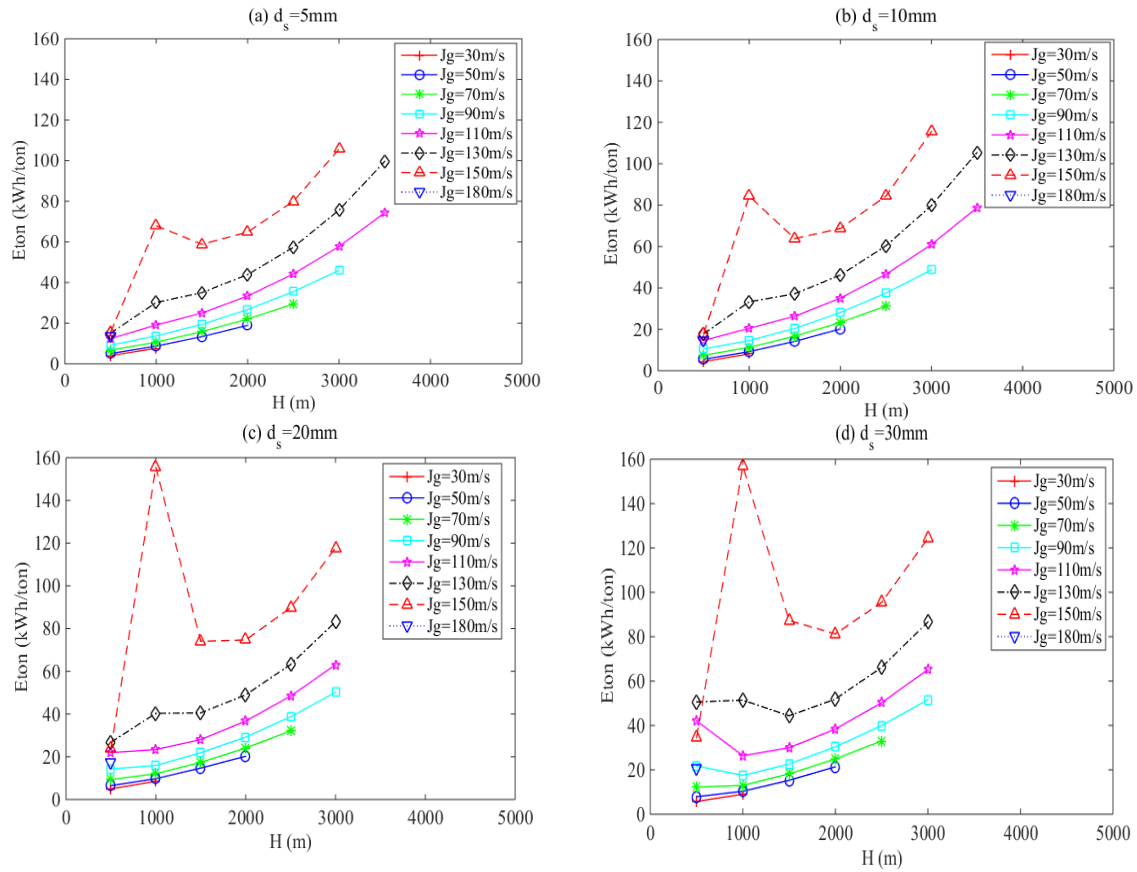

Figure 4.10: Figure of energy consumption per tonnage of mineral *Eton* influenced by particle diameter d_s at different mining depth H and gas flux rate Jg. The particle diameter of figure 4.10 (a), (b), (c), (d) are 5mm, 10mm, 20mm, 30mm respectively.

4.3.4. Profitability per tonnage of mineral Analysis

The given parameters to calculate the profitability per tonnage of mineral are shown in Table 4.2 (Sharma, 2011; Ma et al., 2017a). Profitability per tonnage of mineral is also an important parameter to determine an optimal transport plan of DSM projects. In this section, the relationships between profitability per tonnage of mineral and submergence ratio, pipe diameter, mining depth, particle diameter, and gas flux rate are researched.

Table 4.2: The Calculation Parameters Used for the Economic Comparison Partially Based on References (Ma et al., 2017a; Sharma, 2011).

Parameters	Value	Parameters	Value	Parameters	Value
ε_1 (-)	30	M_{sv} ($10^6 \cdot \$$)	495	M_{c_p} ($10^6 \cdot \$$)	750
W_i ($10^6 \cdot \$$/year)	0.45	R ($\$$/kWh)	0.2	a (-)	4.28%
K_{m_k} ($\$$/ton)	1.2	K_{t_k} ($\$$/ton)	1.2	K_{p_k} ($\$$/ton)	0.8
s (day)	300	N (year)	20	$M_{\_ot}$ ($10^6 \cdot \$$)	35

Figure 4.11 depicts the relationship between the profitability per tonnage of mineral and submergence ratio at different mining depth and gas flux rate with pipe diameter of 0.40 m and particle diameter of 5.0 mm. Although there is not a big scale difference among Figure 11a to Figure 11b, by analyzing the data in Figure 4.11, the airlifting system with a larger submergence ratio has a slightly better performance than that with a smaller submergence ratio in terms of the profitability per tonnage of mineral. This is also correct in terms of the minerals solid production rate; see Figure 4.5, and energy consumption per tonnage of mineral, see Figure 4.8. It is obvious that lifting minerals from a smaller mining depth have a significantly better performance of airlifting systems in terms of profitability lifting per tonnage of mineral. Additionally, only when the mining depth is less than roughly 2500 m, DSM projects can be profitable, or it will lose money. It means that the applicable mining depth range of airlifting technology utilized in DSM systems is limited. For instance, when the submergence ratio is 0.985, see Figure 11d, the DSM system with airlifting mining depth of 3000 m is not profitable at all. Comparing Figures 4.5, 4.8, and 4.11, the solid production rate decreases with the mining depth increase which may also lead to a significant decrease of profitability per tonnage of mineral. Additionally, when airlifting approaches its maximum applicable depth, there may be a sudden decrease of profitability lifting per tonnage of mineral, e.g., the airlifting system with gas flux rate of 50 m/s and submergence ratio of 0.990, see Figure 4.11c, which is also manifested on the sudden decrease of solid production rate, see Figure 4.5, and sudden increase of energy consumption per tonnage of mineral, see Figure 4.8.

Figure 4.11. Figure of profitability per tonnage of mineral *Mton* influenced by submergence ratio S_r at different mining depth H and gas flux rate Jg. The submergence ratio of figure 4.11 (a), (b), (c), (d) are 1.000, 0.995, 0.990, 0.985 respectively.

Figure 4.12 depicts the relationship between the profitability per tonnage of mineral and pipe diameter at different mining depth and gas flux rate with the submergence ratio of 0.990 and particle diameter of 5.0 mm. Comparing Figure 4.12a to Figure 4.12d, it can be concluded that airlifting system with a larger pipe diameter, e.g., 0.40 m, has a better performance than that with a small pipe diameter, e.g., 0.25 m, in terms of the profitability per tonnage of mineral. For instance, when the mining depth is 500 m and gas flux rate is 180 m, the profitability of airlifting system with 0.40 m pipe diameter is 95.2 $/ton which is much larger than 16.8 $/ton of airlifting system with 0.25 m pipe diameter. Additionally, analyzing Figure 4. 12a to Figure 4. 12d, neither the largest, nor the smallest gas flux rate generates the maximum profitability per tonnage of mineral. It is because for each set of mining depth and pipe diameter, there exists an optimal gas flux rate to obtain the maximum profitability per tonnage of mineral. Furthermore, comparing the airlifting performances in Figure 4.12a, d, it is notable that airlifting system is more suitable working with a large pipe diameter in terms of profitability lifting per tonnage of mineral, which is also consistent with the results of solid production rate, see Figure 4. 6, and energy consumption per tonnage of mineral, see Figure 4. 9. It is because the pipe diameter has become a bottleneck to the performances of airlifting system in Figure 4. 12.
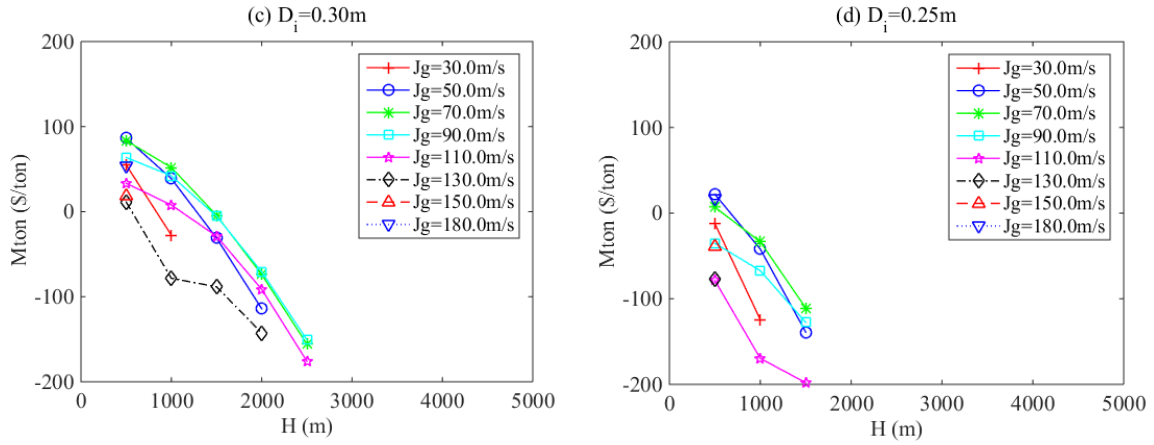
Figure 4. 12: Figure of profitability per tonnage of mineral *Mton* influenced by pipe diameter D_i at different mining depth H and gas flux rate Jg. The pipe diameter of figure 4. 12 (a), (b), (c), (d) are 0.40m, 0.35m, 0.30m, 0.25m respectively.
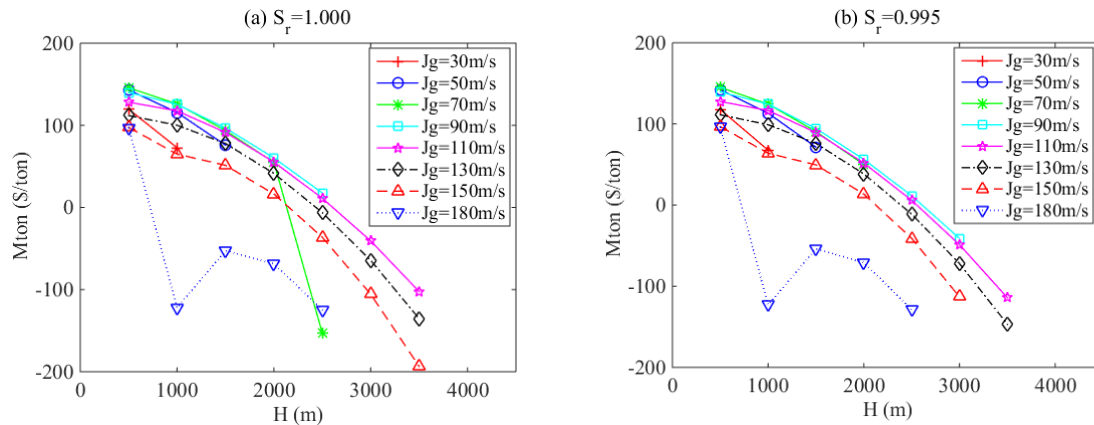
Figure 4. 13 depicts the relationship between the profitability per tonnage of mineral and particle diameter at different mining depth and gas flux rate with the submergence ratio of 0.990 and pipe diameter of 0.30 m. Analyzing Figure 4. 13a to Figure 4. 13d, it is notable that lifting small particles has a better performance than large particles, which is almost correct in terms of total solid production rate, see Figure 4. 7, and energy consumption per tonnage of mineral, see Figure 4. 10. Additionally, when the particles diameter is small, e.g., 5 mm, airlifting system working at a small mining depth has a better performance than at a larger depth, which is caused by the significant increase of anti-gravitational energy consumption. In Figure 4. 13c,d, for the airlifting system with gas flux rate of 70, 90, and 110 m/s, there is a profitability decrease at the mining depth of 500 m. It can be explained as that the profitability lifting per tonnage of mineral is influenced by the mining depth, particle diameter and gas flux rate together. The particle diameter plays as a bottleneck to the airlifting performances in Figure 4. 13c,d.
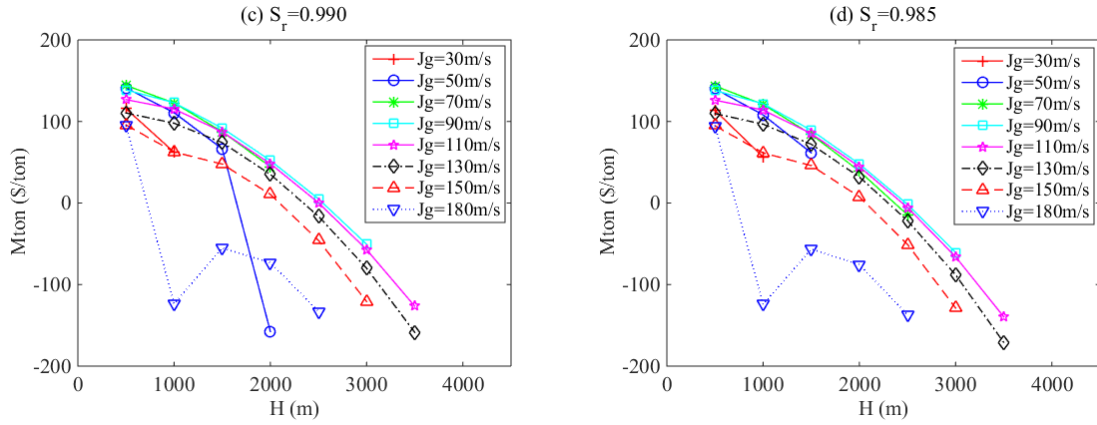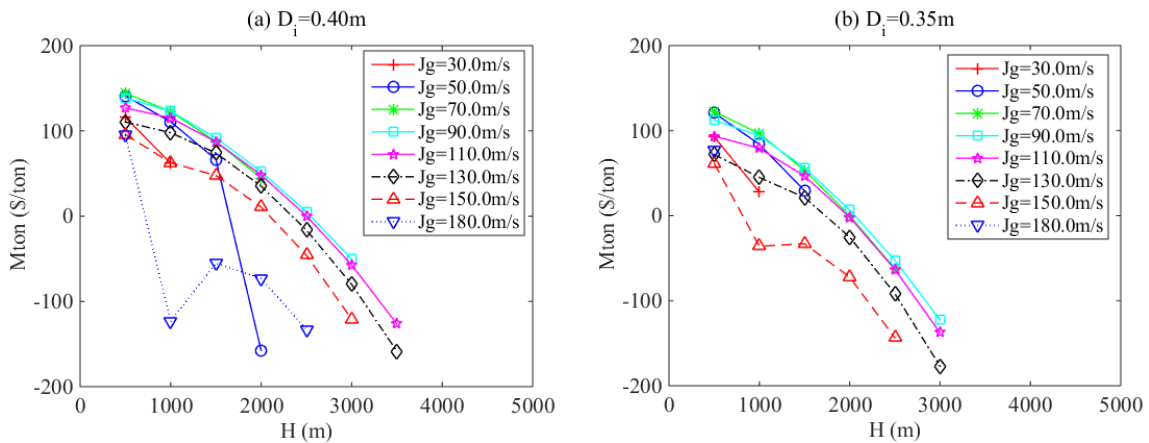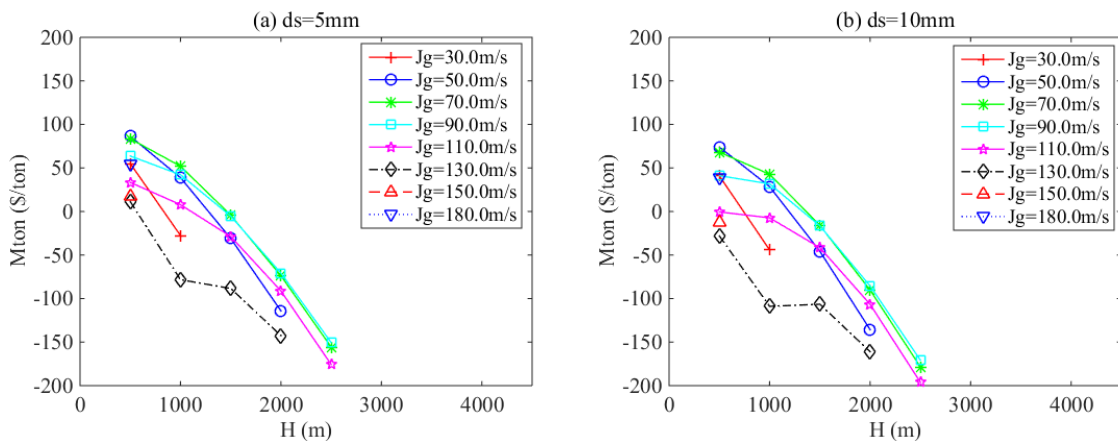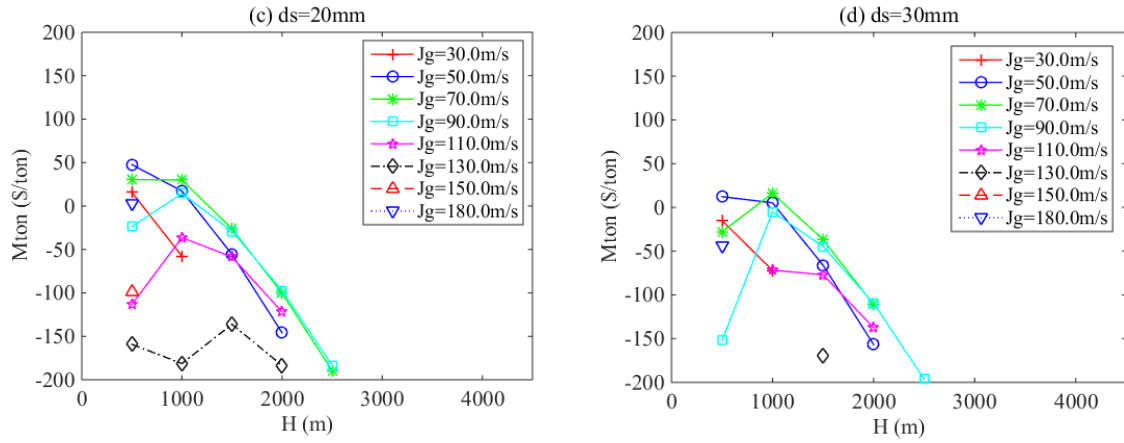
Figure 4.13: Figure of profitability per tonnage of mineral *Mton* influenced by particle diameter d_s at different mining depth H and gas flux rate Jg. The particle diameter of figure 4.13 (a), (b), (c), (d) are 5mm, 10mm, 20mm, 30mm respectively.

4.4. Conclusions

The research in this chapter focuses on technological feasibility and profitability analyses of DSM projects utilizing airlifting technology. The conclusions are as follows:

- The numerical calculation method considers the compressibility of the gas, which is caused by the large mining depth in engineering conditions, on the basis of the original models of Yoshinaga and Sato, and Kassab et al. Additionally, the numerical calculation method considers complete set of parameters, which consists of the submergence ratio, mining depth, pipe diameter, particle diameter, and gas flux rate.

- A higher submergence ratio of airlifting system in DSM projects has slightly better performances than that with a smaller one in terms of the solid production rate, energy consumption per tonnage of mineral, and the profitability per tonnage of mineral.

- Large pipe diameter can increase the solid production rate significantly; see Figure 6. Analysing Figure 9a to Figure 9d, it is notable that airlifting with a larger pipe diameter can be used for a deeper mining depth. Additionally, when airlifting approaches its maximum applicable depth, there may exist a sudden increase of energy consumption per tonnage of mineral, see Figure 9, and a sudden decrease of profitability lifting per tonnage of mineral, see Figure 12. A larger pipe diameter and gas flux rate cannot guarantee a better airlifting performance. It is because for each set of mining depth and pipe diameter, there exists an optimal set of gas flux rate and pipe diameter to obtain the maximum profitability per tonnage of mineral.

- Transporting small particles has a better performance than large particles in terms of its profitability, which is almost correct in terms of total solid production rate and energy consumption per tonnage of mineral.

In future research, the method how to obtain an optimal transport plan considering the solid production rate, energy consumption per tonnage of mineral, and profitability per tonnage of

mineral should be researched. In addition, the scale effect elaborated in Section 3.1.3 should be considered further combining with some industrial scaled prototype parameters of airlifting in DSM projects. Besides the scale effects existing between the up-scaled model and industrial scaled prototype of airlifting model, flow pattern differences should also be considered in the future research.

Chapter 5

Numerical Calculations of Environmental Impacts for Deep Sea Mining Activities*

After the technological performance analysis in chapter 3 and economic profitability analysis in chapter 4, to analyse the sustainability of DSM transport plans, the environmental impact research caused by DSM activities is still missing. Then in this chapter, the caused environmental impacts from DSM activities are discussed taking into consideration the physical seabed disturbances, sediment plume, species disturbances, and tailings disposal. In this chapter, section 5.1 gives an introduction of the current research status of DSM environmental impacts. Section 5.2 presents the selected numerical calculation methods for the DSM environmental impacts. Section 5.3 proposes a quantification of influences of the sediment plume and sedimentation on species disturbances. The section 5.4 shows the calculation results and discussions. The discussion of the calculation results of interconnections between sediment plume and species disturbances are noted in section 5.5. Finally, in section 5.6, the conclusions and recommendations are given.

5.1. Introduction

With the rapid consumption of terrestrial mineral resources, deep sea mining (DSM) was proposed as an innovative idea to solve the crisis of world resource shortage. The coming of DSM era represents not only a leap developing opportunity to the world economy, but also a potential environmental challenge to deep ocean water system, seafloor habitat, and species community (Chung et al., 2001; Chung, 2003; Chung, 2009).

For DSM projects, the most intensive DSM environmental influencing areas are located at the seafloor, ocean surface, tailings release outlet, and the nearby water columns (Ma et al., 2018b). In this paper, the major DSM environmental impacts cover the initial DSM disturbances and plume source, sediment plume, tailings, and species disturbance (Ma et al., 2018b). The initial DSM disturbance was used by Ma et al. (2018), which refer to the disturbing rate of the seafloor, disturbed sediment estimation, and also including plume source

theoretically. However, considering its important research position, the plume source is individually highlighted.

For the initial DSM disturbances and plume source, research focuses on the disturbed seafloor area, gross mining mass rate, resuspended sediment estimation, and the volume of wake flow (Sharma, 2011; Oebius et al., 2001). For the sediment plume, the influencing phenomena, e.g., particles deposition, seafloor erosion, etc., sediment deposition thickness, and various current conditions are taken into considerations in experimental tests (Ohlhorst, 1981; Lavelle, 1987; Jankowski et al., 1996; Segschneider et al., 1998; Taguchi et al., 1995). For tailings disposal, many researchers conducted much qualitative research and experimental tests focusing on the contaminants monitoring and water systems recovery. DSM tailings disposal is a complex issue. It relates to the production rate, the distance between mining site and the processing plan on-land, and discharged depth. Its calculation could refer to the theory of sediment plume transport (Ma et al., 2018a). For species disturbance, only relying on the numerical calculation method is not sufficient to determine the species disturbances, which also require the in situ measurement. Species disturbance is related to abundance, biomass, number of taxa, taxon richness and species diversity (Jewett et al., 1999).

In addition, there is seldom quantitative research addressing the interconnections between different environmental impacts in DSM project. The quantification of the influence of the sediment plume and sedimentation on species disturbances, as one of the most important and most noticeable and eye-catching issue, is emphasized. This relationship is analysed by introducing the related theories in the fields of dredging, ocean farming, fishery, coastal mining, and estuary ecosystem protection into DSM industry (Newcombe and Jensen, 1996; Kjelland et al., 2015; Cyrus and Blaber, 1987a; Dyer, 1972; Müller and Suess, 1979; Thrush and Dayton, 2002; Lohrer et al., 2006; Trueblood and Ozturgut, 1997). The driving factors of species disturbances resulting from sediment plumes are changes of ocean water turbidity, total organic carbon content, sedimentation rate, and sedimentation thickness, and the result of species disturbance is reflected by the severity of ill effect.

This chapter builds on the literature review paper of the author (Ma et al., 2018a) where the numerical calculation method of DSM environmental impact is selected. This chapter is developed on the basis of the literature review paper, which is also an application of the selected method (literature review major contributions). Besides the numerical calculations of DSM environmental impacts focusing on the initial disturbances and plume source, sediment plume, and species disturbances, the most novelty part is to analyse the interconnection between the sediment plume and the species disturbances particularly. The objective of this chapter is to demonstrate the application of the selected numerical calculation model for DSM environmental impacts. The chapter is arranged as follows: The method section describes the selected numerical calculation method. Section three proposes a quantification of influences of the sediment plume and sedimentation on species disturbances. The fourth section shows the calculation results and discussions. The discussions of the calculation results of interconnections between sediment plume and species disturbances are noted in section five. Then, in section six, conclusions and recommendations are given.

5.2. Research Method

5.2.1. Description of the numerical calculation method for DSM environmental impacts

Based on a systematic literature review paper of the author (Ma et al., 2018a), a numerical calculation framework for DSM environmental impacts is proposed in Figure 5.1.
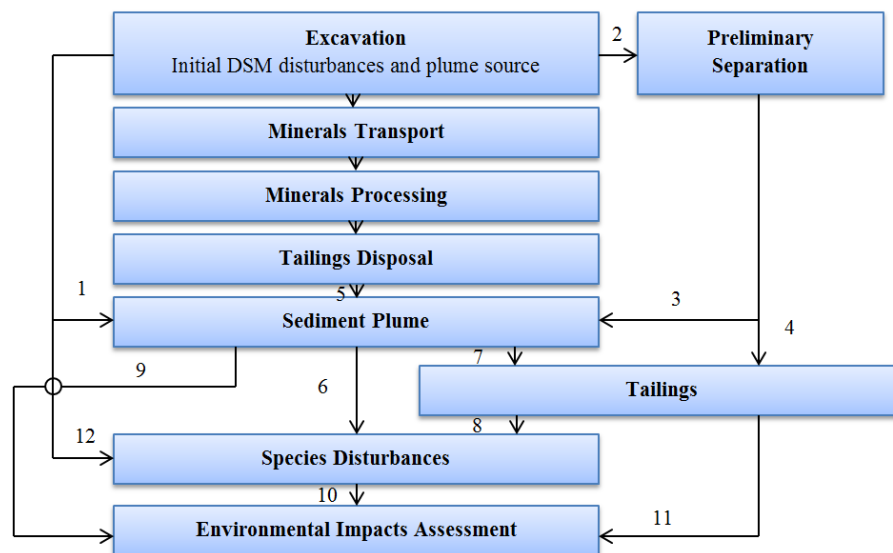
Figure 5.1: Schematic diagram of DSM environmental impacts framework. Notes: the numbers of 1-11 represent the relationship between different environmental impacts, and also the relations between different DSM activities. The initial DSM disturbances and plume source are one of the major causes of sediment plume (1). In the DSM project of manganese nodules, the preliminary separation could be used to decrease the useless sediment in the minerals mixtures (2), and a part of tailings would be piled on the seafloor (4). Simultaneously, the minerals separation process would be another source of sediment plume (3). After undertaking the minerals transport and processing processes, a new sediment plume source will be caused by the tailings disposal (5). The deposited sediment on the seafloor is another cause of DSM tailings (7). The species disturbance could be influenced by the tailings (8), and sediment plume (6). The environmental impacts resulting from DSM activities, e.g., sediment plume, are selected to be emphasized in this chapter. It is because we believe these kinds of influences would give a large impact on the ocean environment. Finally, the whole environmental impacts assessment derived from DSM industry is evaluated by the initial DSM disturbances and plume sources, sediment plume, tailings, and species disturbances (9-11). The seafloor sediment excavation, i.e., the physical disturbances, would also influence the benthic marine species (12) (Ma et al., 2018a).

The DSM environmental impacts depicted in Figure 5.1 consist of the following aspects: (i) the initial DSM disturbances and plume source; (ii) species disturbances; (iii) sediment plume; and (iv) tailings.

Following the research framework described in Figure 5.1, the detailed numerical calculations of different environmental impacts are explained as follows. Here, we would like to emphasize that the framework in Figure 5.1 and the following researches are designed specifically for deep ocean manganese nodules mining projects. For the analysed deep sea mining activities in this chapter, mineral nodule storages are assumed to be sufficient within the mining period. In addition, the complex topography of seafloor is also not taken into consideration, which is assumed to be horizontal in this chapter.

5.2.2. The initial DSM disturbances and plume source

The initial DSM disturbances and plume source are researched first. The numerical calculation in this section is based on the empirical formulas and estimations (Ma et al., 2018a).

- Disturbing rate

The disturbing rate of the seafloor are firmly connected with the dimension of seafloor working vehicles and its working velocity v_m, sediment mined thickness t_m, and the in-situ density of seafloor sediment ρ_d (Ma et al., 2018a; Sharma, 2011).

- Resuspended sediment

Then the resuspended sediment could be estimated with Eq. 5.1 (Sharma, 2011; Thiel and Tiefsee-Umweltschutz, 2001; Becker et al., 2001).

$$m_p = m_s \cdot \lambda_p \tag{5.1}$$

in which m_p is the particles resuspended rate [kg/s], λ_p is a estimation coefficient which depicts the percentage of resuspended particles. The value of λ_p would be highly depended on the excavation method of the mining device (jetting/cutting), which is estimated to be approximately 16% by Thiel and Tiefsee-Umweltschutz (2001) according to a series of in situ experiments with a hybrid (mechanical and hydrodynamic) miner.

- Wake flow

Wake flow, which is described as a turbulent flow around the seafloor vehicles, is proposed by Oebius et al. (2001), which is also determined by the seafloor working vehicle dimension (width W_m and height h_w).

- Sediment plume source

The sediment plume source is defined as follows. Firstly, the maximum mass concentration along the vertical direction is assumed to decrease according to a negative exponential principle, see Eq. 5.2 (Jankowski et al., 1996).

$$C_s(z) = C_{s0} \cdot e^{-0.5 \cdot z} \tag{5.2}$$

in which the superscript symbol z is the vertical coordinate above the seafloor [m], C_s is the mass concentration of suspended particles [kg/m^3], C_{s0} is the mass concentration of suspension particles nearby the sediment plume source. Secondly, after the estimation of maximum mass concentration, the distribution of mass concentration in each horizontal plane is according to a Gaussian distribution as follows (Jankowski et al., 1996).

$$C_s = C_{s\_max} \cdot exp\left(-\frac{\left(x - x_{max}\right)^2 + \left(y - y_{max}\right)^2}{2 \cdot \sigma_{xy}^2} \right) \tag{5.3}$$

in which x_{max} and y_{max} are the coordinates for the maximum point which is assumed to be initial sediment plume source point, σ_{xy} is the standard deviation representing the sediment plume influencing range.

5.2.3. Species disturbances

Based on the literature review, almost all of these numerical calculation methods of species disturbances need experimental tests to obtain the species information as the input. The collected species information, e.g., number of species and individuals' number of different species, would undertake a mathematical processing following Eq. 5.4-5.5 (Margalef, 1958; Simpson, 1949; Shannon, 2001). These parameters in Eq. 5.4-5.5 analyse the species disturbances focusing on different species characteristics (Ma et al., 2018a; Jewett et al., 1999; Oebius, 1997). An integrated species index is proposed characterising the benthic species communities. The integrated species index is composed of Margalef's indices, Shannon diversity index, and Simpson diversity index, see Eq. 5.4, which could be understood as a standard multi-metric parameter (Ma et al., 2018a).

$$SD_{bef/aft} = \begin{bmatrix} I_1 & I_2 & I_3 & I_3' & I_4 & D_V & D_N & D_H & D_S \end{bmatrix} \tag{5.4}$$

in which SD represents the integrated species index, subscripts of 'bef' and 'aft' represent the species information sampling before and after the DSM activities respectively, $\begin{pmatrix} I_1 & I_2 & I_3 & I_3' & I_4 & D_V & D_N \end{pmatrix}$, D_H, and D_S are the Margalef's indices, Shannon diversity index, and Simpson diversity index respectively, which are calculated with Eq. 5.5 (Jewett et al., 1999; Oebius, 1997; Margalef, 1958; Simpson, 1949; Shannon, 2001).

$$
\begin{cases}
I_1 = 1.443 \cdot ln(N) \\[2mm]
I_2 = 1.443 \cdot ln\left(\dfrac{(N-1)!}{(N-S)!(S-1)!} \right) \\[2mm]
I_3 = 1.443 \cdot ln\left(\dfrac{N!}{N_1! N_2! \cdots N_S!} \right) \\[2mm]
I_3{}' = 1.443 \cdot ln\left(\dfrac{N!}{(N/S)!} \right) \\[2mm]
I_4 = 1.443 \cdot ln(N!) \\[2mm]
D_V = \dfrac{1.443}{V} \cdot ln\left(\dfrac{N!}{N_1! N_2! \cdots N_S!} \right) \\[2mm]
D_N = \dfrac{1.443}{N} \cdot ln\left(\dfrac{N!}{N_1! N_2! \cdots N_S!} \right) \\[2mm]
D_H = -\displaystyle\sum_{i=1}^{S} p_i \cdot ln(p_i) \\[2mm]
D_S = 1 - \dfrac{\displaystyle\sum_{i=1}^{S} N_i \cdot (N_i - 1)}{N \cdot (N-1)}
\end{cases}
\tag{5.5}
$$

in which N is the total number of different kinds of species, S is the number of species, N_1, N_2,…, and N_S are the individuals' number of different species, p_i is the proportion of specie i.

The species disturbance is reflected by the variance of the integrated species index before and after the DSM activity (Ma et al., 2018a).

$$
Var(SD) = E\left[\sum_{i=1}^{9} \left(1 - \frac{SD_{aft}(i)}{SD_{bef}(i)} \right)^2 \right]
\tag{5.6}
$$

in which $Var(SD)$ is the variance of the two sets of species disturbances indices. The criteria judging the species disturbance resulting from DSM activity is that: the smaller the variance is, the smaller the DSM impacts are.

5.2.4. Sediment plume

Based on the systematic literature review, Jankowski's model is selected as the numerical calculation method for sediment plume caused by DSM activity. The transport of sediment plume could be calculated by an advection-diffusion model, see Eq. 5.7 (Jankowski et al., 1996; Ancey et al., 2015; Mirza and Vieru, 2017).

$$
\frac{\partial C_s}{\partial t} + u \cdot \frac{\partial C_s}{\partial x} + v \cdot \frac{\partial C_s}{\partial y} + w \cdot \frac{\partial C_s}{\partial z} + \frac{\partial (w_s \cdot C_s)}{\partial z} = \frac{\partial}{\partial x}\left(\varepsilon_x \cdot \frac{\partial C_s}{\partial x} \right) + \frac{\partial}{\partial y}\left(\varepsilon_y \cdot \frac{\partial C_s}{\partial y} \right) + \frac{\partial}{\partial z}\left(\varepsilon_z \cdot \frac{\partial C_s}{\partial z} \right) + q_c \tag{5.7}
$$

in which w_s is settling velocity [m/s], u, v, w are the fluid velocity in the directions of x, y, z respectively [m/s], x, y, and z are the coordinate axis of the sediment plume calculation area which is set to be a cuboid lying on the seafloor, axis x represents the east direction, axis y represents the north direction, the original point of the coordinate system is located on the seafloor, t is the time [s], ε_x, ε_y, ε_z are the dispersion coefficient of sediment plume in three different directions respectively, the horizontal dispersion coefficients , i.e., ε_x and ε_y, are set to be constant, i.e., 1.0 m^2/s, the vertical dispersion coefficient, i.e., ε_z, is determined by $\varepsilon_z = f(Ri) \cdot l^2 \cdot \sqrt{(\partial u / \partial z)^2 + (\partial v / \partial z)^2}$, l is the mixing length which is related to the bottom boundary layer thickness, $f(Ri)$ is the damping function (Sheng, 1983), Ri is the Richardson number which could be calculated by $Ri = -\dfrac{g}{\rho} \dfrac{\partial \rho}{\partial z} / \left(\left(\dfrac{\partial u}{\partial z} \right)^2 + \left(\dfrac{\partial v}{\partial z} \right)^2 \right)$ (Jankowski et al., 1996), q_c is the source term describing discharge [$kg / m^3 \cdot s$].

To calculate a more accurate sediment plume transport, Jankowski et al. (1996) claimed that the following aspects should be taken into consideration the settling velocity, particles deposition and seafloor erosion, particles flocculation and breakup, and particles scavenging phenomena. In which the explanation of the numerical calculation of current velocity conditions is listed in **Appendix A** (Jankowski et al., 1996).

- **Settling velocity**

The calculation method of settling velocity is closely related to the particles diameter, see Eq. 5.8 (Cheng, 1997; Van Wijk et al., 2014; Khatmullina and Isachenko, 2017).

$$\begin{cases} w_s = \dfrac{1}{18} \dfrac{\Delta \cdot g \cdot d_s^2}{\nu} & (d_s \leq 0.1mm) \\ w_s = 10 \dfrac{\nu}{d_s} \left(\sqrt{1 + 0.01 d_*^3} - 1 \right) & (0.1mm < d_s < 1mm) \\ w_s = 1.1 \sqrt{\Delta \cdot g \cdot d_s} & (d_s \geq 1mm) \end{cases} \tag{5.8}$$

in which d_s is the particles diameter [m], $\Delta = (\rho_s - \rho_l) / \rho_l$, ρ_s is the density of solid sediment [kg/m^3], and $d_* = \left(\Delta \cdot g / \nu^2 \right)^{1/3} \cdot d_s$.

- **Particles deposition and seafloor erosion**

The phenomena of particles deposition and seafloor erosion are related closely to the current velocity nearby the seafloor. The sediment flux rate nearby the seafloor is formulated as Eq. 5.9 (Jankowski et al., 1996).

$$\left[w_s \cdot C_s - \varepsilon_z \dfrac{\partial C_s}{\partial z} \right]_{bot} = w_s \cdot C_s \big|_{bot} \cdot f_d + M_{res} \cdot f_e \tag{5.9}$$

in which M_{res} is the erosion rate [$kg \, / \, m^2 \cdot s$], f_d and f_e are the probabilities for particles deposition and erosion, which are determined by the differences between bed shear stress and the critical shear stress of deposition and erosion, τ_b is the bed shear stress [Pa], τ_{cd} is the critical deposition shear stress [Pa], τ_{ce} is the critical erosion shear stress [Pa].

- **Particles flocculation and breakup**

Flocculation is a process in which particles of clay and organic matter stick together to form large flocs (Buffle et al., 1998). The flocculation phenomenon is closely related to the particles collisions. The breakup of particles coagulation can be determined by Kolmogorov length. It is assumed that the particles coagulation will breakup when its size is larger than Kolmogorov length (Jankowski et al., 1996). The Kolmogorov length is a characteristic parameter in turbulent flow which is influenced by both molecular viscosity of fluid and dissipation of turbulent kinetic energy, see Eq. 5.10 (Murhammer and Goochee, 1990). The density of flocculation is set to be 2985 kg/m^3 in this chapter.

$$\eta = \left(v^3 \, / \, \xi \right)^{1/4} \tag{5.10}$$

in which ξ is the dissipation of turbulent kinetic energy, which is set to be 5.0×10^{-8} m^2/s^3 (Monin and Ozmidov, 1985).

The particles flocculation probabilities could be calculated as follows (McCave, 1984; Williams, 1986).

$$\beta = K \cdot E \tag{5.11}$$

in which β represents the flocculation (collision) coefficient [m^3/s], E is the collision efficiency.

The diameters of particles researched in this chapter are set to be $10 \, \mu m$, $50 \, \mu m$, $100 \, \mu m$ respectively. The comparisons of flocculation probabilities are calculated, which is shown in Figure 5.2.
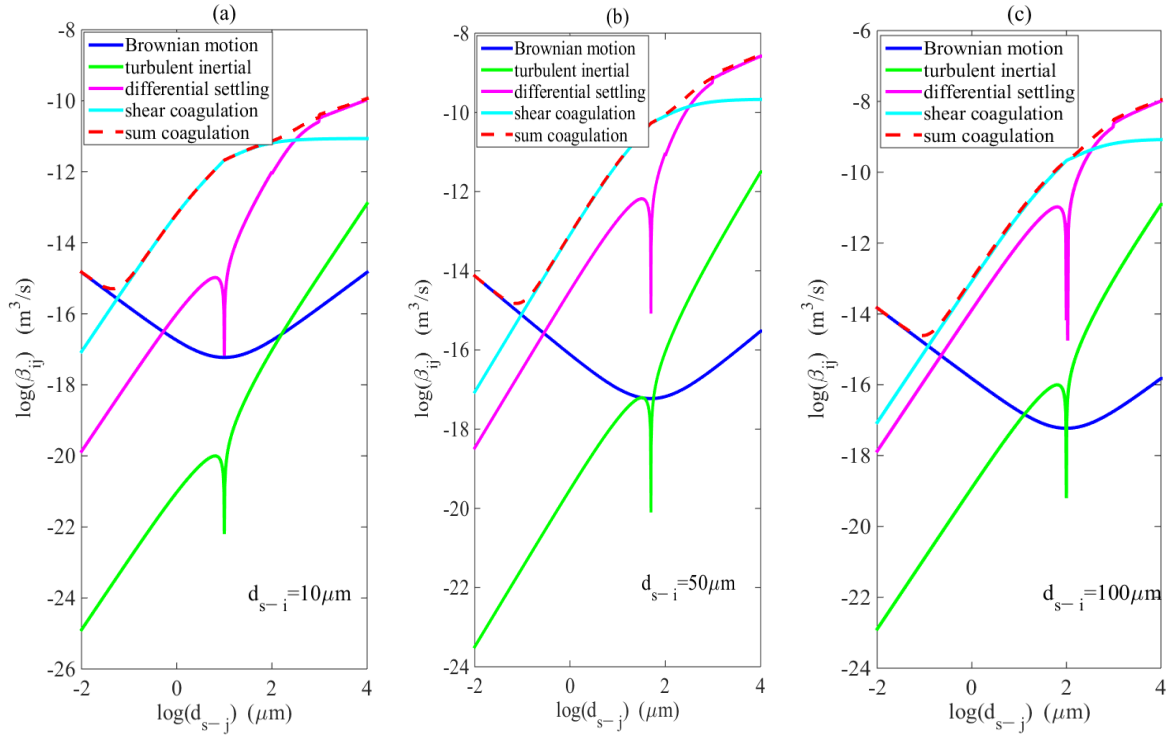
Figure 5.2: Comparisons of collision probabilities derived from Brownian motions, turbulent inertial, differential settling, and laminar and turbulent shear. Note: both d_{s_i} and d_{s_j} represent the collision particles, in which d_{s_i} represents the selected target particles colliding with the variable particle d_{s_j}.

Analysing the figure above, it shows that Brownian motion and differential settling coagulation play the major role in particles collision, when impact particles are smaller than roughly $0.1\,\mu m$ and larger than roughly $1000\,\mu m$ respectively (Jankowski et al., 1996). For impacts particles ranging from $0.1\,\mu m$ to $100\,\mu m$, in Figure 5.2 (a-c), laminar and turbulent shear determines the flocculation probabilities. Additionally, the sum of flocculation probability is usually determined by the dominant influencing factor.

After considering the coagulation kernel and probabilities, the number and mass concentration decreases of suspension particles can be calculated as follows (Jankowski et al., 1996).

$$\frac{dn}{dt} = -n \cdot \beta \tag{5.12}$$

$$\frac{dC_s}{dt} = -\frac{\pi \cdot \rho_s \cdot d_s^3}{6} \cdot \frac{dn}{dt} \tag{5.13}$$

- **Particles scavenging**

The suspension particles in the sediment plume might also be scavenged by the external particles originating in the upper ocean layers – marine snow (Jankowski et al., 1996). The marine snow, which is defined as macroscopic aggregates of detritus, living organisms and

inorganic matter (Alldredge and Silver, 1988), is assumed to be another important source for suspended particles scavenging in the deep ocean. The relationship of mass concentration decrease of suspended particles in the deep ocean can be calculated as follows (Jankowski et al., 1996).

$$\frac{dC_s}{dt} = -\frac{\pi}{4} \cdot E_\beta \cdot n_s \cdot d_{s\_ms}^2 \cdot w_{s\_ms} \cdot C_s \tag{5.14}$$

in which E_β is the scavenging efficiency by marine snow, n_s is the particles in marine snow, which is determined by the particles number concentration, i.e., $n_s = V \cdot O$, in which V is the marine snow volume, O is the particles number concentration [partic./m^3], d_{s_ms} is the particles diameter in marine snow [m], w_{s_ms} is the settling velocity of marine snow particles [m/s].

5.2.5. Tailings disposal

After the minerals processing, one perspective is that the generated tailings could be discharged in the ocean through a pipe system extended to the depth of 1100 m in the ocean (Gideiri, 1984; Nawab, 1984). Another perspective regarding tailings disposal is to send tailings to the seabed (ECORYS, 2014). In this chapter, tailings are assumed released on the seafloor. Therefore, the tailings transport principle could be regarded as the same as the sediment plume transport in section 5.2.4. The difference exists on the generating rate of tailings, which could be estimated as Eq. 5.15 (Chung et al., 2001).

$$m_{ts} = m_s \cdot \lambda_{ts} \cdot \lambda_s \tag{5.15}$$

in which m_{ts} is the mass rate of solid tailings [kg/s], λ_{ts} is the mean percentage of tailings in gross minerals mixtures, λ_s is the percentage of tailings which can be separated after a preliminary processing on the sea.

5.3. Quantification of influences of sediment plume and sedimentation on species disturbances

As different environmental impacts are closely related to each other, in this section, the quantification of influences of sediment plume and sedimentation on species disturbances, as one of the most important and most noticeable and eye-catching DSM environmental issue, is emphasized. Both the sediment plume cloud, i.e., suspended sediment, and the subsequent sedimentations, i.e., deposited sediment, would pose a threat, or challenge to the benthic marine species. The research in this section tries to collect a series of ecological indicators to explain the influencing intensities of sediment plume and sedimentation on the marine species. Its relationship could be majorly explained as the species responses to sediment plume, and is drawn as Figure 5.3.
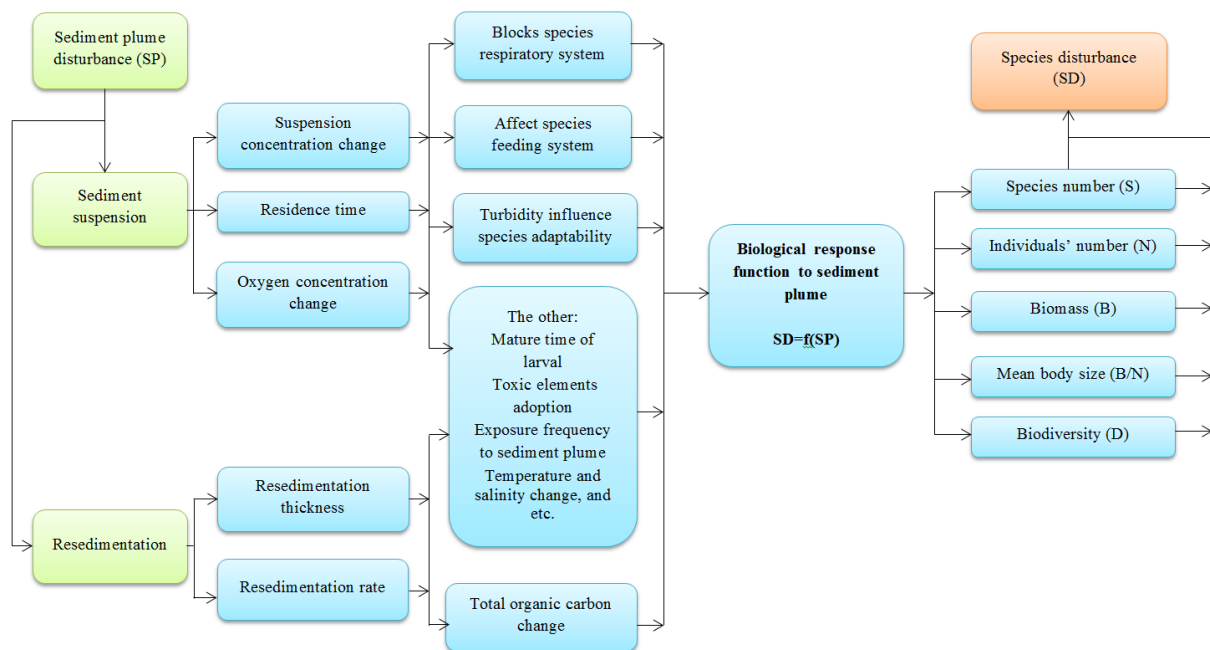
Figure 5.3: The schematic diagram describing the relationship between sediment plume and species disturbances.

The sediment plume influencing species could be explained in two major ways: particles suspension and resedimentation. The influences caused by suspension particles might consist of suspension particles concentration change, residence time of this event (also named exposure time and duration) and oxygen concentration change related to the concentration change. The increased solids concentration can affect the species respiratory system and species feeding system. The resedimentation rate and thickness are the most important influencing aspects when particles settle from the sediment plume. In addition, the total amount of organic carbon is closely related to the sediments depositions. Besides all the influencing aspects aforementioned, there are other insignificant aspects which are also mentioned by researchers in different degrees including mature time changes of larval, toxic elements adoption, temperature and salinity changes (Van Dover, 2014; Rodrigues et al., 2001; Sharma and Nath, 1997; Trueblood and Ozturgut, 1997; Raghukumar et al., 2001).

The biological response function to sediment plume is set to be a bridge between sediment plume and species disturbances. The research on species responses to DSM activities have been emphasized for a long time (Hughes et al., 2015; Morello et al., 2016; Brooks et al., 2015; Simpson and Spadaro, 2016; Haywood et al., 2016; Ramirez-Llodra et al., 2015). For instance, Brooks et al. (2015) analysed the blue mussel reflections to the discharged tailings from an iron ore mine focusing on the integrated biomarker assessment. In their research, the biomarkers consist of stress on stress (SS), condition index (CI), cellular energy allocation (CEA), micronuclei formation (MN), lysosomal membrane stability (LMS), basophilic cell volume (VvBAS), and neutral lipid accumulation (NL). Brooks et al. (2015) integrated the whole above mentioned individual biomarkers into an integrated biological response (IBR) index. The working principle of the integrated biological response is based on the change rate or relative difference between all the biomarkers in each given data set, which could be defined as a simple multi-metric approach. Simpson and Spadaro (2016) analysed the benthic

marine invertebrate responses to deep ocean sulfides mineral exploration in terms of bioavailability and chronic toxicity, which results indicate that the parameter of dilute-acid extractable metal concentration is firmly connected with ecosystem risk assessment by the mine-derived materials. The research conducted by Brooks et al. (2015) and Simpson and Spadaro (2016) raised very frontier species responses to tailings disposal and seabed exploration focusing on the some too much meticulous indicators, such as cellular energy allocation. However, these ecological indicators and biomarkers are difficult to connect directly with the calculation results of sediment plume. Haywood et al. (2016) focused on the coral responses to mine tailings disposal which results prove that the tailings disposal would reduce coral species richness and coral cover proportion within a specific limited impact range.

However, although the qualitative theoretical research is available, there is seldom such quantitative research addressing this problem directly and completely for DSM activities and connecting firmly and directly with the calculation results in sediment plume (Van Dover, 2014; Richmond, 1993; Glover and Smith, 2003). Various kinds of models, empirical formulas, and semi-quantitative researches in the other fields, e.g., dredging, ocean farming, fishing and estuary ecology protection, are introduced in DSM industry trying to address this problem focusing on the severity of ill effect, deep ocean water turbidity, total amount of organic carbon content change (Wenger et al., 2017; Berner, 2013; Hitchcock and Bell, 2004; Fukushima et al., 2000; Sharma et al., 2000; Sharma and Nath, 1997; Newcombe and Jensen, 1996; Müller and Suess, 1979). The species disturbances caused by sediment plume could be reflected on the changes of species' number, individuals' number, biomass, mean body size, and biodiversity (Newell et al., 2002).

5.3.1. Severity of ill effect

Severity of ill effect was proposed by Newcombe and Jensen (1996) through a meta-analysis of 80 collected reports addressing fish responses to sediment plume in streams and estuaries. The limitation of this model is that it only considers the suspension particles concentration and duration time neglecting the other aspects such as the particles dimension, suspension rate and resedimentation thickness. In addition, the model only takes into consideration the ill effect, but no beneficial effect.

The severity of ill effect is classified into four categories: nil effect, behavioural effects, sublethal effects and lethal and paralethal effects, see table 5.1 (Newcombe and Jensen, 1996).

Table 5.1: Severity of ill effect on marine species description (Newcombe and Jensen, 1996).

Severity		Description of effects
Nil effect	0	No behavioural effects
Behavioural effects	1	Alarm reaction
	2	Abandonment of cover
	3	Avoidance responses
Sublethal effects	4	Short-term reduction in feeding rates; Short-term reduction in

		feeding success;
	5	Minor physiological stress; Increase in rate of coughing; Increase respiration rate;
	6	Moderate physiological effects;
	7	Moderate habitat degradation; Impaired home;
	8	Indications of major physiological stress; Long-term reduction in feeding rate; Long-term reduction in feeding success; Poor condition;
Lethal and paralethal effects	9	Reduced growth rate; Delayed hatching; Reduced fish density;
	10	0-20% mortality; Increased predation; Moderate to severe habitat degradation;
	11	>20%-40% mortality
	12	>40-60% mortality
	13	>60-80% mortality
	14	>80-100% mortality

Based on the meta-analysis, an empirical formula describing the severity of ill effect on fish is proposed by Newcombe and Jensen, which is extended to be applied in marine species disturbances (1996).

$$S_{if} = \alpha + \beta\left(log_e\, t\right) + \chi\left(log_e\, C_s\right) \tag{5.16}$$

in which S_{if} is the severity of ill effect described in table 5.1, α, β', and χ are the regression analysis coefficients.

To keep the disturbed ecological system within a large recovering possibility, the species responses caused by sediment plume should not be worse than the sublethal effects degree, which means the value of severity of ill effect should not be larger than 8, please see Table 5.1.

As the formula of severity of ill effect described in Eq. 5.16, the regression analysis data are derived from the species experiments. The regression coefficients might be different focusing on various benthic ocean species. In this chapter, to analyse the severity of ill effect easily, a set of values for these regression coefficients are based on the experimental analyses carried out by Newcombe and Jensen (1996). As the empirical formulas, i.e., Eq. 5.16-5.17, are derived from some particular fish species in streams and estuaries, it should be validated for deep ocean conditions in the future.

$$S_{if} = 2.4661 + 0.9265 \cdot ln(\, t\,) + 0.5118 \cdot ln(\, C_s\,) \le 8 \tag{5.17}$$

It should also be noted that benthic ocean species, which have a fast moving ability, have more possibilities to survive from a sublethal stress from suspended sediment rather than lethality, because they are able to move away from the disturbance area to a relative natural site compared to the sessile and less mobile species (Kjelland et al., 2015).

5.3.2. Turbidity of Ocean Water

Ocean water turbidity nearby the mining site could be affected by the sediment plume. Increased ocean water turbidity might have a significant influence on the benthic marine species depending on the durations and levels, because, generally, species have a particular preferable turbidity range (Cyrus and Blaber, 1987a; Dyer, 1972). In this chapter, Nephelometric Turbidity Unit (NTU) is used to describe the turbidity conditions, see Eq. 5.18 (Cyrus and Blaber, 1987a).

$$NTU = \gamma \cdot C_S{}^{\lambda} \qquad\qquad (5.18)$$

in which γ and λ are the regression analysis coefficients.

To keep the species influences, resulting from ocean turbidity increase, within an environmental acceptable range as much as possible, its increase should be constrained as Eq. 5.19.

$$NTU = \gamma \cdot C_S{}^{\lambda} \leq \iota_t \cdot T_{nature} \qquad\qquad (5.19)$$

in which T_{nature} is the turbidity value at the site without sediment plume influences [NTU], ι_t is the risk factor which controls the acceptable turbidity changing range. In this chapter, a set of mean values of parameters γ, λ, ι_t, and T_{nature} for analysing the ocean water turbidity is given as follows: $\gamma = 0.2923$, $\lambda = 1.0$, $\iota_t = 1.75$, $T_{nature} = 55$ (Cyrus and Blaber, 1987b).

5.3.3. Total organic carbon & sedimentation rate

Total organic carbon content (TOC) is also a very important and popular widely used ecological indicator connecting firmly with the dissolved concentration of O_2 and CO_2, which ensuing influences consist of the bacteria content within the water column, and even the atmospheric compositions (Smith et al., 2015; Rodríguez-Murillo et al., 2015; Al-Said et al., 2018; Saleem et al., 2016). Total organic carbon (TOC) change is determined by the particles sedimentation rate. As we known, the organic carbon content exists in both the settled sediment and water columns. Compared to the organic carbon increase resulting from sedimentation, the organic carbon content within the water columns is quite small which might be neglected. Therefore, in this chapter, we focus on the total organic carbon content change caused by the sedimentation. Based on abundant experimental data, several empirical formulas focusing on the total organic carbon content and organic carbon accumulation are proposed by Müller and Suess (1979). It presents that there is a linear relationship between the total organic carbon content and the sedimentation rate through a regression analysis. However, these empirical formulas are much more suitable for the natural deposition conditions (with a small value of sedimentation rate), rather than the industrial scaled minerals deposition.

Ibach (1982) noted that when sedimentation rate is smaller than a critical sedimentation rate value the total organic carbon content increases with the increase of sedimentation rate, i.e., positive (preservational effect). When sedimentation rate is larger than the critical value the total organic carbon decreases with the increase of sedimentation rate, i.e., negative (diluent)

effect. The relationship of total organic carbon content with the sedimentation rate could be described by a logarithmic formula, see Eq. 5.20 (Tyson, 2001; Ibach, 1982).

$$log\left(TOC\right)=\begin{cases} a_1 \cdot log\left(Se\right)+b_1 & Se \le S_{cri} \\ a_2 \cdot log\left(Se\right)+b_2 & Se \ge S_{cri} \end{cases} \tag{5.20}$$

in which TOC is the total organic carbon content [%], Se is the sedimentation rate [m/m.y.], a_1, b_1, a_2, b_2 are the coefficients determined through the regression analysis, S_{cri} is the critical sedimentation rate where the maximum total organic carbon content is. In this chapter, to take the total organic carbon content and sedimentation rate into consideration, the following set of values for these coefficients is given: a_1=0.1851, b_1=1.2318, a_2=-0.5255, b_2=2.6530 (Tyson, 2001; Ibach, 1982).

To confine the total organic carbon content change (sedimentation rate) within an environment acceptable degree as much as possible, it forms another constraint for the sediment plume transport in deep sea.

$$TOC_{sp} / TOC_{nat} \le \iota_{toc} \tag{5.21}$$

in which TOC_{sp} is the total organic carbon influenced by the sediment plume, ι_{toc} is a risk factor which should be determined from experimental data, TOC_{nat} is the natural value of total organic carbon content of the DSM sites, which is set to be 1.5%.

5.3.4. Sedimentation thickness

Lohrer et al. (2006) analysed the responses of benthic marine macrobenthos to sediments deposition inside and outside a small harbour in northern New Zealand at thickness of 3 mm and 7 mm respectively. Both deposition conditions could cause a significant change for coarse sand species. The deposition thickness 7 mm, particularly, would also influence a lot on the muddier species community (Lohrer et al., 2006). In DSM industry, although the major resedimentation materials are from the benthic ocean seafloor, which seem to be environmental friendly, its sudden deposition might also form a great threat to the benthic marine species (Thrush and Dayton, 2002). The thicker and faster the sedimentation thickness forms, the more intensive the influences on the species community are. In addition, Thrush and Dayton (2002) also claimed that the most obvious deposition impacts to benthic species community might occur within the first three days after the disturbances.

Cummings et al. (2003) suggested that the impacts on the benthic ocean species community would be a catastrophic event if the sedimentation thickness of solids is more than 10 cm. Based on the deposition experiments focusing on worms, Miller et al. (2002) noted that when analysing the worms responses to deposition thicknesses of 0.5 cm, 1 cm, and 2 cm respectively, only the deposition thickness of 2 cm leads to a lethal degree effect for worms. Based on the field tests in BIE (Benthic Impact Experiment Project) and the other projects, the sedimentation thickness resulting from the anthropogenic activities is roughly 1-2 cm, which impacts on benthic ocean species are too much dependent on the disturbance degrees

(Trueblood and Ozturgut, 1997). Based on the in-situ field tests carried out by Metal Mining Agency of Japan (MMAJ) in 1994, the sedimentation thickness caused by seafloor disturbance is up to 19.5 mm (Jones et al., 2017).

Taking into consideration all the information aforementioned and the larger scale and more intensive disturbances in real DSM working conditions, a critical thickness for deposition is preliminarily estimated to be 2 cm to keep the species disturbances within an environmental acceptable degree. In the literature review, we expressed clearly about the source of these experimental data. We refer these data into DSM activities. As the DSM environment is completely different with the estuary or harbour environment, a more accurate data could be determined combining with the deep sea in situ measurement. Therefore, the critical thickness for deposition is assumed to be valid for deep sea.

5.3.5. Others

As the major content of this chapter is specifically focusing on the total framework of DSM environmental impacts, only several typical parameters are discussed and analysed. Except the aforementioned ecological indicators, researchers also proposed many the other related indicators addressing the ecological responses to seabed disturbances (Smit et al., 2008; Aldenberg et al., 2001; Kutti et al., 2015; Trannum et al., 2018). Taking an example of species sensitivity distribution, it is a probabilistic model and originally designed for the risk assessment of biological species for one particular toxicant or a set of toxicants (Aldenberg et al., 2001). Then, Smit et al. (2008) extended the application range of species sensitivity distribution for three nontoxic stressors: suspended clays, sedimentation thickness, and the change in sediment grain size. The nature for species sensitivity distribution is also focusing on its variance between the conditions before and after the seabed distributions in terms of species mortality ratio.

Besides these constraints mentioned above, there are other aspects which should also be considered in the future, including the oxygen concentration change, toxic elements accumulation, changes of species feeding and respiratory system.

5.4. Calculations and Discussion

The calculation method for the quantification of DSM environmental impacts, is illustrated as follows. DSM project: located at 26.5° N, 146° W; target mineral: manganese nodule, with dry density of 3750kg/m^3; depth: 4800m. Other parameters are based on Chung et al., 2001; Oebius et al., 2001; Jankowski et al., 1996; Thiel and Tiefsee-Umweltschutz, 2001, shown in table 5.2.

Table 5.2: Parameters used for numerical calculation of DSM environmental impacts.

Parameters	Values	Parameters	Values	Parameters	Values	Parameters	Values

ρ_d	$2000 kg / m^3$	v_m	$0.75 m/s$	W_m	$6m$	h_m	$3m$
t_m	$0.055m$	λ_p	16%	λ_{ts}	72%	λ_s	60%
ε_x	$1.0 m^2 / s$	ε_y	$1.0 m^2 / s$	E_β	0.001	O	$300 part / m^3$
g	$9.8 m/s^2$	τ_{cd}	$0.10 pa$	τ_{ce}	$0.13 pa$	k	1.38×10^{-23} $m^2 \cdot kg \cdot s^{-2} \cdot K^{-1}$
S_{bef}	9	N_{bef}	166	$N_1:N_2:\cdots:N_9=91:35:15:10:6:5:2:1:1$			
S_{aft}	3	N_{aft}	35	$N_1:N_2:N_3=21:11:3$			

Note: The species sampling information is collected within one week nearby the DSM area in a volume roughly 100 m^3; $N_1 : N_2 : \ldots : N_S$ represents the individuals number of different species; ρ_d - in-situ density of seafloor sediment; v_m - mean velocity of seafloor vehicle; W_m - mining width of the seafloor vehicle; h_m - height of the wake flow; t_m - thickness of the mined sediment (Chung et al., 2001); λ_p - estimation value for percentage of resuspended particles; λ_{ts} - estimation value of percentage of tailings in gross mineral mixtures; λ_s - estimation value for percentage of removed tailings (Oebius et al., 2001; Thiel and Tiefsee Umweltschutz, 2001); ε_x, ε_y - dispersion coefficient in horizontal directions (Jankowski et al., 1996); E_β - scavenging efficiency by marine snow; O - particles density of marine snow; τ_{cd} - critical deposition shear stress; τ_{ce} - critical erosion shear stress (Shi et al., 2015); k - Boltzmann constant; S_{bef}/S_{aft} - species' number before and after the DSM disturbances; N_{bef}/N_{aft} - individuals' number before and after the DSM disturbances.

5.4.1. The initial DSM disturbances and plume source

Based on Eq. 5.1-5.3, the initial DSM disturbances and plume source were calculated. The calculation results are listed in Table 5.3.

Table 5.3: Results of the initial DSM disturbances and plume source following Eq. 5.1-5.3.

Parameters	A_d	V_d	m_d	m_s	m_p	V_w
Results	$4.5 m^2 / s$	$0.25 m^3 / s$	$495 kg/s$	$177.1 kg/s$	$28.3 kg/s$	$40.5 m^3 / s$

Notes: A_d is the disturbing rate of seafloor area, V_d is the volume disturbing rate of saturated sediment, m_d is the mass disturbing rate of saturated sediment, m_s is the mass disturbed rate of solid sediment, m_p is the resuspended sediment, V_w represents the volume of wake flow.

Analysing the data (table 5.3), from the quantification of DSM environmental impacts hypothetical project, we observed that the disturbance of the seafloor will have a rate of $4.5 m^2 / s$, i.e., A_d. If we set the workdays in 300 days per year, the total influencing area of this DSM project will be up to 2332.8 km^2 with estimated period of 20 years of intense

mining. Besides the seafloor disturbing parameters, the resuspended rate of sediment could be estimated based on the total amount of disturbed sediment.

Therefore, the mass rate of suspension particles (m_p in table 5.3) was used to estimate the initial mass concentration of sediment plume nearby the seafloor, see Eq. 5.22. Then the vertical distribution of the maximum mass concentration above the source point was calculated with Eq. 5.2. In the horizontal transport of sediment plume, its distribution complies with the Gaussian equation, as Eq. 5.3.

$$C_{s0} = \frac{m_p \cdot t_d}{dx \cdot dy \cdot dz} \tag{5.22}$$

in which t_d is the total disturbance time, which is set to be 50 h, dx , dy , dz are the resolutions of the calculation space [m].

5.4.2. Species disturbances

Based on Eq. 5.4-5.6 and the species sampling information given in table 5.2, the species disturbances indices before and after the DSM activities were calculated and presented in table 5.4.

Table 5.4. Species characteristic parameters comparisons before and after the DSM activities.

Parameters	Before DSM	After DSM	Parameters	Before DSM	After DSM
I_1	7.38	5.13	D_V	3.12	0.40
I_2	43.39	9.13	D_N	1.88	1.13
I_3	311.98	39.63	D_H	1.38	0.88
I_3'	937.47	107.70	D_S	0.64	0.55
I_4	989.99	132.95	---	----	---
SD	$SD_{bef} = [7.38\ 43.39\ 311.98\ 937.47\ 989.99\ 3.12\ 1.88\ 1.38\ 0.64]$ $SD_{aft} = [5.13\ 9.13\ 39.63\ 107.70\ 132.95\ 0.40\ 1.13\ 0.88\ 0.55]$				
Var	$Var(SD) = E\left[\sum_{i=1}^{9} \left(1 - \frac{SD_{aft}(i)}{SD_{bef}(i)} \right)^2 \right] = 0.45$				

Based on the given species information in Table 5.2, the most significant change on deep-sea communities is the decrease of total biomass and biological species categories. The variance of the integrated species index before and after DSM activity could be used to reflect the deep sea species disturbances. The variance here 0.45 represents the DSM influencing degrees on the deep sea communities. A larger variance represents a higher influencing degree on the deep sea communities.

5.4.3. Sediment plume

Besides the parameters given in Table 5.2, the current velocity nearby the seafloor is required for the sediment plume calculation. The current velocity of 100 m above the seafloor is assumed as Figure 5.4. Based on the given velocity profile in Figure 5.4, the deep sea current model in Appendix A was used to calculate the velocity profiles in the researched area considering the long gravity wave and geostrophic equilibrium current (Jankowski et al., 1996).
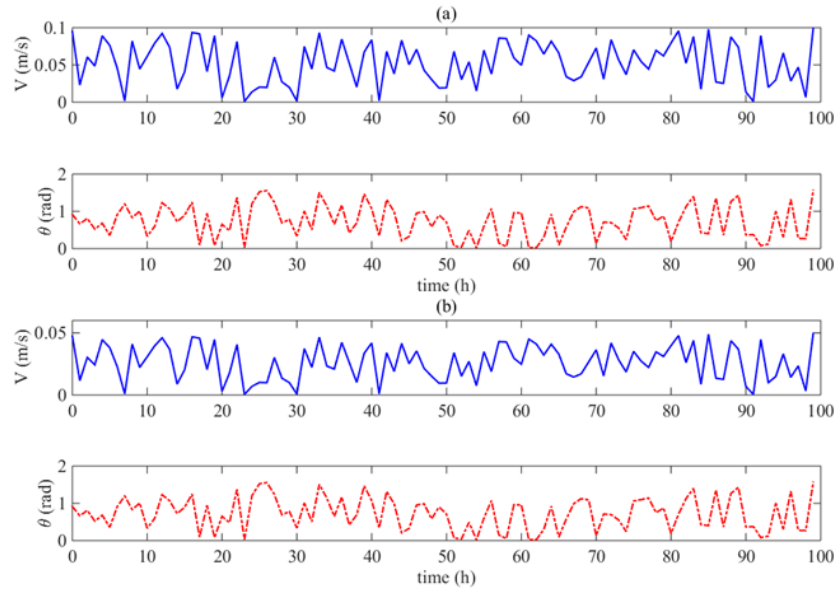
Figure 5.4: The assumed current velocity profile at 100 m above the seafloor. Notes: *V* represents the speed of the current velocity profile, and *θ* represents the angle between the velocity and the latitude direction.

- **Effect of seafloor erosion and particles deposition, flocculation and breakup and marine scavenging**

Compared to the other conventional sediment plume transport methods, the model adopted in this chapter considers the phenomena of seafloor erosion and particles deposition, flocculation and coagulations breakup, and marine scavenging. Figure 5.5 compares the influencing degrees on sediment plume transport by seafloor erosion, particles deposition, flocculation, coagulations breakup, and marine scavenging phenomena.
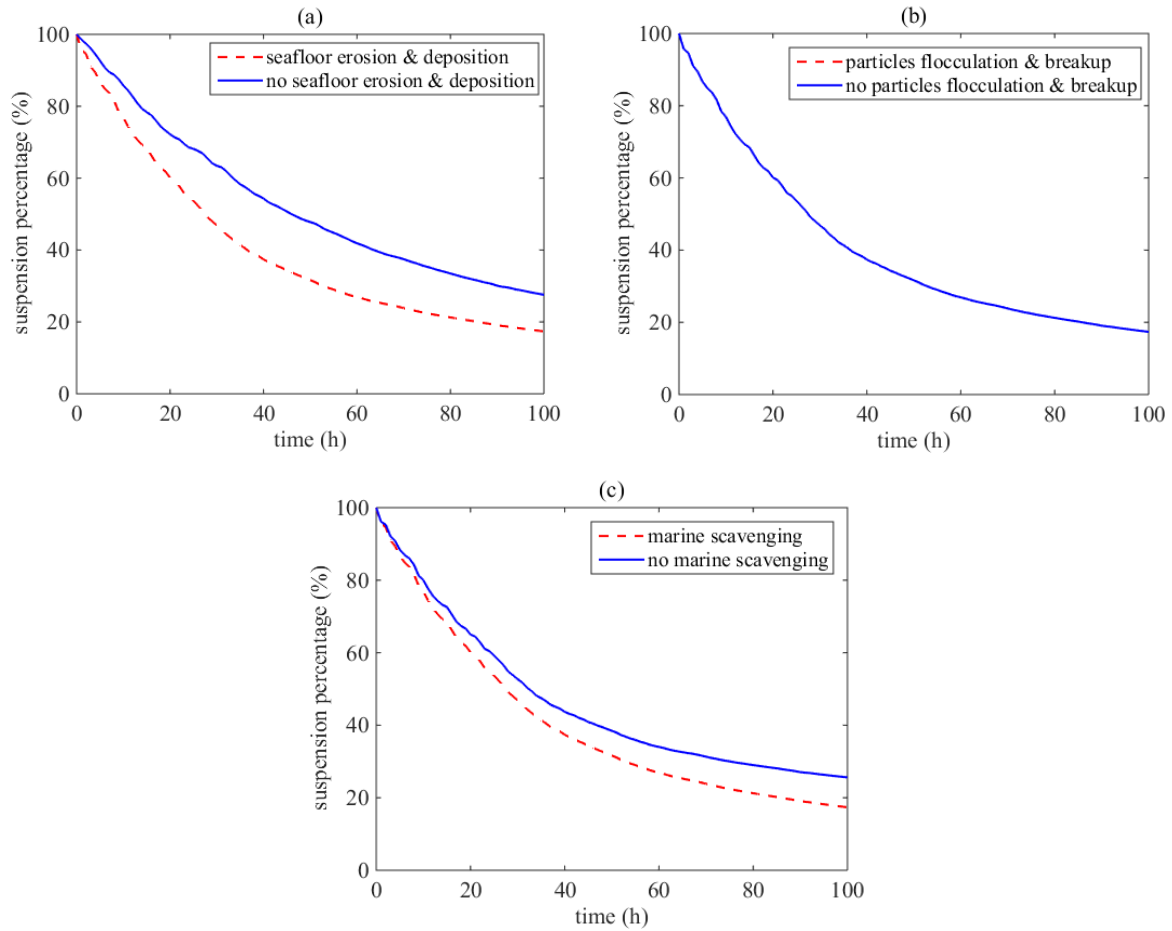
Figure 5.5: Comparisons of influencing degrees of seafloor erosion and deposition, particles flocculation and breakup and marine scavenging phenomena on sediment plume. Notes: Suspension percentage is the ratio between the suspended particles mass at time t and the initial suspended particles mass.

Analysing Fig. 5.5 (a), it presents that the suspended particles transport is influenced greatly by seafloor erosion and particles deposition. This phenomenon accelerates the suspension particles deposition process. The increase of suspended percentage could be caused by the seafloor erosion by adding more particles into the water columns, while its decrease might be caused by the particles deposition. These two phenomena are determined by the differences between the bed shear stress and the critical shear stress of seafloor erosion and deposition, which is closely related to the bottom current velocity profiles. Moreover, as the deep sea current velocity is generally small (<0.15m/s) (Jankowski et al., 1996), the phenomenon of particles deposition plays a more conspicuous role than seafloor erosion. However, if the sediment plume occurs at places with a relative high velocity (with a large erosion rate), the influencing degrees of phenomenon of seafloor erosion might be significant. Analysing Fig. 5.5 (b), the suspension percentage lines with and without influenced by particles flocculation and breakup are basically coincide together. It is because the particles flocculation probability caused by the Brownian motion, turbulent inertial, differential settling and laminar and turbulent shear is quite small, which value ranges from 10^{-17} m^3/s to 10^{-8} m^3/s. The small value of particles flocculation probability makes its influencing degree on sediment plume

transport negligible. However, if the environment friendly coagulant is added into the sediment plume, it might be helpful to accelerate the suspended particles deposition process. Obviously, Fig. 5.5 (c) presents that the phenomenon of marine scavenging is beneficial to decrease the mass concentration of suspended particles. Cooperating with Eq. 5.14, it shows that the scavenging rate is closely related to the scavenging particles diameter and its density nearby water columns. In order to understand clearly how these parameters, e.g., scavenging particles diameter and its density, affect the suspension particles deposition process, the corresponding sensitivity analyses are given in Figure 5.6.
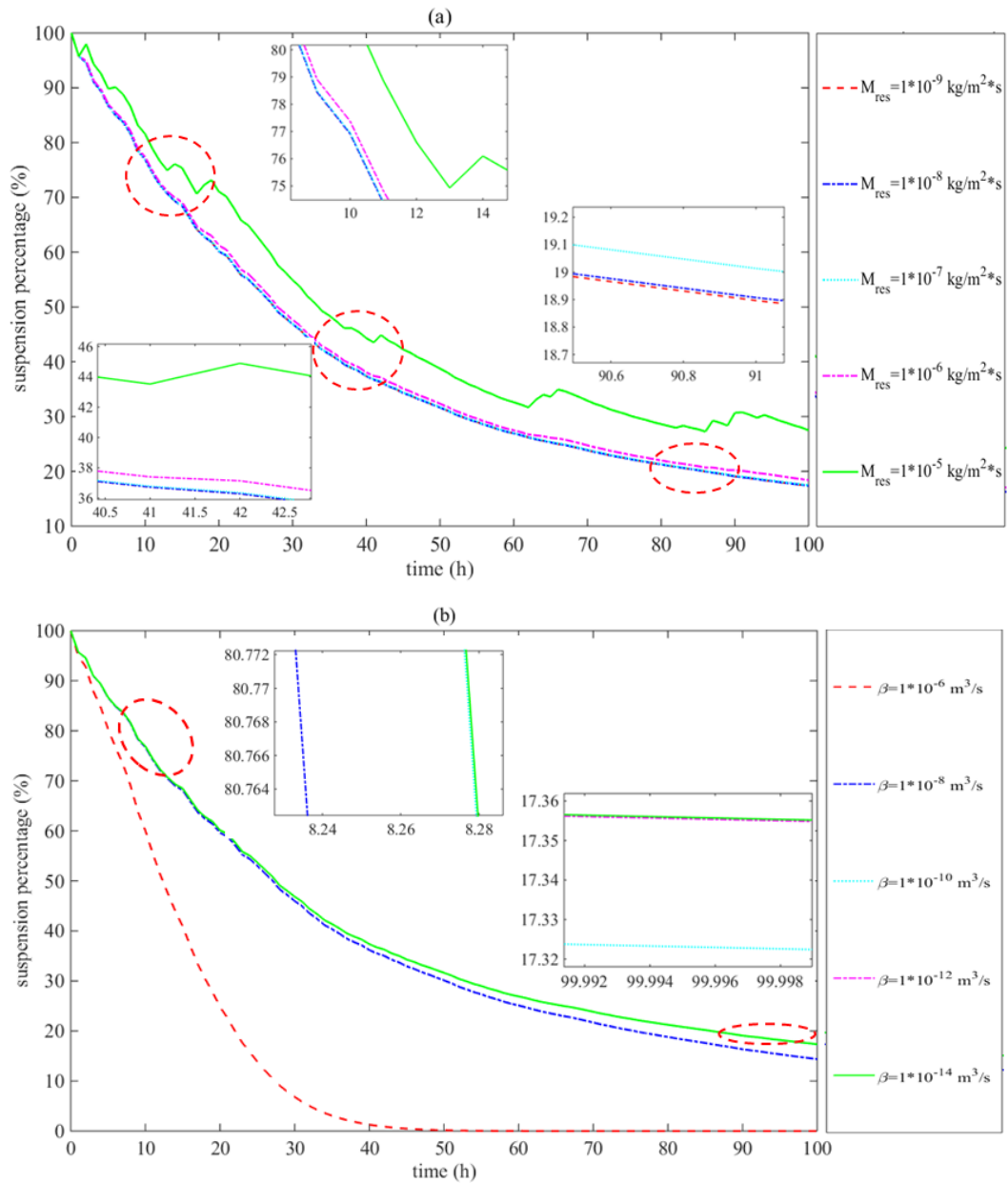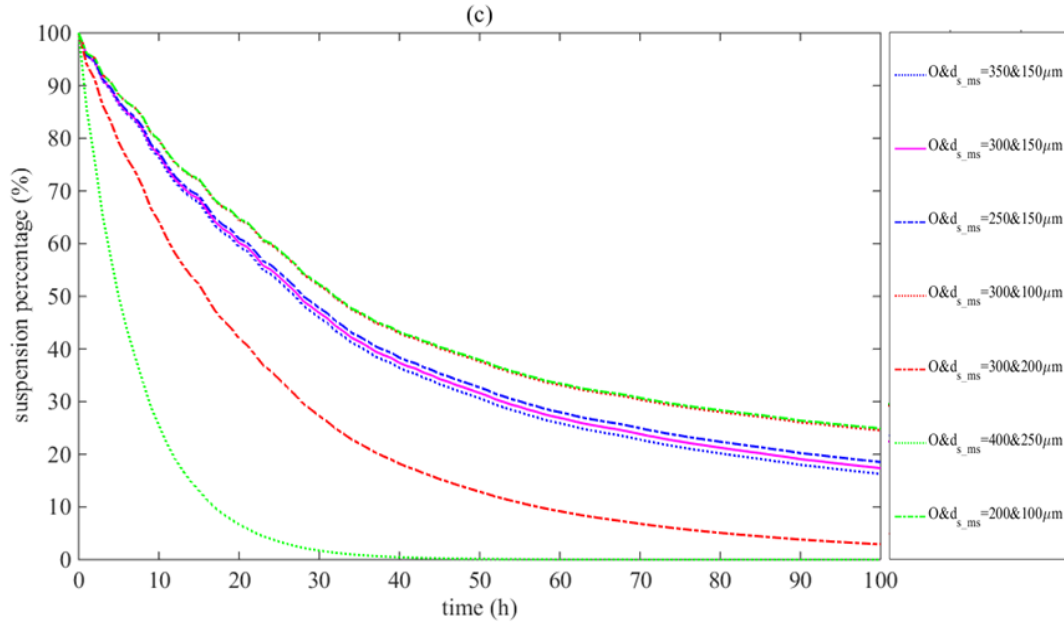
Figure 5.6: Sensitivity analyses of parameters in phenomena of seafloor erosion and particles deposition, particles flocculation and breakup, and marine scavenging. Notes: Figure 5.6 (a-c) represent the sensitivity analyses of seafloor erosion and particles deposition, particles flocculation and break, and marine scavenging respectively.

Analysing Fig. 5.6 (a), when the erosion rate is large enough, e.g., $1\times10^{-5}\,kg\,/\,m^2\cdot s$, the suspension sediment percentage could be influenced significantly by the phenomena of seafloor erosion and deposition. After 100 hours transport, the suspension particles percentage of erosion rate at $1\times10^{-5}\,kg\,/\,m^2\cdot s$, i.e., the green line, is roughly 28%, which is much larger than the sediment plume with erosion rate at $1\times10^{-6}\,kg\,/\,m^2\cdot s$ (roughly 19%). Although suspended particles still decreased with the time going on, there exist some fluctuations in the line of suspension sediment percentage, which might be caused by the sudden increase of mass concentration resulting from the seafloor erosion. In these conditions, the sediment plume would require more time to settle down completely. In Fig. 5.6 (b), the sensitivity of phenomena particles flocculation and breakup is analysed focusing on the particles flocculation possibility. Analysing Fig. 5.6 (b),, when the particles flocculation possibility is smaller than magnitude of 10^{-8} m^3 partic./s, there is almost no impacts on the suspension particles percentage resulting from particles flocculation and breakup. In these conditions the decreased suspension particles from flocculation account for only a small proportion. When the particles flocculation possibility is larger than magnitude of 10^{-6} , the suspension particles would be deposited much faster resulting from flocculation phenomenon. Therefore, in DSM project, adding the natural environmental friendly coagulant within the sediment plume area could accelerate the deposition process of sediment plume. In Fig. 5.6 (c), the density and dimensions of marine scavenging particles are focused on analysing the sensitivity of phenomenon of marine scavenging. Fig. 5.6 (c) shows that both a larger scavenging particle diameter and more of them would be helpful to speed up the suspension particles deposition process. In addition, the parameter of scavenging particles dimension plays a more conspicuous role than the parameter of its density. This could be explained by Eq. 5.14, where

shows that the decrease of suspension particles percentage has a quadratic relationship with scavenging particles diameter.

- **Influencing degrees on sediment plume transport from various current conditions**

Sediment plume could also be influenced by the current conditions nearby the seafloor (Thiel and Tiefsee-Umweltschutz, 2001). Figure 5.7 shows the sediment plume transport under different current conditions.
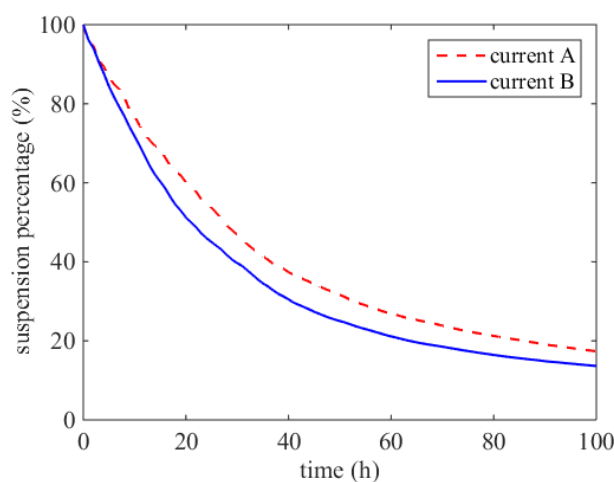
Figure 5.7: Comparisons of influencing degrees from two different kinds of current conditions. Current A is a random assumed current which maximum velocity is no more than 0.10 m/s, current B is another assumed current which maximum velocity is no more than 0.05 m/s. Both current conditions are shown in Figure 5.4. Particle diameter of sediment plume is set to be $10\mu m$.

The calculation results in Figure 5.7 show that the sediment plume mass distribution could be influenced significantly by the current conditions. Analysing the lines of suspension particles percentage, when the current is strong, i.e., current A, the residence time of sediment plume is longer than that in weak current. It means that a weak current condition is more suitable for suspension particles deposition than a current condition with larger velocity. However, if sediment plume deposits fast, it might also be a threat to the benthic ocean species community. It could be caused by that benthic ocean species have less time to adapt the fast increased sedimentation on them (Duckworth et al., 2017; Rogers, 1990; Gutiérrez et al., 2003; Thatje et al., 2005).

- **Influencing degrees on sediment plume transport from different particle diameters**

Figure 5.8 depicts the sediment plume transport for three different particles sizes.
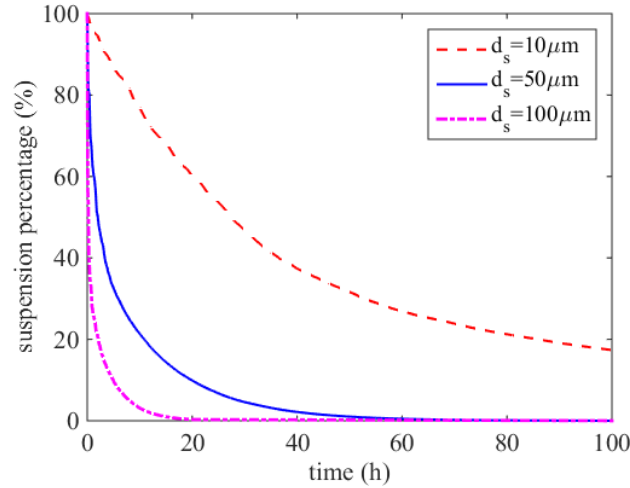
Figure 5.8: Comparisons of three different kinds of sediment plume conditions influenced by various particles diameters.

Figure 5.8 compares sediment plume influencing degrees by different particles diameter with $10\mu m$, $50\mu m$, and $100\mu m$ respectively. It shows that the fine particles can be transport for a longer time compared to the coarse particles. Based on the calculation results, it could be estimated that the residence time for fine particles, i.e., $d_s = 50\mu m$, is roughly 60 h, and that of the coarse particles, i.e., $d_s = 100\mu m$, is roughly 20 h. The calculation results are approximately consistent with the data given in DISCOL experiment that the residence time of particles with settling velocity $w_s \approx 10^{-4}$ m/s is at the order of 1.5-6 days (Jankowski et al., 1996; ISA, 2018b). The large scale DISCOL experiments were carried out during 1989-1996 at Pacific and Indian Oceans focusing on the environmental impacts assessment and recolonization process after a series of seabed disturbances with a plow harrow device. The results given in DISCOL project are determined by in-situ measurements, which try to simulate the real DSM working conditions as much as possible with a real seabed disturber (Schriever et al., 1997; Foell et al., 1990). The calculation result depends largely on the assumed initial mass concentration distribution. However, if the calculation results are almost consistent with the project data, it might be an evidence to prove the results.

- **Thickness of resedimentation**

In addition to the suspended percentage, the thickness of resedimentation on the seafloor is also a very important parameter. Figure 5.9 depicts the thickness profiles of resedimented particles.
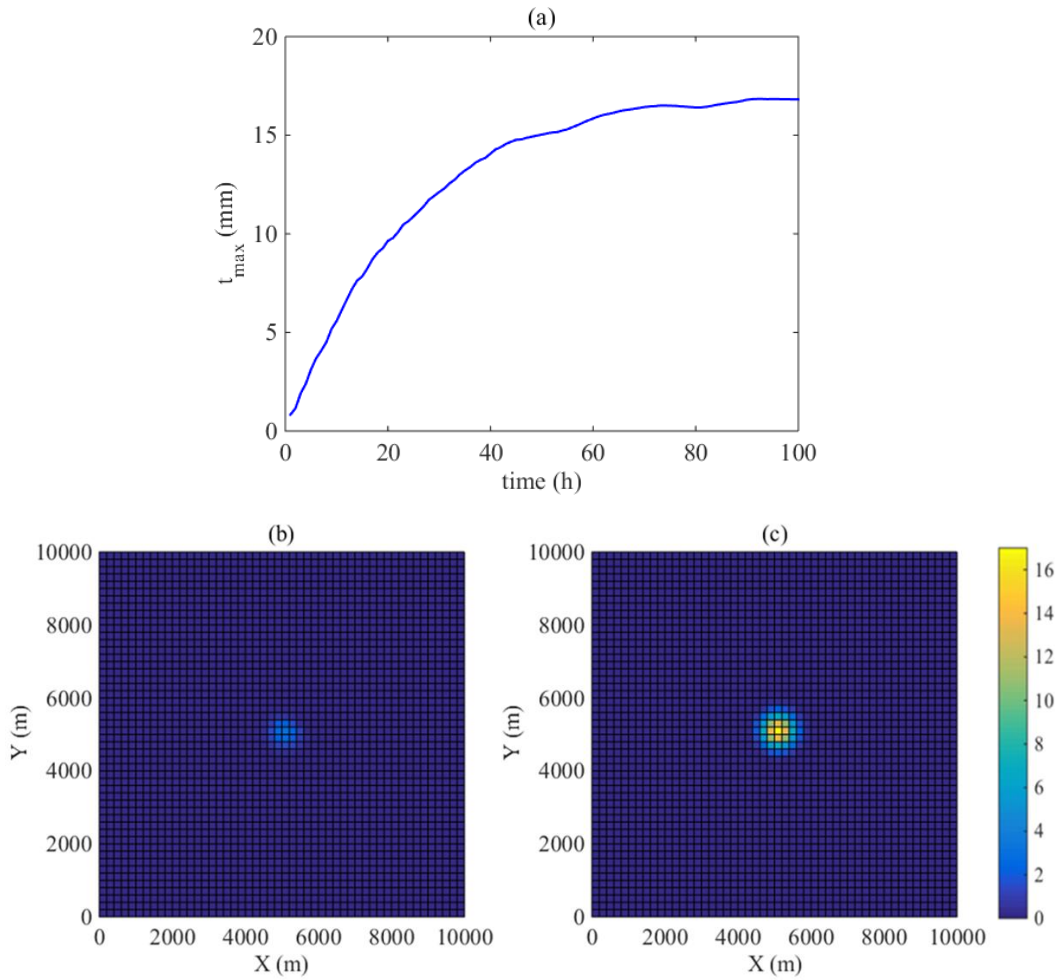
Figure 5.9: Thickness of resedimented particles. (a) t_{max} means the maximum thickness of resedimented particles on seafloor [mm]; (b) and (c) represent the top view of the resedimentation thickness profile within the researched area, which is measured at time of 5 h and 100 h respectively after the sediment release; The particles diameter here is $10 \mu m$.

Analysing Figure 5.9, it presents the maximum thickness of resedimented sediment after DSM activity. The maximum value of t_{max} in this case is approximately 17 mm. It is a bit larger than the experiment data measured in Benthic Impact Experiment Project (BIE), i.e., 10 mm, and Japan Experimental Test (JET), i.e., 1.9 mm (Jankowski and Zielke, 1997). It might be caused by: (i) the assumed initial sediment plume distribution is not completely consistent with the test conditions; (ii) the current conditions are different; (iii) the DSM disturbing degrees are different. The maximum sedimentation thickness of 16 mm is also smaller than 2.0 cm, which is set to be a critical sedimentation thickness controlling the influences within an environmental acceptable degree, as explained in section 3.4. In addition, Figure 5.9 also shows that the maximum thickness of the resedimented sediment, i.e., t_{max}, increases with the time going on, and its increasing speed decreases at the same time. It proves the most intensive influencing period occurs within the first 55 hours (roughly 2-3 days) after the sediment disturbances. Furthermore, analysing Figure 5.9 (b-c), although the thickness of the sediments deposition increases within this period and the sediment plume could transport far

away from the sediment source position, the evident influencing area of the resedimentation is approximately limited within the initial sediment plume area.

5.5. Analysis of interconnections between sediment plume and species disturbances

The analyses of interconnections between sediment plume and species disturbances focus on the parameters of severity of ill effect, turbidity of ocean water, total organic carbon content change and sedimentation thickness, which work as a series of constraints or evaluation standards for DSM projects. In Figure 5.9, the sedimentation thickness is calculated and is smaller than 2 cm, which meets the requirements of restrictions. Therefore, in this section, only the calculations of severity of ill effect, turbidity of ocean water, total organic carbon content, and sedimentation rate are discussed.
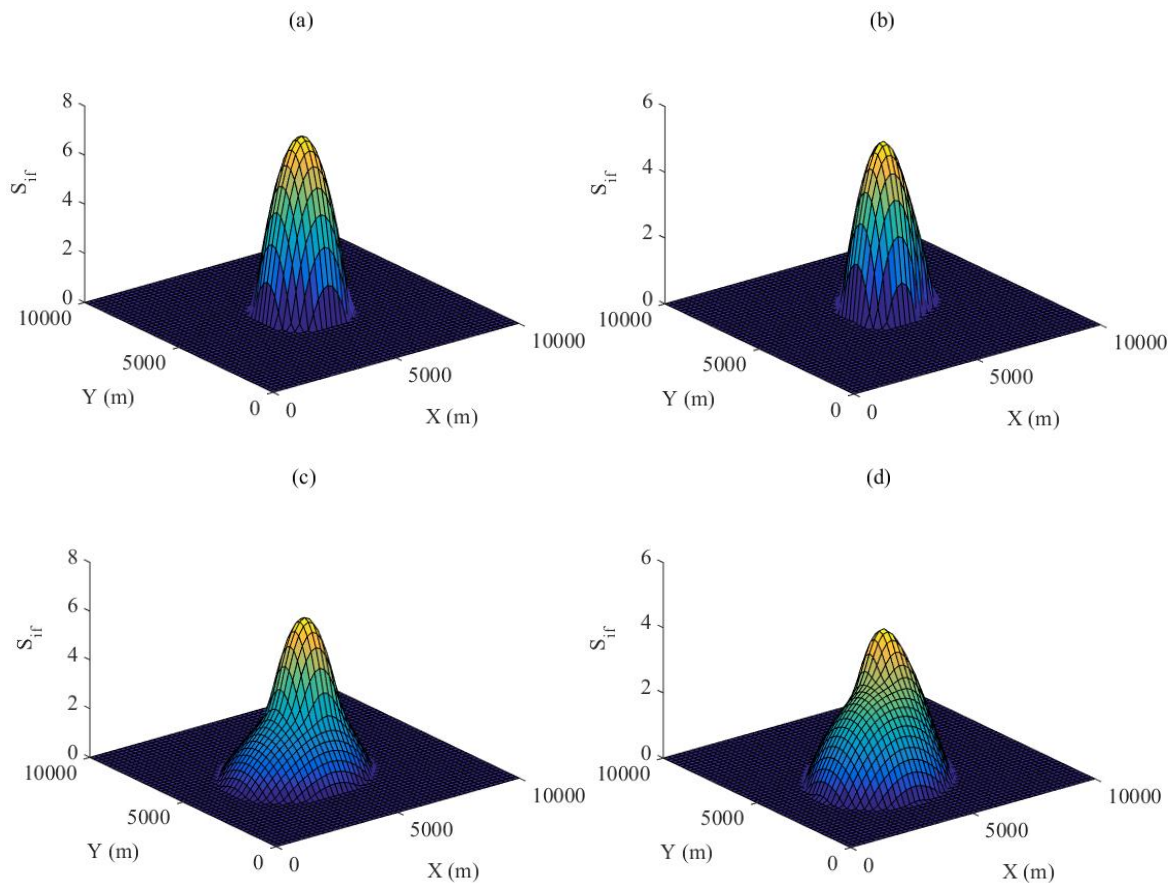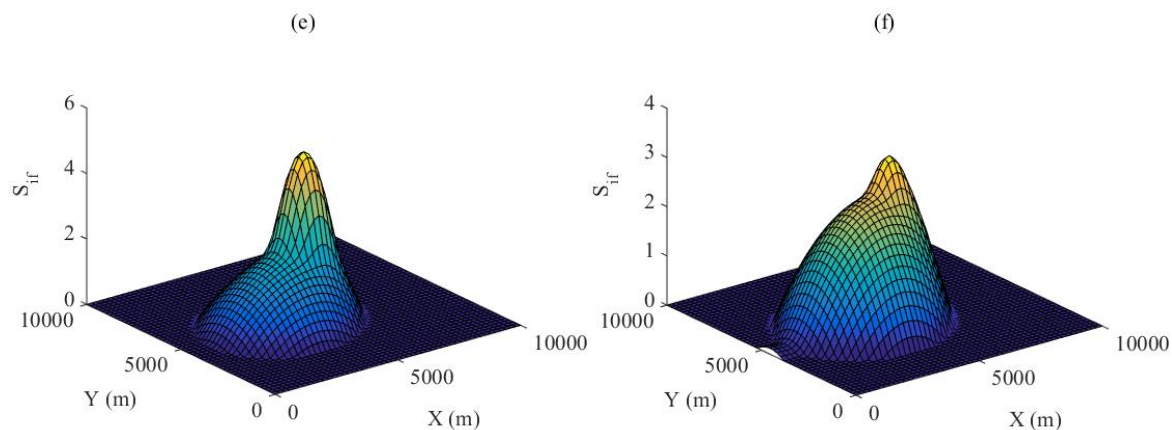
Figure 5.10: Calculation results of severity of ill effect within the influencing area of sediment plume. (a-b), (c-d), and (e-f) describe the severity of ill effect at the time of 5 h, 50 h and 100 h after the sediment plume transport respectively; (a, c, e) describe the severity of ill effect of the plane nearby the seafloor, and (b, d, f) describe the severity of ill effect of the plane 10 m above the seafloor.

Figure 5.10 presents the calculation results of severity of ill effect nearby the seafloor plane and the plane of 10 m above the seafloor, and the time of 5 h, 50 h, and 100 h after the sediment plume transport respectively. As the mass concentration of suspended particles is a time-dependent parameter, the results focus on the severity of ill effect within one hour. Analysing Figure 5.10, it presents that, with the time going on, the maximum value of severity of ill effect within the influencing area is decreasing. In addition, the severity of ill effect marked area is also increasing at the same time of sediment plume expansion process. Compared to the conditions of severity of ill effect at 10 m above the seafloor, see Figure 5.10 (b, d, f), the severity of ill effect nearby the seafloor, see Figure 5.10 (a, c, e), is larger, which means the impact on marine species communities is greater. Furthermore, although the mass concentration of suspension particles at time of 5 h and 100 h after the sediment plume is different with each other roughly 2-3 magnitudes, the values of severity of ill effect do not have such a big difference, and are at the same magnitude at least (Chang, 2016; Van Wijk et al., 2014; Elimelech et al., 2013). This is because the huge difference of mass concentration of suspension particles is reduced greatly by the logarithmic calculations in Eq. 5.16-5.17. Calculation results of severity of ill effect show that all values are smaller than 8, which means the species disturbances are kept away from lethal and paralethal effects.
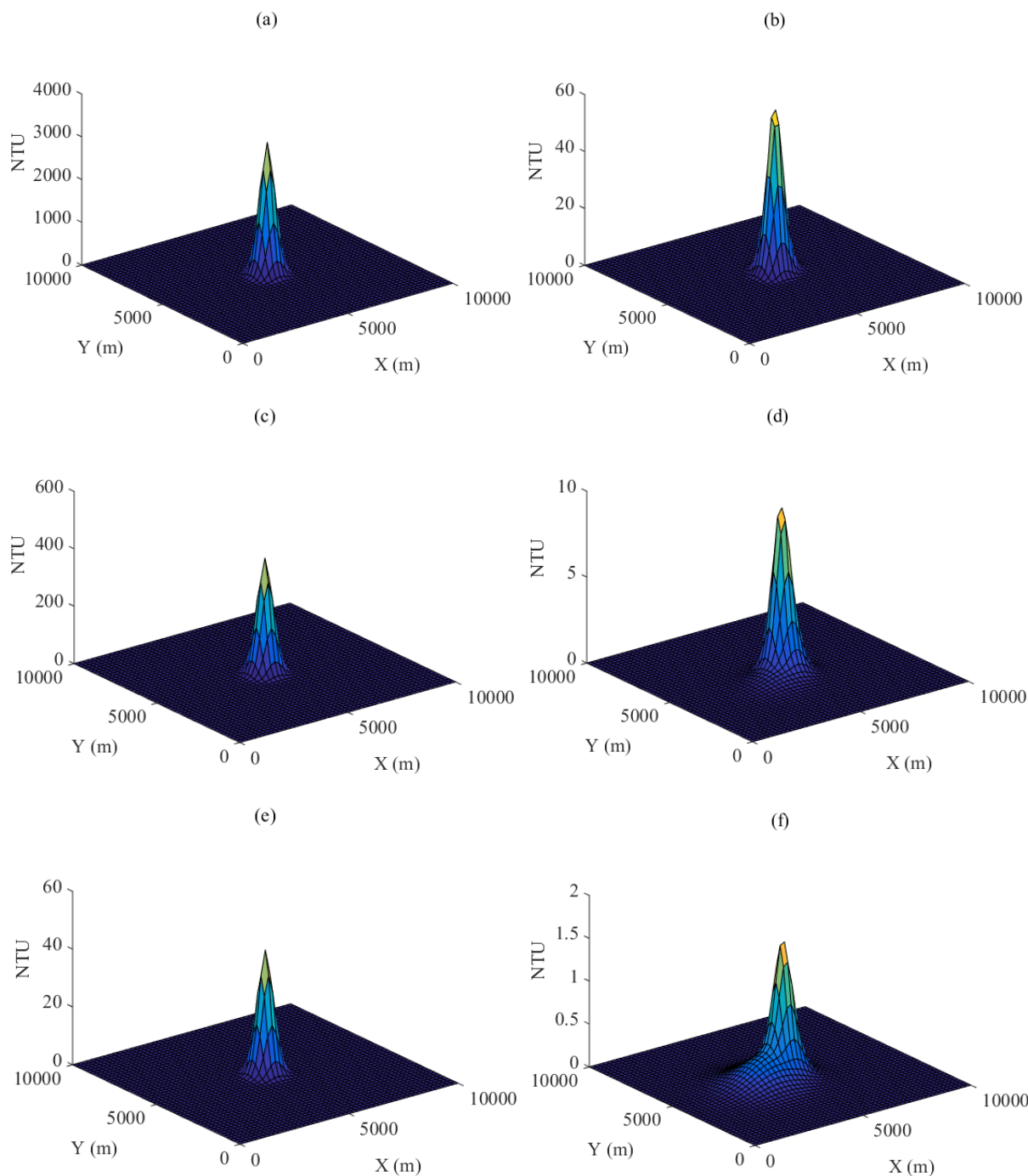
Figure 5.11: The calculation results of turbidity of ocean water in unit of NTU. (a-b), (c-d), and (e-f) describe the turbidity of ocean water at the time of 5 h, 50 h and 100 h after the sediment plume transport; (2) (a, c, e) describe the turbidity of ocean water of the plane nearby the seafloor, and (b, d, f) describe the severity of ill effect of the plane 10 m above the seafloor.

Taking into consideration Eq. 5.18-5.19, the calculation of turbidity of ocean water only considers the parameters of mass concentration of the suspension particles. Analysing Fig. 5.11, with the time going on, the turbidity of ocean water decreases significantly. For instance, at the time of 5 h after the sediment plume transport nearby the seafloor, see Fig. 5.11 (a), the maximum turbidity of ocean water is more than 3000, which is far beyond the

defined environmental acceptable restriction ($t_t \cdot T_{nature} = 96.3$ NTU and 100 NTU). While 95 hours later, the maximum turbidity of ocean water has decreased to 40.5, which is located within the defined environmental acceptable restriction. In addition, compared to the plane nearby the seafloor, the plane of 10 m above the seafloor has a quite small turbidity of ocean water at the same time. Almost all of the calculated turbidity of ocean water at the plane of 10 m above the seafloor could be regarded as environmental acceptable to benthic ocean species. Furthermore, in terms of the parameter of turbidity of ocean water, the environment conditions influenced by the sediment plume could revert to an environmental acceptable degree after 100 hours (roughly four days later).
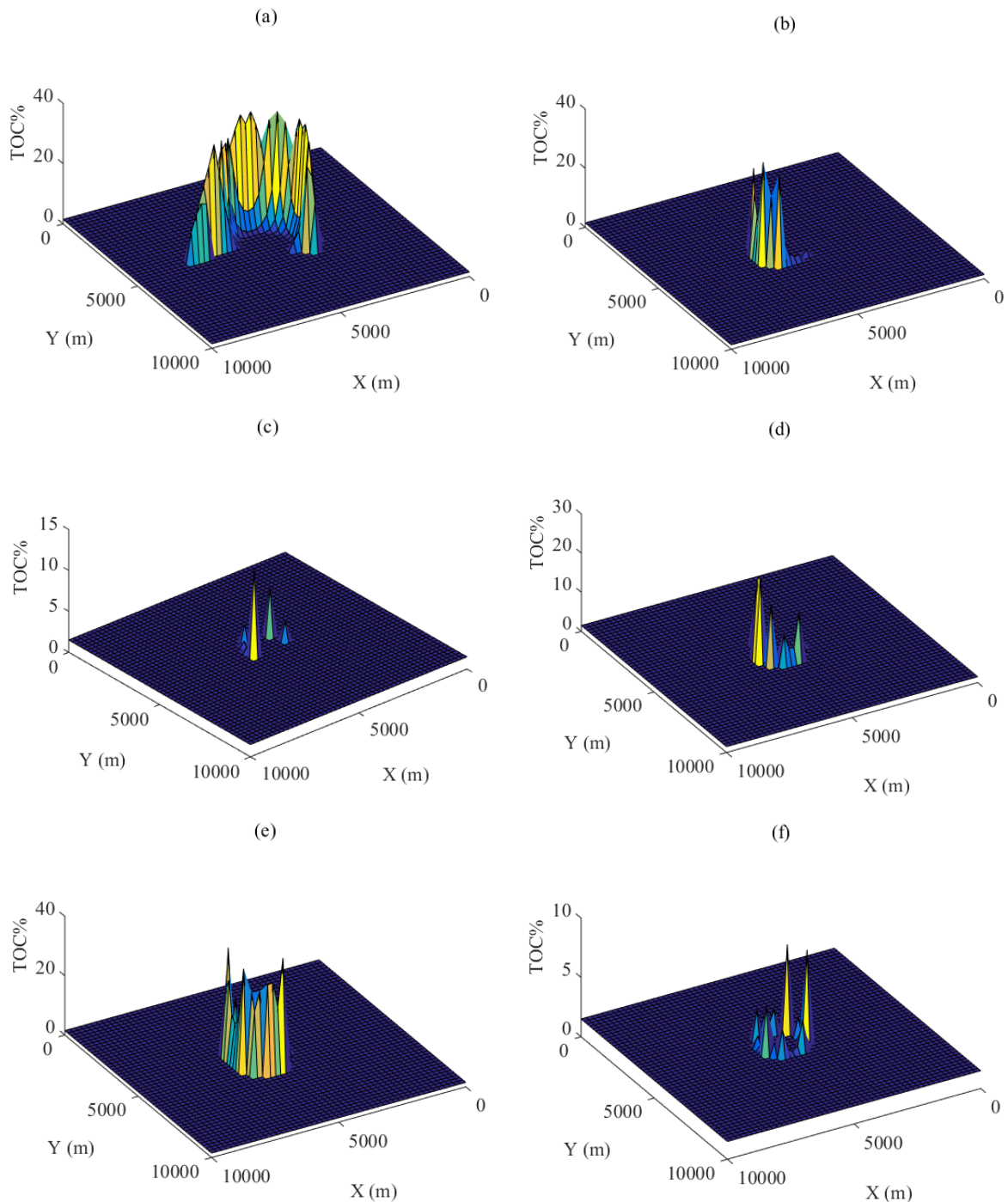
Figure 5.12: Results for total organic carbon within the sediment plume influencing area. (a-f) describes the total organic carbon content at time of 5 h, 20 h, 35 h, 50 h, 65 h, and 80 h later after the sediment plume transport.

Taking into consideration Eq. 5.21 and the selected regression coefficients in section 5.3.3, the critical sedimentation rate is calculated to be $100\, m/m.y.$ Analysing Figure 5.12 (a, b, c), the total organic carbon content (TOC%) decreases with the time going on. It is because the sedimentation rates at such conditions are located in the range of negative effect of TOC% parameter, which also means the sedimentation rates are larger than the critical sedimentation rate. Comparing Figure 5.12 (c, d, e), the maximum total organic carbon content increases from roughly 15%, i.e., figure (c), to 40%, i.e., figure (e). It is because most of sediment plume would settle down within the first 50-60 hours after the formation of sediment plume, while its increase velocity of sedimentation rate also decreases. In Figure 5.12 (c, d, e), the sedimentation rate gets closer and closer to critical point which is reflected on the increase of total organic carbon content. Comparing Figure 5.12 (e, f), the maximum total organic carbon decreases from roughly 40%, i.e., figure (e), to 10%, i.e., figure (f). It presents that these conditions of sedimentation rates are located in the positive effect rage. Combining the increasing principle of total organic carbon content and the law of sedimentation resulting from DSM activities, if the calculation resolution of sediment plume is dense enough, the top view of total organic carbon content should be similar to a ring-like shape, which surrounding values of total organic carbon is larger than the middle of ring-like area. Comparing figure (a) with the left figures, it shows that the obvious increasing area of total organic carbon content is larger than that of figures (b-f). It might be caused by the assumption of initial sediment plumes, while the extraordinary large unit of sedimentation rate used in Eq. 5.21, i.e., m/m.y., would also leads to magnify effect of small sedimentation rate at the beginning of the calculation.

The calculation results in this section reflect that the sediment plume has the most significant impacts on the benthic ocean species at the first 2-3 days. For instance, the ocean water turbidity and total organic carbon content calculated results have greatly exceeded the normal conditions where benthic ocean species used to live within this time period. Although the calculation results of severity of ill effect, see Fig. 5.10, have not reached the degree of lethal and paralethal level, it is because we ignored the sediment plume accumulative impacts, but only analysed its real-time impact within one hour.

5.6. Conclusions

In this chapter, the numerical calculations of DSM environmental impacts are implemented majorly focusing on the sediment plume and species responses. In which, the species responses to sediment plume are discussed and quantified through analyzing a series of ecological indicators, such as the severity of ill effect and deposition thickness.

After conducting the numerical calculation methods of DSM environmental impacts, several recommendations are proposed for the future research.

> ➢ Besides the initial DSM disturbances and plume source, species disturbance, sediment plume, and tailings disposal, the DSM environmental impacts are also influenced by other aspects, such as seafloor topography change, food chain change, and heavy metals concentration change.

> ➢ The interconnections between DSM environmental influencing aspects should be analysed further, and not only be analysed by the parameters of turbidity of ocean water, severity of ill effect, total organic carbon content, and deposition thickness. Other aspects, e.g., toxic elements, illumination, and noise influences, should also be considered.

> ➢ Several formulas used in this chapter, e.g., severity of ill effect and turbidity of ocean water, are determined by the regression analyses of data not derived from deep sea environment. The exact deep sea conditions might be different. Therefore, the field tests seem to be necessary to obtain some reliable data and determine the particular coefficients from the deep sea mining activities.

The research conducted in this chapter could be used for the future DSM environmental performance assessment.

Chapter 6

Multi-criteria Decision Making Applied to Sustainable Deep Sea Mining Vertical Transport Plans*

To analyse the sustainability of DSM transport plans, the technological performance, economic profitability, and environmental impacts of DSM activities are analysed in chapter 3, 4, and 5 respectively. We would integrate the DSM technological performance, economic profitability, and environmental impacts together in this chapter. To determine a sustainable DSM vertical transport plan chapter 6 applies a MCMD (Fuzzy-ANP) method into the assessment system taking into consideration the numerical calculations results in the chapter 3-5 integrally. In this chapter, section 6.1 gives an introduction of the current research status of MCMD applications to address the industrial sustainability problems. Section 6.2 explains the MCDM method and evaluating criteria selection. In section 6.3, the numerical calculation principles and definitions of the evaluating criteria are described in detail. Then section 6.4 focuses on a case demonstrating the application procedure of the method. Finally, conclusions and recommendations for the conducted research are given in section 6.5.

6.1. Introduction

Recent advances in deep sea mining (DSM) strategies have led many international marine mining companies to develop implementation plans for the first seabed mining project. For example, the Canadian company Nautilus Minerals has stated its aim to begin mining minerals from the seabed belonging to Papua New Guinea in 2019 (Mining Weekly, 2018). Nautilus Minerals company has also announced that they will be chartering a production support vessel (PSV) from Fujian Mawei Shipbuilding Ltd. for $199,910 per day, for a rental period of at least five years (Nautilus Minerals, 2018b). It seems like that – in the near future – the DSM industry will move forward from this planning phase and begin the process of large-scale industrial mining process. Despite this, no current research exists that looks at the

sustainability of DSM vertical transport plans and takes into account the associated technological, economic, environmental and social factors related.

The schematic diagram of a DSM project is shown in Figure 6.1. The majority of the workload involved in DSM takes place at sea. A key research topic – and one that has received considerable prior attention – is the environmental impact of DSM activities, particularly given the low productivity and vulnerability of deep ocean ecology (Van Dover, 2011; Jones et al., 2017). Beside environmental impacts, both the technological and economic considerations of DSM are key components in the development of a sustainable DSM transport plan (Ma et al., 2017a, b). Furthermore, other researchers also have examined the social implications of DSM in influencing sustainability projects (Roche and Bice, 2013).
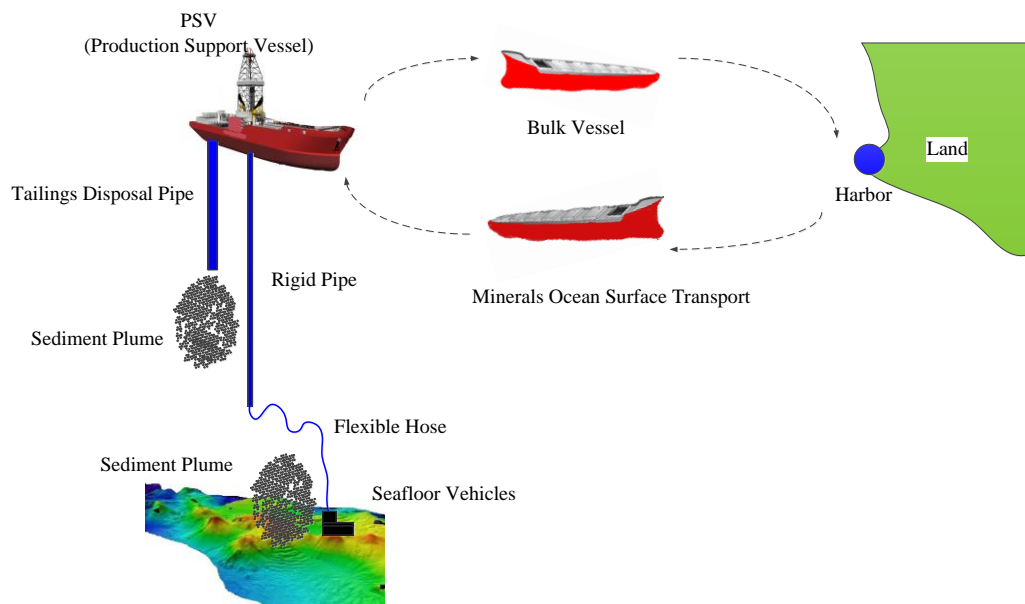
Figure 6.1: Schematic diagram of one kind of DSM project (Ma et al., 2018a, b).

Given that the decision making process for a sustainable DSM transport plan involves the integration of several discrete-related criteria, a traditional cost-benefit model would not be qualified to address this problem. A method of *multi-criteria decision making* (MCDM) has been adopted in this research, following its successful application to a number of industrial fields (e.g. coastal mining, sustainable project planning, manufacturing system scheduling) to address similar multiple criteria problems (Ho et al., 2010; Ha and Krishnan, 2008; Rezaei, 2015; Titus and Liberatore, 1991; Ng, 2008; Liao, Z. and Rittscher, 2007; Padhye and Deb, 2011). The discipline of MCDM was first proposed by Zionts in 1979. Since then, the framework of MCDM has been used extensively throughout a variety of fields. Following review of the existing literature, when applying the MCDM theory in DSM system, three key practices are identified: MCDM method selection, evaluation criteria determination, and the calculation of criteria weights (Kahraman, 2008; Pohekar and Ramachandran, 2004).

Fuzzy set theory is a widely used algorithm that allows imprecise and uncertain information to be examined through rigorous mathematical process (Zadeh, 1965). It has previously been used to integrate qualitative information and allow *fuzzy* date to be expressed as *crispy* evaluation weights (Boran et al., 2009). The method of analytic network process (ANP) was

developed by Saaty in the 1990s taking into consideration of the interdependencies between different evaluation criteria. It represents the development of analytic hierarchy process (AHP) method. Both ANP and AHP methods have the ability to divide a complex MCDM problem into several hierarchies with specific affiliation relationships. ANP has a highly systematic procedure of application and is quite easy to understand. Fuzzy & analytic network process (Fuzzy-ANP) is a typical integrated MCDM method, which integrates fuzzy set theory with ANP methodology. Mohanty et al. (2005) applied a Fuzzy-ANP approach to analysis of the iron and steel industries of Southeast Asia, developing this approach further to describe a structured methodology to evaluate preference ambiguity in decision makers (DMs). Promentilla et al. (2008) redeveloped the Fuzzy-ANP method by redefining the *fuzzy scale* in terms of the degree of fuzziness, confidence level, and attribute toward fuzziness. They used this redeveloped Fuzzy-ANP method to evaluate contaminated site remedial countermeasures. Pang (2009) analysed supplier selection in order to facilitate optimal order allocation, by combining the Fuzzy-ANP method with fuzzy preference programming. Zhou (2012) proposed a systematic analytic framework using Fuzzy-ANP methodology to address project selection and evaluation problems. Given that the Fuzzy-ANP method has been successfully applied to such a wide variety of industrial research fields, it was selected and utilised in this paper for evaluation of sustainability in DSM vertical transport plans.

The objective of this paper is to evaluate the sustainability of DSM vertical transport plans through Fuzzy-ANP analysis. The paper is arranged as follows: the first (previous) section introduces the principles and aims of our research; the second section explains the MCDM methodology and evaluation criteria selection. In the third section, numerical calculation principles and definitions of the evaluation criteria are described in detail. The fourth section focuses on a test case, demonstrating the application procedure for our framework. In the fifth section, conclusions and recommendations for future research are presented.

6.2. Multi-criteria decision making method

6.2.1. Research outline

The research outline of this paper is illustrated in Figure 6.2. The major research components are vertical transport plan generation, questionnaire survey, and MCDM (Fuzzy-ANP) application.
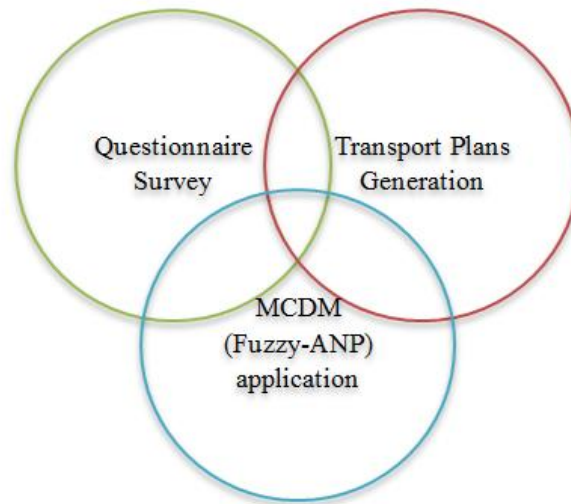
Figure 6.2: Major research components of this chapter.

- **Vertical transport plans generation**

Before the application of MCDM method, a set of DSM vertical transport plans should be generated for evaluation. The formation of the evaluated DSM transport plans is a long vector, and the elements in the vector are the values of all evaluation criteria. The variables involved in a DSM transport plan consist of the type of lifting technology, e.g., continuous line bucket technology (CLB), pipe lifting with centrifugal pumps or with airlifting pumps, working period, maximum winch force (for CLB systems), pipe diameter and gas flux rate for hydraulic lifting and airlifting systems respectively. The vertical transport plans majorly connect with the vertical lifting technologies, e.g., continuous line bucket lifting, hydraulic lifting with centrifugal pump and airlifting systems. In real-life DSM working conditions, different vertical lifting methods require different compatible technology systems, such as tailings disposal systems and mineral processing systems. These may influence sustainability assessments of DSM vertical transport plans (Sharma, 2011; Hoagland et al., 2010). In this paper, however, the influences of such compatible systems on vertical lifting technologies are considered to be negligible. The sustainability evaluation framework described in this paper could be used in whole project assessment in DSM following the initial assessment of the technological, economic, environmental, and social factors at play (presented in this paper).

- **Questionnaire survey**

Expert opinion is elicited through the designed questionnaire in order to determine the evaluation criteria weights. 27 researchers and engineers – in the fields of environmental impact, policy making, marine mining, project sustainability consultancy, and economic profitability – participated in this questionnaire survey.

- **MCDM application**

Through the application of MCDM methodology, all DSM vertical transport plans can be evaluated and ranked, based on a comprehensive performance index that takes into consideration the technological, economic, environmental, and social aspects of these plans. The detailed explanation of the MCDM application is given in the following section.

6.2.2. MCDM application procedure

Following a literature review of existing MCDM applications to sustainable project planning, manufacture scheduling systems, and other, similar, industrial problems, an application procedure for a Fuzzy-ANP MCDM method was derived and is summarised in Figure 6.3. The procedure consists of 4 steps.
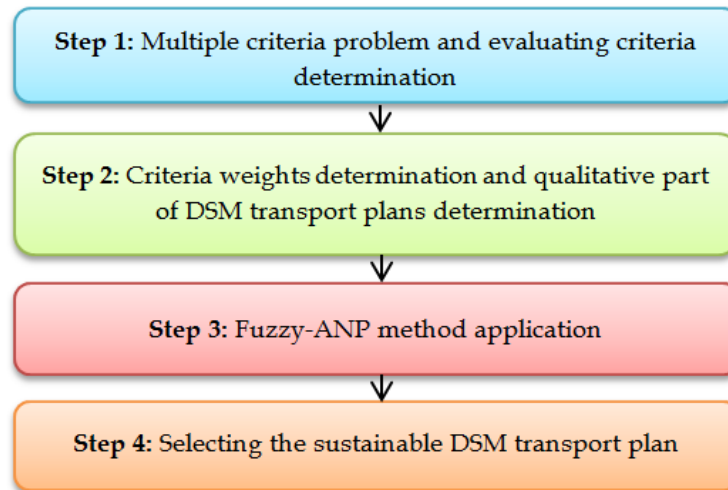
Figure 6.3: Application procedure of Fuzzy-ANP method for sustainable DSM transport plan selection.

- **Step 1: Defining the multi-criteria problem and evaluating criteria determination**

a) Problem definition

Determination of a sustainable DSM vertical transport plan is dependent on technological, economic, environmental, and social factors. These factors are, of course, not completely independent of one another and are likely to exhibit a number of inter factorial relationships with each other. After consideration of the complexities and characteristics involved in selecting a sustainable DSM transport plan, it quickly becomes apparent that the traditional cost-benefit model is unsuitable in this context.

b) Evaluating criteria determination

MCDM has not, until now, been applied to DSM projects. Despite this, a number of useful theories, application frameworks, and evaluation criteria – some of which have potential utility in DSM vertical transport plan sustainability assessment – have been developed in other, related research fields, such as coastal mining, sustainable project planning, and manufacturing system scheduling (Ho et al., 2010; Ha and Krishnan, 2008; Rezaei, 2015; Titus and Liberatore, 1991; Ng, 2008; Liao, Z. and Rittscher, 2007; Padhye and Deb, 2011). Using these pre-existing evaluation criteria, along with knowledge of the real-life working conditions involved in DSM activities, a set of evaluation criteria for use in the decision making process for sustainable DSM vertical transport plans is proposed in Table 6.1.

Table 6.1: Evaluating criteria for selecting the sustainable DSM transport plan (Jovanović et al., 2009; McDowall and Eames, 2007; Pilavachi et al., 2009; Afgan and Carvalho, 2008; Begić and Afgan, 2007; Mamlook et al., 2001; Akash et al., 1999; Chatzimouratidis and Pilavachi, 2009; Yedla and Shrestha, 2003).

Major criteria	Subcriteria	Parameter attribute
Technological aspect	Specific energy consumption for lifting	Quantitative
	Proven technology	Qualitative
	Technology reliability	Qualitative
	Production rate	Quantitative
	Technology availability	Qualitative
Economic aspect	Gross income	Quantitative
	Capital cost	Quantitative
	Operation and maintenance cost	Quantitative
	Investment recovery period	Quantitative
Environmental aspect	Species disturbance variance	Quantitative
	Severity of ill effect	Quantitative
	Turbidity of ocean water	Quantitative
	Total organic carbon content & sedimentation rate	Quantitative
	Sedimentation thickness	Quantitative
Social aspect	Social acceptability	Qualitative
	Policy support & legislation & regulation (PLR)	Qualitative

As presented in Table 6.1, the major criteria in our methodology are the technological, economic, environmental, and social aspects of a sustainable DSM transport plan. These have both quantitative and qualitative subcriteria. For example, *technological* subcriteria include such quantitative parameters as *specific energy consumption for lifting* and *production rate*, and qualitative parameters, such as *technological reliability*. Subcriteria are not completely independent of one another. For instance, there is a relationship between the *proven technology*, *technology reliability* and *technology safety*, because a well-proven technology tends to be associated with good technology reliability and high levels of safety (Haralambopoulos and Polatidis, 2003; Ligus, 2017; Chatzimouratidis and Pilavachi, 2009).

- **Step 2: Criteria weights determination**

In Fuzzy-ANP method, the criteria evaluating weights are determined through pairwise comparison method. The acceptance of pairwise comparison matrix is based on the consistency index (CI) and consistency ratio (CR). If CR is larger than 0.10, the pairwise comparison matrixes are not acceptable (Yüksel and Dagdeviren, 2007). The parameter of CI could be calculated as follows (Zhang et al., 2015; Yüksel and Dagdeviren, 2007).

$$CI = \frac{\lambda_{max} - n}{n - 1} \tag{6.1}$$

in which λ_{max} represents the maximum eigenvalue of pairwise comparison matrix, n represents the matrix dimension.

The parameter of CR could be calculated as follows (Zhang et al., 2015; Yüksel and Dagdeviren, 2007).

$$CR = \frac{CI}{RI} \tag{6.2}$$

in which RI means the random index.

- **Step 3: Fuzzy-ANP method application**

When applying AHP methodology to multiple criteria problems, all criteria and subcriteria are required to be independent of each other. However, in many real-life working conditions, there may be dependencies that exist between the different criteria. To overcome this problem, Saaty developed the ANP method in 1990s (Saaty, 2005). A Fuzzy-ANP method was selected for use in this paper to evaluate the sustainability of DSM transport plans. This methodology has the further advantage of allowing consideration of both qualitative evaluation criteria as well as the dependency relationships between different criteria.

- **Step 4: Sustainable DSM transport plan selection**

After the analyses of Fuzzy-ANP method, all the DSM vertical transport plans could be evaluated based on a comprehensive performance index, see Eq. 6.3 (Xu and Yang, 2001). The transport plan with the maximum comprehensive index is regarded to be more preferable, i.e., the sustainable DSM vertical transport plan.

$$P_j = \sum_{i=1}^{m} w_i \cdot v_{ij} \tag{6.3}$$

in which P_j means the comprehensive performance of DSM transport plan No. j, w_i means the weight of evaluating criterion i, v_{ij} is the transport plan's score in terms of criterion i.

6.3. Evaluating criteria for sustainability of DSM vertical transport plans

In this section, the numerical calculation principles and definitions of these evaluating criteria for sustainable DSM vertical transport plan are explained in detail. The authors' previous work (Ma et al., 2017a-c, 2018a-b) also elaborates these evaluating aspects regarding to the DSM technological, economic and environmental impacts systematically.

6.3.1. Technological subcriteria

- **Specific energy for lifting**

The specific energy consumption for lifting could be calculated as follows (Ma et al., 2017a).

$$EC = \frac{E_t}{Q_s \cdot H} \tag{6.4}$$

in which E_t represents the total energy consumption per time unit, Q_s represents the mineral production rate, H represents the vertical transportation distance. In this chapter we compare three different methods: the mineral vertical transportation technologies, e.g., the continuous line bucket lifting (CLB), hydraulic lifting (HL) with centrifugal pumps and airlifting (AL) systems. Figure 6.4 depicts a schematic diagram of a CLB system and a HL system (Ma et al., 2017a). The arrangement of AL system is quite similar to the centrifugal lifting system, i.e., Figure 6.4 (b). The differences are located at: (i) air compressors are put on the production support vessel (PSV); (ii) an auxiliary pipe is required to transport the compressed air to the lifting pipe (Yoshinaga and Sato, 1996). For CLB systems, its total energy consumption is related closely with the winch force and speed supplied by the steel ropes, see Eq. 6.5 (Schulte, 2013). For HL system, the required pressure drops lifting the mineral mixtures and lifting pipe dimension majorly determine its energy consumption, see Eq. 6.6 (Shook and Bartosik, 1994). The inlet pressure and gas flux rate are very firmly connected with the energy consumption of airlifting systems, see Eq. 6.7 (Yoshinaga and Sato, 1996).

$$E_t = \frac{F_{wi} \cdot v_c}{\eta_f} \tag{6.5}$$

in which F_{wi} represents the winch force, v_c represents the cable moving velocity, and η_f represents the mechanical efficiency.

$$E_t = \frac{v_m \cdot A_p \cdot P_r}{\eta_h \cdot (a_w)^{N_p}} \tag{6.6}$$

in which P_r represents the required pressure difference to lift the mineral mixtures from the seabed to the ocean surface, v_m represents the mineral mixture velocity, N_p is the number of centrifugal pumps, a_w represents the working ability factor of centrifugal pumps, A_p means the cross-section area of the rigid pipe, η_h means the hydraulic efficiency.

$$E_t = J_{g\_atm} \cdot A_p \cdot ln \frac{P_I}{P_{atm}} \tag{6.7}$$

in which J_{g_atm} means the gas flux rate under the atmospheric pressure, P_I and P_{atm} mean the inlet pressure and the atmospheric pressure respectively.

- **Proven technology**

Proven technology could be defined as the maturity of the utilized technology. For a good proven technology, its initial working faults and inherent problems have been decreased or even eliminated through a long developing and application process (Chapman, 2016; Anuar et al., 2015).

- **Technology reliability**

Technology reliability could be defined as the technical ability of continuous working properly according to its specifications. A reliable technology has a large possibility to complete its target under a normal working condition (Johnson and Ettlie, 2001).

- **Production rate**

For CLB systems, its production rate is determined by the cable lifting velocity and bucket dimensions, see Eq. 6.8 (Schulte, 2013).

$$Q_s = \frac{v_c \cdot l^3 \cdot \gamma \cdot \rho_m}{l + l_s} \tag{6.8}$$

in which Q_s represents the mineral production rate, l_s means the span length of the adjacent buckets, γ is the bucket filling ratio, ρ_m represents the density of in-situ sediment, l means the bucket side length, v_c means the cable moving velocity.

For AL systems, the mineral production rate could be calculated taking into consideration the flux rate of solid particles and cross-section area of lifting pipes, see Eq. 6.9 (Yoshinaga and Sato, 1996).

$$Q_s = J_s \cdot A_p \cdot \rho_m \tag{6.9}$$

in which J_s means the solid particle flux rate.

- **Technology availability**

Technology availability refers to the possibility and accessibility of utilizing the technology in DSM specific working conditions with the correct format (Pick et al., 2013).
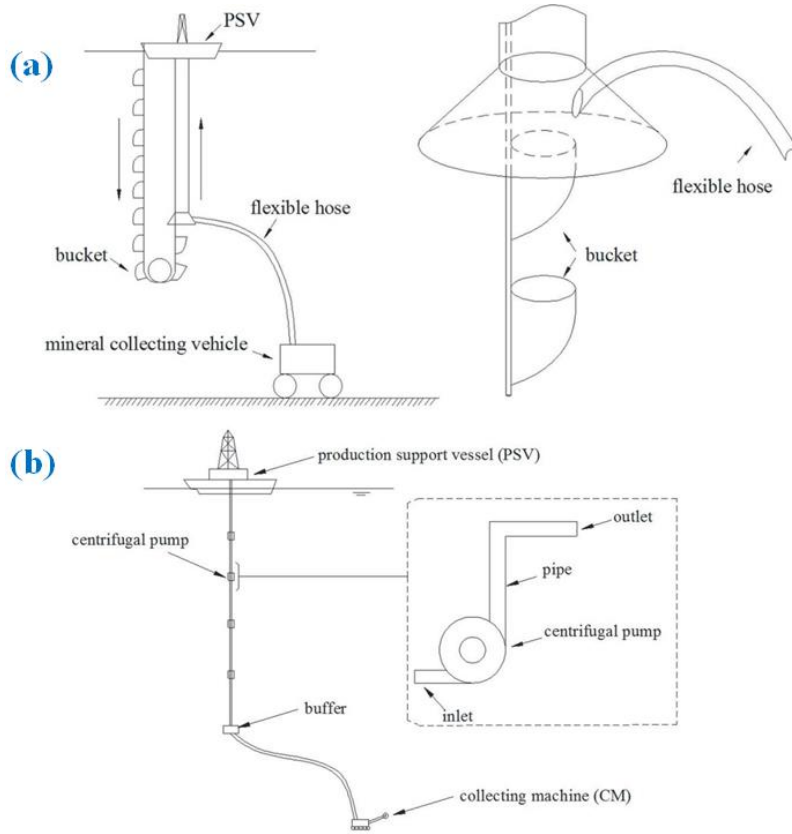
Figure 6.4: Schematic diagrams of a CLB and a HL system.

6.3.2. Economic subcriteria

- **Gross income**

Gross income represents the income derived from the mineral extraction in DSM activities, which could be calculated as follows (Ma et al., 2017a).

$$M_{in} = \sum_{i=1}^{N}\left(3.6 \cdot h_o \cdot s \cdot \lambda_s \cdot Q_s \cdot M_{i,mm} \cdot (1+a)^N\right) \qquad (6.10)$$

in which N represents the mining period in year, h_o represents the mean working hours per day, λ_s is the percentage of gross minerals left after processing, s represents the working days per year, $M_{i,mm}$ represents the mineral ores price, a represent the inflation rate.

- **Capital cost**

Capital cost could be explained as the one-time expenditure purchasing the equipment and constructions for production. It is the whole initial expenditure to bring a DSM project to a commercially operable status (UKessays, 2018).

- **Operation and maintenance cost**

Operation and maintenance cost is defined as the expenditure to support the normal running of a DSM project, which covers the maintenance cost (repairing & replacing), labour cost and energy consumption cost (Sharma, 2011; Nyhart et al., 1978). Nyhart et al. (1978) categorized both the capital cost and operation and maintenance cost into three aspects: mining, transport and processing sectors, see Eq. 6.11.

$$
\begin{cases}
M_c = M_{c\_m} + M_{c\_t} + M_{c\_p} \\
M_o = M_{o\_m} + M_{o\_t} + M_{o\_p}
\end{cases}
\tag{6.11}
$$

in which M_c and M_o represent the capital cost and operation plus maintenance cost, the subscripts of m, t, p represent the mining, transport and processing sectors respectively.

- **Investment recovery period**

The investment recovery period, also known as payback period, refers to the period to recover the investment of a DSM project. It is an important economic parameter to determine whether a DSM project is profitable or not. For DSM project investors, they would prefer the investment recovery period to be as small as possible (Investopedia, 2018). Investment recovery period is determined by comparing the net cash inflow with net cash outflow. In this chapter, it could be simply understood as the period when the gross income is larger than the initial capital cost and operation and maintenance cost.

6.3.3. Environmental impact subcriteria

- **Species disturbance variance**

Species disturbance variance is an integrated ecological index by comparing the species conditions before and after the DSM activities, which could be calculated as follows (Ma et al., 2018b).

$$
Var(SD) = E\left[\sum_{i=1}^{9} \left(1 - \frac{SD_{aft}(i)}{SD_{bef}(i)} \right)^2 \right]
\tag{6.12}
$$

in which the subscripts of *aft* and *bef* reflect the species conditions after the DSM disturbances and before disturbances respectively, *SD* represents the integrated species index including Margalef's indices, Shannon diversity index, and Simpson diversity index, see Eq. 6.13 (Ma et al., 2018b).

$$
SD_{bef/aft} = \begin{bmatrix} I_1 & I_2 & I_3 & I_3' & I_4 & D_V & D_N & D_H & D_S \end{bmatrix}
\tag{6.13}
$$

in which $(I_1 \quad I_2 \quad I_3 \quad I_3' \quad I_4 \quad D_V \quad D_N)$, D_H, and D_S represent the Margalef's indices, Shannon diversity index, and Simpson diversity index respectively.

- **Severity of ill effect**

Severity of ill effect is another important ecological parameter proposed by Newcombe and Jensen (1996) through a meta-analysis, which is introduced in DSM activities (Ma et al., 2018b). The severity of ill effect is defined as Table 6.2.

Table 6.2: Severity of ill effect on marine species description (Newcombe and Jensen, 1996).

Severity		Description of effects
Nil effect	0	No behavioural effects
Behavioural effects	1	Alarm reaction
	2	Abandonment of cover
	3	Avoidance responses
Sublethal effects	4	Short-term reduction in feeding rates; Short-term reduction in feeding success;
	5	Minor physiological stress; Increase in rate of coughing; Increase respiration rate;
	6	Moderate physiological effects;
	7	Moderate habitat degradation; Impaired home;
	8	Indications of major physiological stress; Long-term reduction in feeding rate; Long-term reduction in feeding success; Poor condition;
Lethal and paralethal effects	9	Reduced growth rate; Delayed hatching; Reduced fish density;
	10	0-20% mortality; Increased predation; Moderate to severe habitat degradation;
	11	>20%-40% mortality
	12	>40-60% mortality
	13	>60-80% mortality

Severity of ill effect could be calculated as Eq. 6.14 (Newcombe and Jensen, 1996).

$$S_{if} = \alpha + \beta\left(log_e\, t\right) + \chi\left(log_e\, C_s\right) \tag{6.14}$$

in which S_{if} represents the severity of ill effect, α, β and χ represent the regression analysis coefficients, C_s and t represent the sediment plume mass concentration and residence time respectively, which could be determined by solving the plume advection-diffusion model (Ma et al., 2018b).

- **Turbidity of ocean water**

Based on the literature review, most species have their particularly preferable ocean turbidity range (Cyrus and Blaber, 1987a; Dyer, 1972). To control the benthic species community impacts within an environmental acceptable range, the changing rate of turbidity of ocean water should be constrained, see Eq. 6.15 (Cyrus and Blaber, 1987a, b).

$$CR_{NTU} = \frac{\gamma \cdot C_S{}^{\lambda}}{T_{nature}} \tag{6.15}$$

in which CR_{NTU} represents the changing rate of turbidity of ocean water, γ and λ are the regression analysis coefficients, T_{nature} is the historical turbidity at the mining site before mining disturbances.

- **Total organic carbon content**

Total organic carbon content is an important ecological indicator which could be influenced significantly by DSM activities (Saleem et al., 2016). Similarly like the turbidity of ocean water, in order to minimize the impact on benthic ocean species, the changing rate of total organic carbon content should also be taken into consideration. It could be understood as the smaller the changing rate of total organic carbon content is, the less the caused environmental impacts are. The total organic carbon content could be calculated as Eq. 6.16.

$$log(TOC) = \begin{cases} a_1 \cdot log(Se) + b_1 & Se \leq S_{cri} \\ a_2 \cdot log(Se) + b_2 & Se \geq S_{cri} \end{cases} \tag{6.16}$$

in which Se represents the sedimentation rate, a_1, a_2, b_1, and b_2 are the coefficients determined through the regression analysis, S_{cri} is the critical sedimentation rate where the maximum total organic carbon content is.

- **Sedimentation thickness**

Different benthic ocean species, e.g., coral, sponges, holothurian and other macrofauna, have different resistance abilities to the sedimentation burial thickness (Lohrer et al., 2006; Thrush and Dayton, 2002; Cummings et al., 2003). The larger the sedimentation thickness is, the more intensive the DSM impacts on the ecological community are. The most direct connection between the technological and environmental impact aspects is the minerals production rate (Ma et al., 2018b).

6.3.4. Social subcriteria

- **Social acceptability**

Social acceptability is regarded as one of the most important parameters, which is closely related to the success of a DSM project (Brunson et al., 1996). In this chapter, social acceptability is a qualitative parameter which value is derived from the experts' opinions.

- **Policy (legislation & regulation) support**

Policy support refers to the possibility to be supported by the marine policy, mining legislation and regulation, which is also regarded as one of the most important parameters for the implementation of a DSM project (Lewis and Wiser, 2007).

6.4. Demonstrate case: Fuzzy-ANP method application

6.4.1. Criteria weights determination

After collating experts' opinions provided through the completion of the questionnaire, the data were checked through the functions of consistency index (CI) and consistency ratio (CR), as Eq. 6.1-6.2. The weights of the major criteria, including technological (TEC), economic (ECO), environmental (ENV), and social (SOC) aspects, can then be determined (assuming independence of one another).

$$w_1 = \begin{bmatrix} \text{TEC} \\ \text{ECO} \\ \text{ENV} \\ \text{SOC} \end{bmatrix} = \begin{bmatrix} 0.3490 \\ 0.3563 \\ 0.1706 \\ 0.1241 \end{bmatrix} \quad (6.17)$$

Following this, the interconnections (or dependencies) between the major criteria can be examined, see Figure 6.5 (Ma et al., 2017a). Depending on the pairwise comparison matrices derived from the experts' opinions, dependency weight vectors for technological, economic, environmental, and social factors can be listed subsequently.

$$\begin{cases} w_2 = \begin{bmatrix} 0.4471 & 0.3074 & 0.2455 \end{bmatrix}^{\text{T}} \\ w_3 = \begin{bmatrix} 0.4659 & 0.2759 & 0.2581 \end{bmatrix}^{\text{T}} \\ w_4 = \begin{bmatrix} 0.3553 & 0.4041 & 0.2407 \end{bmatrix}^{\text{T}} \\ w_5 = \begin{bmatrix} 0.3089 & 0.4027 & 0.2884 \end{bmatrix}^{\text{T}} \end{cases} \quad (6.18)$$
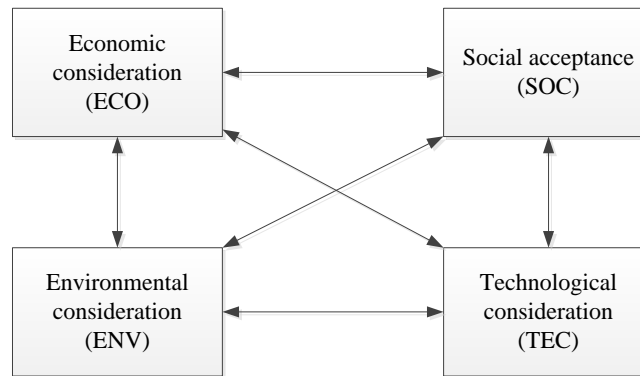
Figure 6.5: Schematic diagram reflecting the interconnection relationship between the major criteria (Ma et al., 2017c).

The interconnection matrix for the major criteria is determined as follows.

$$w_6 = \begin{bmatrix} 1.0000 & 0.4659 & 0.3553 & 0.3089 \\ 0.4471 & 1.0000 & 0.4041 & 0.4027 \\ 0.3074 & 0.2759 & 1.0000 & 0.2884 \\ 0.2455 & 0.2581 & 0.2407 & 1.0000 \end{bmatrix} \tag{6.19}$$

Next, the evaluating weighs of major criteria taking into consideration the interconnections could be calculated as follows.

$$w_7 = \begin{bmatrix} TEC \\ ECO \\ ENV \\ SOC \end{bmatrix} = w_6 \cdot w_1 = \begin{bmatrix} 1.0000 & 0.4659 & 0.3553 & 0.3089 \\ 0.4471 & 1.0000 & 0.4041 & 0.4027 \\ 0.3074 & 0.2759 & 1.0000 & 0.2884 \\ 0.2455 & 0.2581 & 0.2407 & 1.0000 \end{bmatrix} \times \begin{bmatrix} 0.3490 \\ 0.3563 \\ 0.1706 \\ 0.1241 \end{bmatrix} = \begin{bmatrix} 0.6139 \\ 0.6313 \\ 0.4120 \\ 0.3428 \end{bmatrix} \xrightarrow{\text{unitization}} \begin{bmatrix} 0.3070 \\ 0.3156 \\ 0.2060 \\ 0.1714 \end{bmatrix}$$

$$\tag{6.20}$$

Comparing the weights of major criteria considering the interconnection relationship or not, i.e., w_1 and w_7, we found that the evaluating weights order of major criteria has not been changed, i.e., ECO>TEC>ENV>SOC . However, after considering the interconnection relationship between all evaluating criteria, the evaluating criteria, e.g., social impact consideration, which are easily overlooked, have been evaluated more objectively and fairly (Liao et al., 2018; Azis, 2003).

Weights determinations for subcriteria follow the similar principles to those of the major criteria. However, in order to reduce the difficulty of data collection and to reduce the number of calculations, we treated the evaluation subcriteria as independent of each other. The subcriteria for each major criterion are listed as follows. Technological: energy consumption (EC), proven technology (PT), technology reliability (TR), production rate (PR), and technology availability (TA). Economic: gross income (GI), capital cost (CC), operation and maintenance cost (OM), and investment recovery period (IRP). Environmental: species disturbance variances (SD), severity of ill effect (SIE), turbidity of ocean water (TOW), total organic carbon content (TOC), and sedimentation thickness (ST). Social: social acceptability (SA) and policy support (PS). The weights for all subcriteria can be calculated based on the pairwise comparison matrices, as follows:

$$\begin{cases} w_8 = \begin{bmatrix} EC & PT & TR & PR & TA \end{bmatrix}^T = \begin{bmatrix} 0.1373 & 0.1808 & 0.2533 & 0.2302 & 0.1984 \end{bmatrix}^T \\ w_9 = \begin{bmatrix} GI & CC & OM & IRP \end{bmatrix}^T = \begin{bmatrix} 0.2339 & 0.2454 & 0.2684 & 0.2523 \end{bmatrix}^T \\ w_{10} = \begin{bmatrix} SD & SIE & TOW & TOC & ST \end{bmatrix}^T = \begin{bmatrix} 0.2435 & 0.2597 & 0.1410 & 0.1750 & 0.1808 \end{bmatrix}^T \\ w_{11} = \begin{bmatrix} SA & PS \end{bmatrix}^T = \begin{bmatrix} 0.3857 & 0.6143 \end{bmatrix}^T \end{cases} \tag{6.21}$$

The global weights of all evaluating subcriteria (w_{12}) could be determined by multiplying the individual weights, e.g., w_{8-11}, with the major criteria weight, i.e., w_7, see Figure 6.6.

$$w_{12} = \begin{bmatrix} EC & PT & TR & PR & TA & GI & CC & OM... \\ IRP & SD & SIE & TOW & TOC & ST & SA & PS \end{bmatrix}^{T}$$

$$= \begin{bmatrix} 0.0421 & 0.0555 & 0.0778 & 0.0707 & 0.0609 & 0.0738 & 0.0774 & 0.0847... \\ 0.0796 & 0.0502 & 0.0535 & 0.0290 & 0.0361 & 0.0373 & 0.0661 & 0.1053 \end{bmatrix}^{T}$$

(6.22)
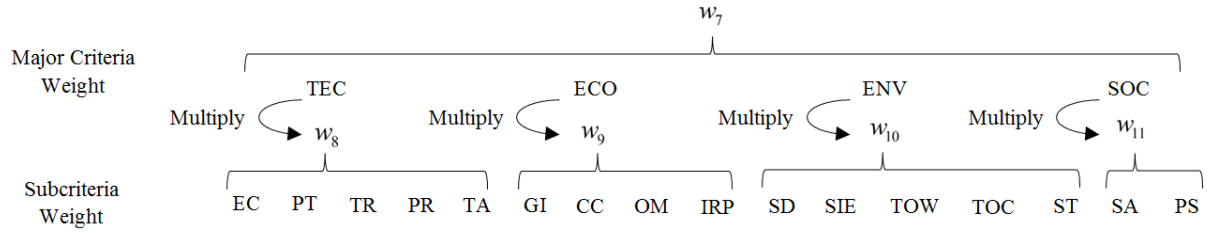
Figure 6.6: Schematic diagram of the global subcriteria weights determination.

6.4.2. Qualitative evaluating criteria

In this chapter, besides the quantitative evaluating criteria, there are a series of qualitative evaluating criteria. As shown in table 6.1, the qualitative evaluating criteria consist of proven technology (PT), technology reliability (TR), technology availability (TA), social acceptability (SA) and policy support (PS). In this chapter, we compared three kinds of vertical lifting technologies in DSM activities, i.e., continuous line bucket lifting (CLB), hydraulic lifting (HL), and airlifting (AL) systems. As we all known, the most accurate evaluations of these qualitative criteria should be combined with the specific DSM transport plans. Here, in this chapter, the scores of these qualitative evaluating parameters for all DSM transport plans are simplified to be directly connected with the vertical lifting technologies. Based on the collected data through questionnaire, the scores of all these DSM transport plans in terms of proven technology could be calculated through the Mean of Maxima (MOM) defuzzification method (Ozdemir, 2010).

$$PT_{CLB} = \frac{\left(\sum_{j=1}^{n} \frac{f_{x1j}}{n} \quad \sum_{j=1}^{n} \frac{f_{x2j}}{n} \quad \sum_{j=1}^{n} \frac{f_{x3j}}{n} \quad \sum_{j=1}^{n} \frac{f_{x4j}}{n} \right)}{4} = \frac{\left(0.2909 \quad 0.3727 \quad 0.4364 \quad 0.5364 \right)}{4} = 0.4091 \ (6.23)$$

Following the same principle, the scores for the other qualitative evaluating parameters are listed as follows.

$$\begin{cases} PT_{CLB} = 0.4091 \\ PT_{HL} = 0.6250 \\ PT_{AL} = 0.2159 \end{cases} \begin{cases} TR_{CLB} = 0.3545 \\ TR_{HL} = 0.6455 \\ TR_{AL} = 0.2909 \end{cases} \begin{cases} TA_{CLB} = 0.5341 \\ TA_{HL} = 0.6364 \\ TA_{AL} = 0.2250 \end{cases} \begin{cases} SA_{CLB} = 0.2725 \\ SA_{HL} = 0.6200 \\ SA_{AL} = 0.4375 \end{cases} \begin{cases} PS_{CLB} = 0.3575 \\ PS_{HL} = 0.6950 \\ PS_{AL} = 0.5100 \end{cases}$$

(6.24)

6.4.3. DSM vertical transport plans evaluation

Before the application of MCDM to DSM vertical transport plan evaluation, two assumptions are first made, as follows: (i) the minerals storage richness is sufficient for the whole mining period, and (ii) reduction in marine species numbers is simplified to be related to the mineral production rate (see Table 6.3).

The parameters involved in the MCDM methodology for selecting a sustainable DSM vertical transport plan are presented in Table 6.3.

Table 6.3: Given parameters in MCDM application for sustainable DSM vertical transport plan selection.

Mining period	20 years	Minerals type	Polymetallic nodules	Minerals solid density	$2350\,kg\,/\,m^3$
Mining depth	2000 m	Working period	36 / 43 weeks per year	Ocean water density	$1025\,kg\,/\,m^3$
Mean particles diameter	9 mm	Gravitational acceleration	9.8 m/s^2	In-situ sediment density	$1500\,kg\,/\,m^3$
Fill ratio of bucket	0.85	Dynamic viscosity	$1.88\times10^{-3}\,N\cdot s\,/\,m^2$	Air kinematic viscosity	$1.48\times10^{-5}\,m^2\,/\,s$
Atmospheric pressure	$1.01\times10^5\,pa$	Mean suspension particle diameter	$10\,\mu m$	Staff number	30 person
Price of seafloor mining vehicles	500 million	Price of mineral processing facility	750 million	Price of PSV (ships)	495 million
Seawater temperature	$-4^\circ C$	Von Karman coefficient	0.41	Dissipation of turbulent kinematic energy	$5.0\times10^{-8}\,m^2\,/\,s^3$
Boltzmann constant	1.38×10^{-23} $m^2\cdot kg\cdot s^{-2}\cdot K^{-1}$	Critical deposition shear stress	$0.10\,pa$	Critical erosion shear stress	$0.13\,pa$
Original species number	13	Original species distribution	[66, 32, 16, 6, 5, 3, 3, 2, 2, 1, 1, 1, 1]		
Species number after disturbances (simplification, required experiments)	*if $Qs \le 400ton\,/\,h$* , then, [60, 29, 13, 3, 3, 2, 2, 1, 1, 1, 1, 1]; *if $400ton\,/\,h < Qs \le 600ton\,/\,h$* , then, [55, 25, 10, 3, 2, 2, 2, 1, 1, 1, 1]; *if $600ton\,/\,h < Qs \le 800ton\,/\,h$* , then, [50, 23, 9, 2, 2, 2, 2, 1, 1, 1]; *if $Qs > 800ton\,/\,h$* , then, [45, 20, 7, 2, 2, 2, 2, 1];				
Winch force - CLB	600, 700, 800, 900, 1000 KN	Pipe diameter – centrifugal pump lifting	0.20, 0.25, 0.30, 0.35, 0.40 m		
Pipe diameter – airlifting	0.35, 0.40 m	Ming site	$26^\circ 30'00''N$ $126^\circ 30'00''E$		

The DSM vertical transport plans with different changing variables are listed as follows:

Table 6.4: The calculated DSM vertical transport plans.

Continuous line bucket lifting DSM transport plans										
TR No.	1	2	3	4	5	6	7	8	9	10
WP - weeks	36	43	36	43	36	43	36	43	36	43
F_{wi} - kN (CLB)	600	600	700	700	800	800	900	900	1000	1000

Centrifugal pump lifting DSM transport plans										
TR No.	11	12	13	14	15	16	17	18	19	20
WP - weeks	36	43	36	43	36	43	36	43	36	43
D_i - m (CPL)	0.20	0.20	0.25	0.25	0.30	0.30	0.35	0.35	0.40	0.40

Airlifting DSM transport plans												
TR No.	21	22	23	24	25	26	27	28	29	30	31	32
WP - weeks	36	43	36	43	36	43	36	43	36	43	36	43
D_i - m (AL)	0.35	0.35	0.35	0.35	0.35	0.35	0.40	0.40	0.40	0.40	0.40	0.40
J_g - m/s (AL)	100	100	110	110	120	120	100	100	110	110	120	120

Using the numerical calculation theories and equations presented in section 6.3, the quantitative parameters for DSM vertical transport plans can be calculated. Combining the results of the quantitative evaluation criteria with the qualitative evaluation criteria allows for comprehensive assessment for all DSM vertical transport plans through MCDM. The preference value trend for all evaluation criteria is presented in Table 6.5.

As the evaluation criteria have different preferable trends and desired values, prior to the specific operations of the evaluation process of all DSM vertical transport plans, the evaluation matrix of these DSM transport plans should first be normalised (Mateo, 2012). Vafaei et al. (2016) examined the use of normalization techniques in analytic hierarchy process method (AHP), and here we extend their findings to the Fuzzy-ANP method presented in this paper. Except the unsuitable logarithmic normalisation method, the combined application of Linear-Max normalisation and Linear-Sum normalisation is suggested to be the most suitable normalisation method, see Eq. 6.25 (Vafaei et al., 2016).

Table 6.5: Preferable or desired value trend for all evaluating criteria.

Major criteria	Subcriteria	Desired value
Technological aspect	Specific energy consumption for lifting	Low
	Proven technology	High
	Technology reliability	High
	Production rate	High
	Technology availability	High
Economic aspect	Gross income	High
	Capital cost	Low
	Operation and maintenance cost	Low
	Investment recovery period	Low
Environmental aspect	Species disturbance variance	Low
	Severity of ill effect	Low
	Turbidity of ocean water	Low
	Total organic carbon content & sedimentation rate	Low
	Sedimentation thickness	Low
Social aspect	Social acceptability	High
	Policy support & legislation & regulation (PLR)	High

$$\text{Linear-Max:}\begin{cases} R_{ij} = \dfrac{r_{ij}}{r_{max}} & \text{desired-high} \\[2ex] R_{ij} = 1 - \dfrac{r_{ij}}{r_{max}} & \text{desired-low} \end{cases} \quad \& \quad \text{Linear-Sum:}\begin{cases} R_{ij} = \dfrac{r_{ij}}{\sum\limits_{i=1}^{m} r_{ij}} & \text{desired-high} \\[3ex] R_{ij} = \dfrac{1/r_{ij}}{\sum\limits_{i=1}^{m} 1/r_{ij}} & \text{desired-low} \end{cases} \quad (6.25)$$

After the normalization with Eq. 6.25, the super-matrix of all DSM vertical transport plans is changed into the following format, i.e., M_{DSM}.

$M_{DSM} =$

$$
\begin{bmatrix}
0.0357 & 0.0357 & 0.0263 & 0.0150 & 0.0371 & 0.0150 & 0.0557 & 0.0459 & 0.0000 & 0.0478 & 0.0605 & 0.0486 & 0.0801 & 0.0486 & 0.0192 & 0.0215 \\
0.0357 & 0.0357 & 0.0263 & 0.0179 & 0.0371 & 0.0179 & 0.0557 & 0.0435 & 0.0000 & 0.0478 & 0.0527 & 0.0454 & 0.0655 & 0.0454 & 0.0192 & 0.0215 \\
0.0350 & 0.0357 & 0.0263 & 0.0179 & 0.0371 & 0.0179 & 0.0552 & 0.0433 & 0.0000 & 0.0478 & 0.0526 & 0.0454 & 0.0655 & 0.0454 & 0.0192 & 0.0215 \\
0.0350 & 0.0357 & 0.0263 & 0.0214 & 0.0371 & 0.0214 & 0.0552 & 0.0404 & 0.0180 & 0.0478 & 0.0448 & 0.0416 & 0.0512 & 0.0416 & 0.0192 & 0.0215 \\
0.0350 & 0.0357 & 0.0263 & 0.0215 & 0.0371 & 0.0215 & 0.0547 & 0.0401 & 0.0180 & 0.0347 & 0.0460 & 0.0422 & 0.0533 & 0.0422 & 0.0192 & 0.0215 \\
0.0350 & 0.0357 & 0.0263 & 0.0257 & 0.0371 & 0.0257 & 0.0547 & 0.0367 & 0.0288 & 0.0347 & 0.0382 & 0.0378 & 0.0396 & 0.0378 & 0.0192 & 0.0215 \\
0.0350 & 0.0357 & 0.0263 & 0.0240 & 0.0371 & 0.0240 & 0.0542 & 0.0383 & 0.0252 & 0.0347 & 0.0401 & 0.0390 & 0.0429 & 0.0390 & 0.0192 & 0.0215 \\
0.0350 & 0.0357 & 0.0263 & 0.0287 & 0.0371 & 0.0287 & 0.0542 & 0.0344 & 0.0324 & 0.0347 & 0.0322 & 0.0339 & 0.0297 & 0.0339 & 0.0192 & 0.0215 \\
0.0350 & 0.0357 & 0.0263 & 0.0274 & 0.0371 & 0.0274 & 0.0542 & 0.0354 & 0.0324 & 0.0347 & 0.0348 & 0.0356 & 0.0339 & 0.0356 & 0.0192 & 0.0215 \\
0.0350 & 0.0357 & 0.0263 & 0.0328 & 0.0371 & 0.0327 & 0.0542 & 0.0310 & 0.0396 & 0.0347 & 0.0269 & 0.0299 & 0.0217 & 0.0299 & 0.0192 & 0.0215 \\
0.0000 & 0.0455 & 0.0478 & 0.0296 & 0.0442 & 0.0304 & 0.0457 & 0.0094 & 0.0360 & 0.0347 & 0.0298 & 0.0322 & 0.0261 & 0.0322 & 0.0437 & 0.0418 \\
0.0000 & 0.0455 & 0.0478 & 0.0363 & 0.0442 & 0.0363 & 0.0457 & 0.0000 & 0.0432 & 0.0347 & 0.0220 & 0.0257 & 0.0149 & 0.0257 & 0.0437 & 0.0418 \\
0.0327 & 0.0455 & 0.0478 & 0.0355 & 0.0441 & 0.0355 & 0.0436 & 0.0271 & 0.0432 & 0.0220 & 0.0232 & 0.0268 & 0.0165 & 0.0268 & 0.0437 & 0.0418 \\
0.0327 & 0.0455 & 0.0478 & 0.0424 & 0.0442 & 0.0424 & 0.0436 & 0.0211 & 0.0468 & 0.0220 & 0.0153 & 0.0193 & 0.0071 & 0.0193 & 0.0437 & 0.0418 \\
0.0454 & 0.0455 & 0.0478 & 0.0406 & 0.0442 & 0.0405 & 0.0415 & 0.0337 & 0.0468 & 0.0220 & 0.0175 & 0.0214 & 0.0094 & 0.0214 & 0.0437 & 0.0418 \\
0.0454 & 0.0455 & 0.0478 & 0.0485 & 0.0442 & 0.0484 & 0.0415 & 0.0290 & 0.0504 & 0.0220 & 0.0096 & 0.0129 & 0.0023 & 0.0129 & 0.0437 & 0.0418 \\
0.0506 & 0.0455 & 0.0478 & 0.0456 & 0.0442 & 0.0456 & 0.0394 & 0.0363 & 0.0504 & 0.0000 & 0.0124 & 0.0161 & 0.0044 & 0.0161 & 0.0437 & 0.0418 \\
0.0506 & 0.0455 & 0.0478 & 0.0545 & 0.0441 & 0.0545 & 0.0394 & 0.0320 & 0.0540 & 0.0000 & 0.0045 & 0.0064 & 0.0000 & 0.0064 & 0.0437 & 0.0418 \\
0.0536 & 0.0455 & 0.0478 & 0.0507 & 0.0441 & 0.0507 & 0.0368 & 0.0370 & 0.0504 & 0.0000 & 0.0078 & 0.0107 & 0.0013 & 0.0107 & 0.0437 & 0.0418 \\
0.0536 & 0.0455 & 0.0478 & 0.0606 & 0.0442 & 0.0605 & 0.0368 & 0.0329 & 0.0540 & 0.0000 & 0.0000 & 0.0000 & 0.0001 & 0.0000 & 0.0437 & 0.0418 \\
0.0260 & 0.0157 & 0.0216 & 0.0204 & 0.0156 & 0.0203 & 0.0063 & 0.0373 & 0.0144 & 0.0347 & 0.0471 & 0.0428 & 0.0553 & 0.0428 & 0.0309 & 0.0306 \\
0.0260 & 0.0157 & 0.0216 & 0.0243 & 0.0156 & 0.0243 & 0.0063 & 0.0333 & 0.0252 & 0.0347 & 0.0393 & 0.0385 & 0.0415 & 0.0385 & 0.0309 & 0.0306 \\
0.0223 & 0.0157 & 0.0216 & 0.0204 & 0.0156 & 0.0204 & 0.0063 & 0.0354 & 0.0144 & 0.0347 & 0.0469 & 0.0427 & 0.0550 & 0.0427 & 0.0309 & 0.0306 \\
0.0223 & 0.0157 & 0.0216 & 0.0244 & 0.0156 & 0.0244 & 0.0063 & 0.0310 & 0.0252 & 0.0347 & 0.0391 & 0.0384 & 0.0412 & 0.0384 & 0.0309 & 0.0306 \\
0.0171 & 0.0157 & 0.0216 & 0.0203 & 0.0156 & 0.0203 & 0.0063 & 0.0335 & 0.0108 & 0.0478 & 0.0473 & 0.0429 & 0.0557 & 0.0429 & 0.0309 & 0.0306 \\
0.0171 & 0.0157 & 0.0216 & 0.0242 & 0.0156 & 0.0242 & 0.0063 & 0.0287 & 0.0252 & 0.0478 & 0.0395 & 0.0386 & 0.0418 & 0.0386 & 0.0309 & 0.0306 \\
0.0290 & 0.0157 & 0.0216 & 0.0284 & 0.0156 & 0.0284 & 0.0000 & 0.0310 & 0.0324 & 0.0347 & 0.0328 & 0.0343 & 0.0307 & 0.0343 & 0.0309 & 0.0306 \\
0.0290 & 0.0157 & 0.0216 & 0.0339 & 0.0156 & 0.0339 & 0.0000 & 0.0257 & 0.0396 & 0.0347 & 0.0249 & 0.0283 & 0.0188 & 0.0283 & 0.0309 & 0.0306 \\
0.0260 & 0.0157 & 0.0216 & 0.0289 & 0.0156 & 0.0288 & 0.0000 & 0.0284 & 0.0324 & 0.0347 & 0.0321 & 0.0338 & 0.0296 & 0.0338 & 0.0309 & 0.0306 \\
0.0260 & 0.0157 & 0.0216 & 0.0345 & 0.0156 & 0.0345 & 0.0000 & 0.0226 & 0.0396 & 0.0347 & 0.0242 & 0.0277 & 0.0179 & 0.0277 & 0.0309 & 0.0306 \\
0.0216 & 0.0157 & 0.0216 & 0.0290 & 0.0156 & 0.0290 & 0.0000 & 0.0258 & 0.0324 & 0.0347 & 0.0319 & 0.0337 & 0.0293 & 0.0337 & 0.0309 & 0.0306 \\
0.0216 & 0.0157 & 0.0216 & 0.0346 & 0.0156 & 0.0346 & 0.0000 & 0.0196 & 0.0396 & 0.0347 & 0.0241 & 0.0276 & 0.0177 & 0.0276 & 0.0309 & 0.0306
\end{bmatrix}
$$

$$(6.26)$$

Finally, the scores for all these DSM vertical transport plans could be determined by multiplying the normalization matrix, i.e., Eq. 6.26, by the global weights of all evaluating criteria, i.e., w_{12}.

$F_{DSM} = M_{DSM} \cdot w_{12}$

$= [0.0334 \quad 0.0325 \quad 0.0324 \quad 0.0329 \quad 0.0324 \quad 0.0324 \quad 0.0322 \quad 0.0319 \quad 0.0322 \quad 0.0319... \qquad\qquad \text{- CLB}$

$\quad\ 0.0342 \quad 0.0336 \quad 0.0366 \quad 0.0361 \quad 0.0376 \quad 0.0374 \quad 0.0370 \quad 0.0370 \quad 0.0370 \quad 0.0371... \qquad\qquad \text{- HL}$

$\quad\ 0.0267 \quad 0.0266 \quad 0.0264 \quad 0.0262 \quad 0.0264 \quad 0.0265 \quad 0.0262 \quad 0.0258 \quad 0.0258 \quad 0.0254 \quad 0.0254 \quad 0.0250]^{T} \text{ - AL}$

$$(6.27)$$

The scores for all evaluated DSM vertical transport plans are transferred into a two-dimensional column figure as follows.
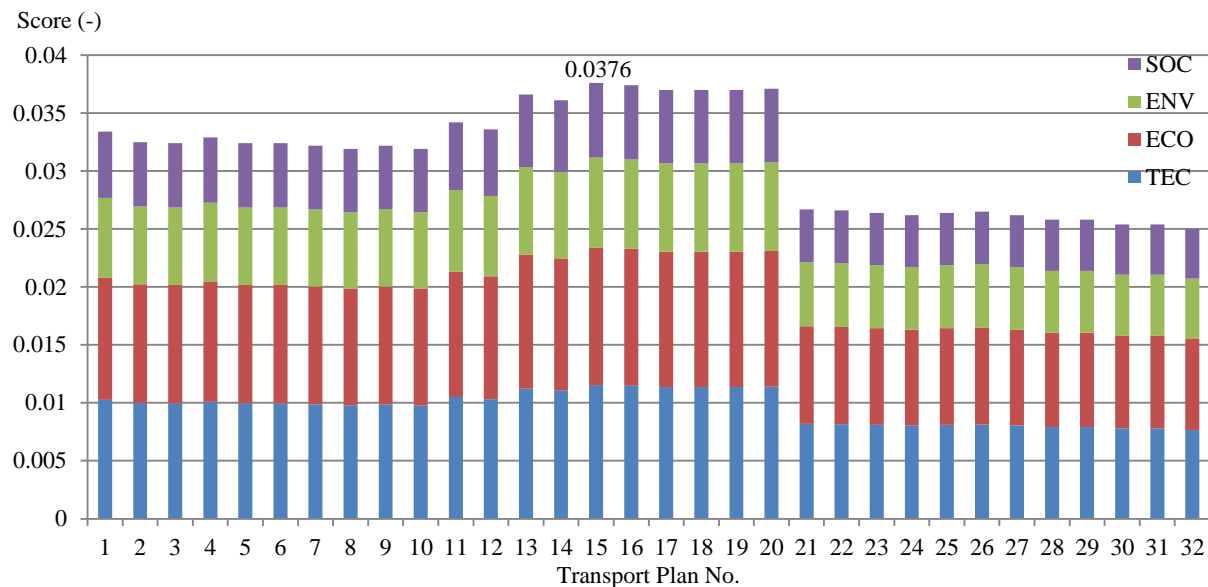
Figure 6.7: Score diagram of the evaluated DSM transport plans. Note: the maximum score is marked in the figure, which is transport plan (TR) No. 15 with the score of 0.0376; TRs. No (1-10), (11-20) and (21-32) are CLB, HL and AL systems respectively.

Analysing Figure 6.7, it clearly expresses the following information: (i) TR. 15 is calculated with the maximum score, i.e., 0.0376, which is selected as the most sustainable DSM transport plan taking into consideration the technological, economic, environmental and social considerations; TR. 15 is not the working plan with the maximum gross income, neither does it have the least environmental impacts. However, it is the working plan with the highest integrated evaluating index. Based on the multiple criteria evaluating results, TR. 15 is suggested to be the most preferable or sustainable vertical transport plan for the selected DSM working condition. (ii) Compared to continuous line bucket lifting and airlifting systems, centrifugal pump lifting system seems to be more preferable with relative larger evaluating scores. The advantages of centrifugal pump lifting system could be explained as follows: (a) centrifugal pump lifting system could achieve a larger solid production rate at the depth of 2000 m than continuous line bucket lifting and airlifting systems. This advantage will be furtherly expanded with the increase of mining water depth (Ma et al., 2017a). (b) To obtain a relatively large mineral production rate, the mineral particle velocity could be another problem for airlifting system. In airlifting system, pressure inside the pipe lifting system decreases with the continuous lifting of minerals. The volumetric concentration of mineral particles could be very small, which will lead to a fast moving velocity of solid particles, roughly 20 – 80 m/s (Ma et al., 2017d). (c) Compared to the centrifugal pumps which could be added along the pipe lifting system to improve its mining capacity, the strength standard of steel rope is an important limitation for continuous line bucket lifting system, which limits its maximum lifting depths and maximum solid production rate (Ma et al., 2017a).

In future application of this evaluating system, a large number of DSM vertical transport plans would be calculated to determine an optimal sustainable working plan. It would be a huge workload when applying Fuzzy-ANP evaluating methods (Yüksel and Dagdeviren, 2007). In order to improve the multiple criteria evaluating efficiency, all evaluating candidates could

receive a pre-filtering process to decrease the number of evaluated DSM transport plans. For instance, if the DSM working period is set to be 20 years, the investors would like a large profitability. It means the investment recovery period should be smaller than the mining period. Analysing Figure 6.8, transport plans No. 1-3 could be excluded in the evaluating process because these DSM working conditions are unprofitable.
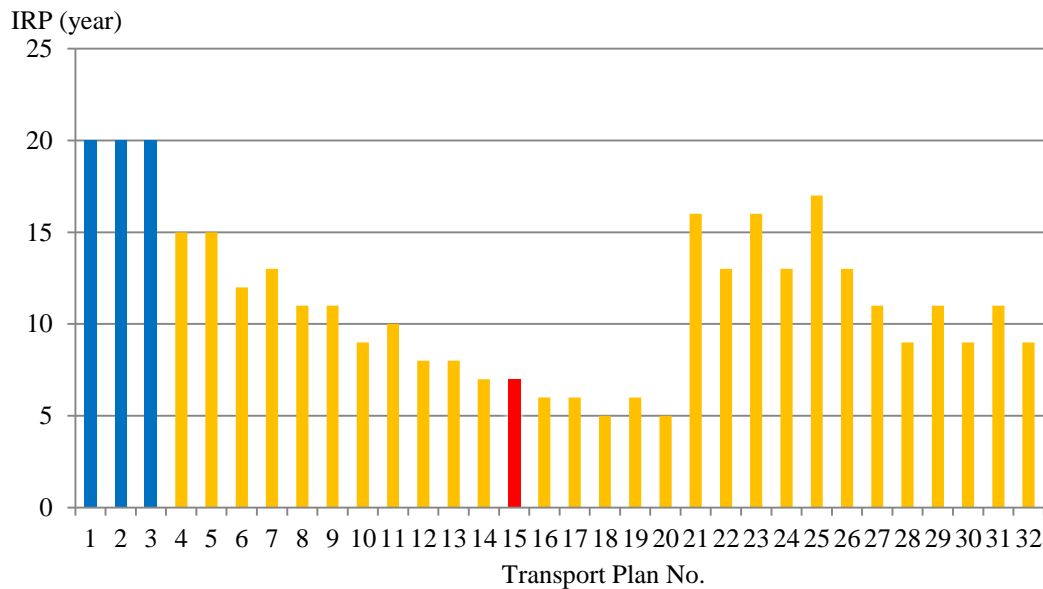
Figure 6.8: Investment recovery period (IRP) of all evaluated DSM vertical transport plans. Notes: the IRP of these transport plans no smaller than 20 year are orange bars; the red bar is the selected most preferable and sustainable DSM vertical transport plan; the IRP of the transport plan No. (1-3) is no less than 20 years. Here, it is simplified as 20 years in blue bars.

Additionally, as suggested by Ma et al. (2018a) in a paper examining the environmental impacts of DSM using a numerical calculation method combined with in-situ tests, an environmental impact standard should be established in order to allow the greatest degree of ecological recovery possibility. The environmental impact standard considers physical disturbances, species disturbances, turbidity of ocean water change, sedimentation rate, and sedimentation thickness. Outcomes are measured in terms of species mortality, the mass concentration of sediment plume, and its residence time (Van Dover, 2011; Jones et al., 2017). These environmental impact standards facilitate the exclusion of many substandard transport plans, thereby further reducing the potential workload and allowing for more accurate and concise identification of the most preferable working condition.

Furthermore, in the evaluation of sustainable DSM vertical transport plans, it is notable that economically advantageous evaluation parameters often have conflicting results with environmentally advantageous evaluation parameters. An economically advantageous DSM transport plan may have a relatively poor environmental impact performance and vice versa. Figure 6.9 illustrates this, presenting the normalised scores for gross income and sedimentation thickness (parameters belonging to economic and environmental impact considerations, respectively). The normalised values can be understood as the preferable levels of all DSM transport plans in terms of all these selected evaluating criteria. Figure 6.9

illustrates that the normalised values for gross income demonstrate a negative correlation with those for sedimentation thickness. That reflects why, in many industrial working conditions, a larger economic profit can be obtained at the expense of the environment (Panayotou, 2016; Ghisellini et al., 2016). Through a systematic use of multiple criteria decision making method, we have tried to find the optimal balance of all included evaluation criteria – encompassing technological, economic, environmental, and social perspectives.
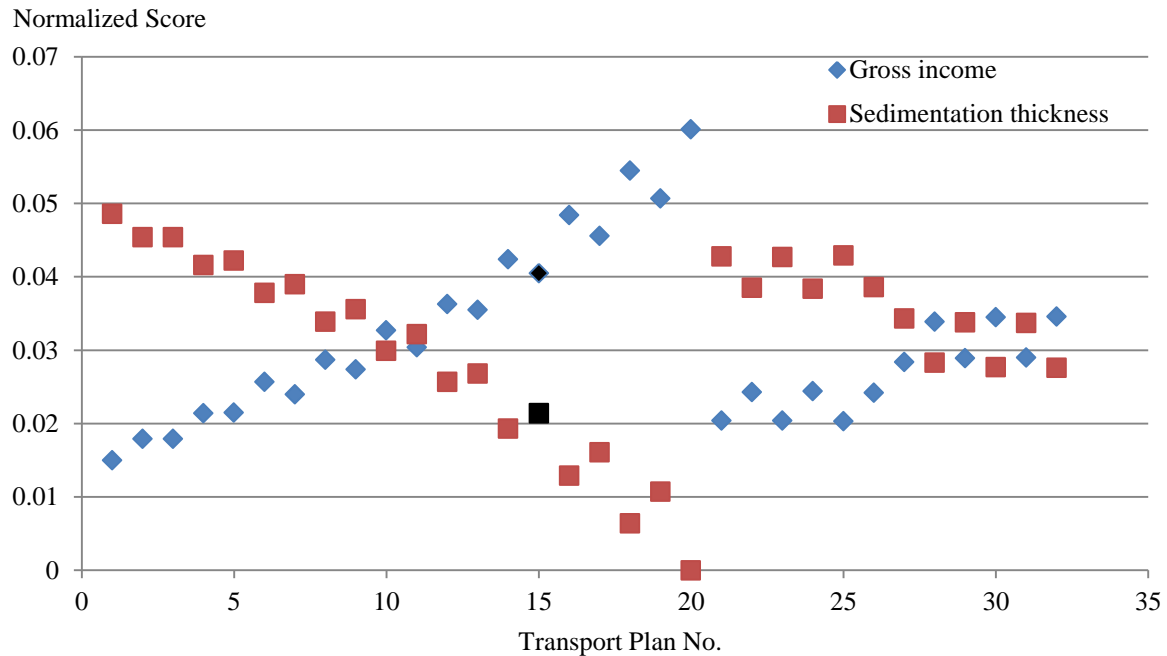
Figure 6.9: Normalized scores of gross income and sedimentation thickness. Notes: the black points represent the selected most preferable and sustainable DSM transport plan.

6.5. Conclusions

In this chapter, Fuzzy-ANP method is utilised for sustainability assessment in DSM vertical transport plans. The decision making criteria constituting the technological, economic, environmental, and social components of these plans possess both quantitative and qualitative attributes. The application of Fuzzy-ANP methodology is demonstrated in section 6.4, in which an example set of DSM vertical transport plans are evaluated. The MCDM results show that transport plans involving centrifugal pump lifting are more competitive compared to bucket lifting and airlifting systems. It can also be concluded that economically advantageous evaluation parameters often demonstrate a conflicting relationship with environmentally advantageous evaluating parameters. Although this chapter focuses on the utility of the proposed framework in vertical lifting technologies, this method of sustainability evaluation allows for sustainability assessment of DSM projects as a whole.

Future improvements of the proposed framework could include (i) consideration of the interconnections of evaluation subcriteria, (ii) sustainability assessment of whole DSM projects, and (iii) global optimisations of DSM working conditions.

Chapter 7

Conclusion and Recommendations

This thesis aims to evaluate and determine the sustainable DSM transport plan. To reflect all the conducted research, in this chapter, conclusions are summarized in section 7.1. Recommendations are presented in section 7.2 guiding the future research.

7.1 Conclusions

The major research question is '*How to evaluate the sustainability of DSM transport plans?*' which is analysed, discussed and answered in this thesis. Taking into consideration that DSM is still an emerging industry and there are many problems in its commercialization, we select its sustainability evaluation as our major research objective. Based on the proposed sustainability evaluation framework in this thesis, different kinds of DSM transport plans are evaluated. The DSM transport plan with the largest comprehensive performance index is selected as the most sustainable. The followings are concluded regarding the research questions.

Based on a literature review in chapter 2, it shows that the DSM technological feasibility, economic profitability and environmental impacts influence the determination of project's sustainability significantly. In addition, the current R&D status on DSM technological, economic, and environmental aspects are analysed and discussed. It is noticeable that almost all these researches stay at the level of theoretical explaining, conceptualisation making, and framework establishment. There is no prior research addressing the sustainability problem of DSM transport plan across these multiple influencing areas.

Compared with the continuous line bucket lifting, hydraulic lifting have a wider application range of mining depth and maximum mineral production rate. When the target solid mineral production rate and mining depth is low, the technological performance of continuous line bucket lifting system might be similar as hydraulic lifting systems.

The economic profitability of DSM transport plans are analysed in chapter 4. For airlifting, a larger pipe diameter can be used for a larger mining depth. However, a larger pipe diameter and gas flux rate cannot guarantee a better airlifting performance. This is because for each set of mining depth and pipe diameter, there will be an optimal set of gas flux rate and pipe diameter to obtain the maximum profitability per tonnage of mineral. Transporting small

particles has a better performance than large particles in terms of its profitability. This advantage could also be reflected in terms of total solid production rate and energy consumption per tonnage of mineral.

Through a systematic literature review, a framework to quantify the DSM environmental impacts with numerical calculation method is proposed in this thesis. The framework consists of the physical seabed disturbance, sediment plume, species disturbance and tailings disposal. Based on the assumed case analysis, see section 5.4, the direct physical seabed disturbance for a normal DSM project is large and extensive, roughly 2500 km^2, which potential ecological influencing scope could be dozens to hundreds of times this figure. Additionally, the species disturbance degree reflecting on the total individual number and biodiversity could be compared and evaluated by analyzing the integrated species index. Although the sediment plume could transport more than thousands of kilometers away from the plume source and suspend within the water for a long time, the most evident influencing area of the resedimentation is limited within the initial sediment plume area. The most intensive influencing period of sediment plume is within the first two to three days in terms of the sedimentation thickness increase. Furthermore, the species responses to sediment plume are quantified by analyzing the severity of ill effect, turbidity of ocean water, total organic carbon content and sedimentation thickness. The calculation results prove that with the time going on the species disturbance degree is decreasing, but the influencing scope increases. The closer to the sediment plume source, the greater the species disturbance would be.

To evaluate and determine a sustainable DSM transport plan, multi-criteria decision making method is selected integrating the technological, economic, environmental and social aspects. By utilizing Fuzzy-ANP method, the DSM vertical transport plans are scored and evaluated. Compared to continuous line bucket lifting and airlifting systems, centrifugal pump lifting systems are calculated to be more preferable and sustainable with a relative larger evaluating score. Additionally, when analysing the influencing factors on the DSM sustainability, it shows that the economically advantageous evaluating parameters often have the conflicting results with the environmentally advantageous evaluating parameters. The conducted research in this thesis could be used by multiple stakeholders, e.g., DSM investors, engineers, and environmentalists, to give a comprehensive evaluation of all DSM influencing aspects on its sustainability. It is meaningful to promote the realization of industrialization of DSM activities.

7.2 Recommendations

Recommendations for the future research are listed as follows.

a) Combining the in-situ field tests to apply and validate the DSM sustainability evaluating systems

The multi-criteria decision making framework evaluating the sustainability of DSM transport plan is proposed in this thesis. Although the framework is demonstrated through a case with a series of assumptions and simplifications, it might not reflect the actual working conditions completely. In the next stage, the research is necessary to apply and validate with an in-situ field test.

b) Scale effect consideration in air pump lifting

In chapter 4, the calculation theories of airlifting pumps for minerals slurry transportation are majorly based on the experimental scale tests. The scale effect with the industrial scale conditions might influence the accuracy of the calculation results, which should also be taken into consideration in the future. For instance, the minerals transportation flow patterns are mostly froth flow in experimental test, but annular flow in large scale calculating conditions. Therefore, the calculation theories of airlifting pumps for mineral slurry transportation should be validated by the large scale experiments or the in-situ tests.

c) Interconnection relationships between the DSM environmental impacts

As mentioned in chapter 5, most of existing researches analyse only a part of environmental impacts individually neglecting the interconnections between different environmental impact aspects. Although we proposed a way to quantify the species responses to sediment plume, there are un-researched interconnection blanks remaining. It is necessary to formulate a comprehensive-systematic model of species responses to the DSM activities in terms of the sound impact, light pollution, and heavy metals contaminations.

d) Establishment of standard for the DSM environmental impacts

In our research, it is mentioned that the sediment plume, tailings disposal, seabed physical disturbances, and species disturbances are very important environmental indicators for DSM activities. However, until now, there is no standard for the DSM environmental impacts based on the experimental or in-situ tests.

Bibliography

Abramowski, T. and Stoyanova, V., 2012. Deep-sea Polymetallic nodules: renewed interest as resources for environmentally sustainable development. *International Multididciplinary Scientific GeoConference: SGEM, Surveying geology and mining ecology management*, *1*, p.515.

Afgan, N.H. and Carvalho, M.G., 2008. Sustainability assessment of a hybrid energy system. *Energy Policy*, *36*(8), pp.2903-2910.

Amos, A.F. and Roels, O.A., 1977. Environmental aspects of manganese nodule mining. *Marine Policy*, *1*(2), pp.156-163.

Alldredge, A.L. and Silver, M.W., 1988. Characteristics, dynamics and significance of marine snow. *Progress in oceanography*, *20*(1), pp.41-82.

Aldenberg, T., Jaworska, J.S. and Traas, T.P., 2001. Normal species sensitivity distributions and probabilistic ecological risk assessment. In *Species sensitivity distributions in ecotoxicology* (pp. 73-126). CRC Press.

Al-Said, T., Naqvi, S.W.A., Al-Yamani, F., Goncharov, A. and Fernandes, L., 2018. High total organic carbon in surface waters of the northern Arabian Gulf: Implications for the oxygen minimum zone of the Arabian Sea. *Marine pollution bulletin*, *129*(1), pp.35-42.

Ancey, C., Bohorquez, P. and Heyman, J., 2015. Stochastic interpretation of the advection-diffusion equation and its relevance to bed load transport. *Journal of Geophysical Research: Earth Surface*, *120*(12), pp.2529-2551.

Anuar, N., Kahar, W.S.W.A. and Manan, J.A.N.A., 2015, April. Defining the "proven technology" technical criterion in the reactor technology assessment for Malaysia's nuclear power program. In *AIP Conference Proceedings* (Vol. 1659, No. 1, p. 020006). AIP Publishing.

Akash, B.A., Mamlook, R. and Mohsen, M.S., 1999. Multi-criteria selection of electric power plants using analytical hierarchy process. *Electric Power Systems Research*, *52*(1), pp.29-35.

Boran, F.E., Genç, S., Kurt, M. and Akay, D., 2009. A multi-criteria intuitionistic fuzzy group decision making for supplier selection with TOPSIS method. *Expert Systems with Applications*, *36*(8), pp.11363-11368.

Begić, F. and Afgan, N.H., 2007. Sustainability assessment tool for the decision making in selection of energy system—Bosnian case. *Energy*, *32*(10), pp.1979-1985.

Brunson, M.W., Kruger, L.E., Tyler, C.B. and Schroeder, S.A., 1996. Defining social acceptability in ecosystem management: a workshop proceedings.

Becker, H.J., Grupe, B., Oebius, H.U. and Liu, F., 2001. The behaviour of deep-sea sediments under the impact of nodule mining processes. *Deep Sea Research Part II: Topical Studies in Oceanography*, *48*(17), pp.3609-3627.

Brooks, S.J., Harman, C., Hultman, M.T. and Berge, J.A., 2015. Integrated biomarker assessment of the effects of tailing discharges from an iron ore mine using blue mussels (Mytilus spp.). *Science of the Total Environment*, *524*, pp.104-114.

Buffle, J., Wilkinson, K.J., Stoll, S., Filella, M. and Zhang, J., 1998. A generalized description of aquatic colloidal interactions: the three-colloidal component approach. *Environmental Science & Technology*, *32*(19), pp.2887-2899.

Berner, R.A., 2013. *Principles of chemical sedimentology*. McGraw-Hill.

Brink, A.N. and Chung, J.S., 1981, January. Automatic Position Control of A30, 000 Tons Ship During Ocean Mining Operations. In *Offshore Technology Conference*. Offshore Technology Conference, Houston, Texas, pp. 205-212.

Bradshaw, C., Tjensvoll, I., Sköld, M., Allan, I.J., Molvaer, J., Magnusson, J., Naes, K. and Nilsson, H.C., 2012. Bottom trawling resuspends sediment and releases bioavailable contaminants in a polluted fjord. *Environmental Pollution*, *170*, pp.232-241.

Borowski, C. and Thiel, H., 1998. Deep-sea macrofaunal impacts of a large-scale physical disturbance experiment in the Southeast Pacific. *Deep Sea Research Part II: Topical Studies in Oceanography*, *45*(1-3), pp.55-81.

Brown, B.J., Hanson, M.E., Liverman, D.M. and Merideth, R.W., 1987. Global sustainability: toward definition. *Environmental management*, *11*(6), pp.713-719.

Brown, L.R., 1982. Building a sustainable society. *Society*, *19*(2), pp.75-85.

Birney, K., Griffin, A., Gwiazda, J., Kefauver, J., Nagai, T. and Varchol, D., 2006. Potential deep-sea mining of seafloor massive sulfides: A case study in Papua New Guinea. *Donald Bren School of Environmental Science and Management Thesis*.

Bath, A.R., 1989, January. Deep sea mining technology: recent developments and future projects. In *Offshore Technology Conference*. Offshore Technology Conference, Houston, Texas, 1(4), pp. 333-340.

Copley, J.T.P., Flint, H.C., Ferrero, T.J. and Van Dover, C.L., 2007. Diversity of meiofauna and free-living nematodes in hydrothermal vent mussel beds on the northern and southern East Pacific Rise. *Journal of the Marine Biological Association of the United Kingdom*, *87*(5), pp.1141-1152.

Chung, J.S., 1996. Deep-ocean mining: technologies for manganese nodules and crusts. *International Journal of Offshore and Polar Engineering*, *6*(04).

Chung, J.S., 2003, January. Deep-ocean mining technology: learning curve I. In *Fifth ISOPE Ocean Mining Symposium*. International Society of Offshore and Polar Engineers.

Collins, P.C., Kennedy, B., Copley, J., Boschen, R., Fleming, N., Forde, J., Ju, S.J., Lindsay, D., Marsh, L., Nye, V. and Patterson, A., 2013. VentBase: Developing a consensus among stakeholders in the deep-sea regarding environmental impact assessment for deep-sea mining– A workshop report. *Marine Policy*, *42*, pp.334-336.

Chung, J.S., 1985. Advances in manganese nodule mining technology. *Marine Technology Society Journal*, *19*(4).

Chung, J.S. and Tsurusaki, K., 1994, January. Advance in deep-ocean mining systems research. In *The Fourth International Offshore and Polar Engineering Conference*. International Society of Offshore and Polar Engineers.

Chung, J.S., Schriever, G., Sharma, R. and Yamazaki, T., 2001, January. Deep seabed mining environment: preliminary engineering and environmental assessment. In *Fourth ISOPE Ocean Mining Symposium*. International Society of Offshore and Polar Engineers.

Chung, J.S., 2009, January. Deep-ocean mining technology III: Developments. In *Eighth ISOPE Ocean Mining Symposium*. International Society of Offshore and Polar Engineers.

Cheng, N.S., 1997. Simplified settling velocity formula for sediment particle. *Journal of hydraulic engineering*, 123(2), pp.149-152.

Chang, Q., 2016. *Colloid and interface chemistry for water quality control*. Academic Press.

Cummings, V., Thrush, S., Hewitt, J., Norkko, A. and Pickmere, S., 2003. Terrestrial deposits on intertidal sandflats: sediment characteristics as indicators of habitat suitability for recolonising macrofauna. *Marine Ecology Progress Series*, *253*, pp.39-54.

Cyrus, D.P. and Blaber, S.J.M., 1987a. The influence of turbidity on juvenile marine fish in the estuaries of Natal, South Africa. *Continental Shelf Research*, *7*(11-12), pp.1411-1416.

Cyrus, D.P. and Blaber, S.J.M., 1987b. The influence of turbidity on juvenile marine fishes in estuaries. Part 1. Field studies at Lake St. Lucia on the southeastern coast of Africa. *Journal of Experimental Marine Biology and Ecology*, *109*(1), pp.53-70.

Chatzimouratidis, A.I. and Pilavachi, P.A., 2009. Technological, economic and sustainability evaluation of power plants using the Analytic Hierarchy Process. *Energy policy*, *37*(3), pp.778-787.

Chapman, R.J., 2016. *The rules of project risk management: Implementation guidelines for major projects*. Routledge.

Dyer, K.R., 1972. Sedimentation in estuaries. *The estuarine environment*, *12*, p.32.

Duckworth, A., Giofre, N. and Jones, R., 2017. Coral morphology and sedimentation. *Marine pollution bulletin*, *125*(1-2), pp.289-300.

Dare, A.A. and Oturuhoyi, O., 2007. Experimental investigation of air lift pump. *African Journal of Science and Technology*, *8*(1), pp.56-62.

Decrop, B., De Mulder, T., Toorman, E. and Sas, M., 2015. Numerical Simulation of Near-Field Dredging Plumes: Efficiency of an Environmental Valve. *Journal of Environmental Engineering*, *141*(12), p.04015042.

Dedegil, M.Y. Principles of Air-Lift Techniques. *Encyclopedia Fluid Mechanics*; Gulf: Houston, TX, USA, 1987; Chapter 12, p. 4.

Doyle, R.L.; Halkyard, J.E. Large scale airlift experiments for application to deep ocean mining. In Proceedings of the 26th International Conference on Offshore Mechanics and

Arctic Engineering, San Diego, CA, USA, 10–15 June 2007; American Society of Mechanical Engineers: New York, NY, USA, 2007; pp. 27–36.

Deepak, C.R., Shajahan, M.A., Atmanand, M.A., Annamalai, K., Jeyamani, R., Ravindran, M., Schulte, E., Handschuh, R., Panthel, J., Grebe, H. and Schwarz, W., 2001, January. Developmental tests on the underwater mining system using flexible riser concept. In *Fourth ISOPE Ocean Mining Symposium*. International Society of Offshore and Polar Engineers.

Edinger, E.N., Siregar, P.R. and Blackwood, G.M., 2007. Heavy metal concentrations in shallow marine sediments affected by submarine tailings disposal and artisanal gold mining, Buyat-Ratototok district, North Sulawesi, Indonesia. *Environmental Geology*, *52*(4), pp.701-714.

Eckert, R.D., 1974. Exploitation of Deep Ocean Minerals: Regulatory Mechanisms and United States Policy. *The Journal of Law and Economics*, *17*(1), pp.143-177.

Elberling, B., Knudsen, K.L., Kristensen, P.H. and Asmund, G., 2003. Applying foraminiferal stratigraphy as a biomarker for heavy metal contamination and mining impact in af iord in West Greenland. *Marine Environmental Research*, *55*(3), pp.235-256.

ECORYS, 2014. Study to investigate state of knowledge of deep sea mining. Final report Annex 6 Environmental Analysis. Retrieved on December 6th, 2017. https://webgate.ec.europa.eu/maritimeforum/sites/maritimeforum/files/Annex%206%20Environmental%20analysis.pdf.

Elimelech, M., Gregory, J. and Jia, X., 2013. *Particle deposition and aggregation: measurement, modelling and simulation*. Butterworth-Heinemann.

Fukushima, T., Shirayama, Y. and Kuboki, E., 2000. The characteristics of deep-sea epifaunal megabenthos community two years after an artificial rapid deposition event.

Foell, E.J., Thiel, H. and Schriever, G., 1990, January. DISCOL: a long-term, large-scale, disturbance-recolonization experiment in the abyssal eastern tropical South Pacific Ocean. In *Offshore Technology Conference*. Offshore Technology Conference.

Fan, W., Chen, J., Pan, Y., Huang, H., Chen, C.T.A. and Chen, Y., 2013. Experimental study on the performance of an air-lift pump for artificial upwelling. *Ocean Engineering*, *59*, pp.47-57.

Fallon, S.J., White, J.C. and McCulloch, M.T., 2002. Porites corals as recorders of mining and environmental impacts: Misima Island, Papua New Guinea. *Geochimica et Cosmochimica Acta*, *66*(1), pp.45-62.

Glasby, G.P., 2002. Deep seabed mining: past failures and future prospects. *Marine Georesources and Geotechnology*, *20*(2), pp.161-176.

Glover, A.G. and Smith, C.R., 2003. The deep-sea floor ecosystem: current status and prospects of anthropogenic change by the year 2025. *Environmental Conservation*, *30*(3), pp.219-241.

Gideiri, Y.B.A., 1984. Impacts of mining on central Red Sea environment. *Deep Sea Research Part A. Oceanographic Research Papers*, *31*(6-8), pp.823-828.

Giurco, D. and Cooper, C., 2012. Mining and sustainability: asking the right questions. *Minerals Engineering*, *29*, pp.3-12.

Griffith, P. The Prediction of Low-Quality Boiling Voids. *J. Heat Transf.* 1964, *86*, 327–333.

Gandhi, B.K., Singh, S.N. and Seshadri, V., 2002. Effect of speed on the performance characteristics of a centrifugal slurry pump. *Journal of Hydraulic Engineering*, *128*(2), pp.225-233.

Gatto, M., 1995. Sustainability: is it a well defined concept?.

Gever, J., Kaufmann, R., Skole, P. and Vorosmarty, C., 1986, January. Beyond oil. Atomic Industrial Forum, Bethesda, MD.

Gutiérrez, J.L., Jones, C.G., Strayer, D.L. and Iribarne, O.O., 2003. Mollusks as ecosystem engineers: the role of shell production in aquatic habitats. *Oikos*, *101*(1), pp.79-90.

Hitchcock, D.R. and Bell, S., 2004. Physical impacts of marine aggregate dredging on seabed resources in coastal deposits. *Journal of Coastal Research*, pp.101-114.

Haywood, M.D.E., Dennis, D., Thomson, D.P. and Pillans, R.D., 2016. Mine waste disposal leads to lower coral cover, reduced species richness and a predominance of simple coral growth forms on a fringing coral reef in Papua New Guinea. *Marine environmental research*, *115*, pp.36-48.

Hughes, D.J., Shimmield, T.M., Black, K.D. and Howe, J.A., 2015. Ecological impacts of large-scale disposal of mining waste in the deep sea. *Scientific reports*, *5*, p.9985.

Hatta, N.; Fujimoto, H.; Isobe, M.; Kang, J.S. Theoretical analysis of flow characteristics of multiphase mixtures in a vertical pipe. *Int. J. Multiph. Flow* 1998, *24*, 539–561.

Hatta, N.; Omodaka, M.; Nakajima, F.; Takatsu, T.; Fujimoto, H.; Takuda, H. Predictable Model for Characteristics of One-Dimensional Solid-Gas-Liquid Three-Phase Mixtures Flow Along a Vertical Pipeline with an Abrupt Enlargement in Diameter. *ASME J. Fluids Eng.* 1999, *121*, 330–342.

Hein, J.R., Mizell, K., Koschinsky, A. and Conrad, T.A., 2013. Deep-ocean mineral deposits as a source of critical metals for high-and green-technology applications: Comparison with land-based resources. Ore Geology Reviews, 51, pp.1-14.

Hong, S.; Choi, J.S.; Hong, S.W. Experimental study on effects of pipe inclination in airlift water pumping. In Proceedings of the Fifteenth International Offshore and Polar Engineering Conference, Seoul, Korea, 19–25 June 2005; International Society of Offshore and Polar Engineers: Mountain View, CA, USA, 2005; pp. 421–425.

Heller, V. Scale effects in physical hydraulic engineering models. *J. Hydraulic Res.* 2011, *49*, 293–306.

Hanafizadeh, P., Ghanbarzadeh, S. and Saidi, M.H., 2011. Visual technique for detection of gas–liquid two-phase flow regime in the airlift pump. *Journal of Petroleum Science and Engineering*, *75*(3-4), pp.327-335.

Hoagland, P., 1993. Manganese nodule price trends: dim prospects for the commercialization of deep seabed mining. *Resources Policy*, *19*(4), pp.287-298.

Haralambopoulos, D.A. and Polatidis, H., 2003. Renewable energy projects: structuring a multi-criteria group decision-making framework. *Renewable energy*, *28*(6), pp.961-973.

Ho, W., Xu, X. and Dey, P.K., 2010. Multi-criteria decision making approaches for supplier evaluation and selection: A literature review. *European Journal of operational research*, *202*(1), pp.16-24.

Investopedia, Payback Period. What is the 'Payback Period'. Retrieved on Oct 1st, 2018. Available at: https://www.investopedia.com/terms/p/paybackperiod.asp.

ISA. International Seabed Authority. Deep Seabed Minerals Contractors. Retrieved on Aug 21st, 2018a. Available at: https://www.isa.org.jm/deep-seabed-minerals-contractors.

ISA. Standardization of Environmental Data and Information – Development of Guidelines. Retrieved on September 7th, 2018b. Available at: https://www.isa.org.jm/files/documents/EN/Pubs/2001-Standards.pdf.

Ingole, B.S., Ansari, Z.A., Rathod, V. and Rodrigues, N., 2001. Response of deep-sea macrobenthos to a small-scale environmental disturbance. *Deep Sea Research Part II: Topical Studies in Oceanography*, *48*(16), pp.3401-3410.

Ibach, L.E.J., 1982. Relationship between sedimentation rate and total organic carbon content in ancient marine sediments. *AAPG Bulletin*, *66*(2), pp.170-188.

Jankowski, J.A. and Zielke, W., 1997, January. Data support for modelling of deep-sea mining impacts. In *The Seventh International Offshore and Polar Engineering Conference*. International Society of Offshore and Polar Engineers.

Jewett, S.C., Feder, H.M. and Blanchard, A., 1999. Assessment of the benthic environment following offshore placer gold mining in the northeastern Bering Sea. *Marine Environmental Research*, *48*(2), pp.91-122.

Jankowski, J.A., Malcherek, A. and Zielke, W., 1996. Numerical modeling of suspended sediment due to deep-sea mining. *Journal of Geophysical Research: Oceans*, *101*(C2), pp.3545-3560.

Jones, D.O., Kaiser, S., Sweetman, A.K., Smith, C.R., Menot, L., Vink, A., Trueblood, D., Greinert, J., Billett, D.S., Arbizu, P.M. and Radziejewska, T., 2017. Biological responses to disturbance from simulated deep-sea polymetallic nodule mining. *PLoS One*, *12*(2), p.e0171750.

Jovanović, M., Afgan, N., Radovanović, P. and Stevanović, V., 2009. Sustainable development of the Belgrade energy system. *Energy*, *34*(5), pp.532-539.

Johnson, M.D. and Ettlie, J.E., 2001. Technology, customization, and reliability. *Journal of Quality Management*, *6*(2), pp.193-210.

Kahraman, C. ed., 2008. *Fuzzy multi-criteria decision making: theory and applications with recent developments* (Vol. 16). Springer Science & Business Media.

Kineke, G.C., Woolfe, K.J., Kuehl, S.A., Milliman, J.D., Dellapenna, T.M. and Purdon, R.G., 2000. Sediment export from the Sepik River, Papua New Guinea: evidence for a divergent sediment plume. *Continental Shelf Research*, *20*(16), pp.2239-2266.

Kotlinski, R., Stoyanova, V., Hamrak, H. and Avramov, A., 2008. An Overview of the Interoceanmetal (IOM) Deep-Sea Technology Development (Mining and Processing). In *Proceedings of the Workshop on Polymetallic Nodule Mining Technology-Current Status and Challenges Ahead, Chennai, India* (Vol. 2, pp. 18-22).

Kato, H.; Miyazawa, T.; Timaya, S.; Iwasaki, T. A study of an air-lift pump for solid particles and its application to marine engineering. *JSME* 1975, *18*, 286–294.

Kice, J. E., 1986. U.S. Patent No. 4,607,987. Washington, DC: U.S. Patent and Trademark Office.

Kassab, S.Z., Kandil, H.A., Warda, H.A. and Ahmed, W.H., 2007. Experimental and analytical investigations of airlift pumps operating in three-phase flow. *Chemical Engineering Journal*, *131*(1-3), pp.273-281.

Khatmullina, L. and Isachenko, I., 2017. Settling velocity of microplastic particles of regular shapes. *Marine pollution bulletin*, *114*(2), pp.871-880.

Kutti, T., Bannister, R.J., Fosså, J.H., Krogness, C.M., Tjensvoll, I. and Søvik, G., 2015. Metabolic responses of the deep-water sponge Geodia barretti to suspended bottom sediment, simulated mine tailings and drill cuttings. *Journal of experimental marine biology and ecology*, *473*, pp.64-72.

Kjelland, M.E., Woodley, C.M., Swannack, T.M. and Smith, D.L., 2015. A review of the potential effects of suspended sediment on fishes: potential dredging-related physiological, behavioral, and transgenerational implications. *Environment Systems and Decisions*, *35*(3), pp.334-350.

Lavelle, J., 1987. Effects of boundary layer structure and macro-particle scavenging on the benthic deposition of fine sediment resuspended during nodule mining. *Final Report to NOAA Office of Ocean and Coastal Resource Management, NOAA Pacific Marine Environmental Laboratory, Seattle. 39pp.*

Lohrer, A.M., Thrush, S.F., Lundquist, C.J., Vopel, K., Hewitt, J.E. and Nicholls, P.E., 2006. Deposition of terrigenous sediment on subtidal marine macrobenthos: response of two contrasting community types. *Marine Ecology Progress Series*, *307*, pp.115-125.

Lohrer, A.M., Thrush, S.F., Hewitt, J.E., Berkenbusch, K., Ahrens, M. and Cummings, V.J., 2004. Terrestrially derived sediment: response of marine macrobenthic communities to thin terrigenous deposits. *Marine Ecology Progress Series*, *273*, pp.121-138.

Leach, S., Smith, G. and Berndt, R., 2012, April. SME SPECIAL SESSION: Subsea Slurry Lift Pump Technology-SMS Development. In *Offshore Technology Conference*. Offshore Technology Conference.

Lander, T.R., Robinson, S.M.C., MacDonald, B.A. and Martin, J.D., 2013. Characterization of the suspended organic particles released from salmon farms and their potential as a food

supply for the suspension feeder, Mytilus edulis in integrated multi-trophic aquaculture (IMTA) systems. *Aquaculture*, *406*, pp.160-171.

Lambert, I.B., 2001, November. Mining and sustainable development: considerations for minerals supply. In *Natural resources forum* (Vol. 25, No. 4, pp. 275-284). Oxford, UK: Blackwell Publishing Ltd.

L. Morgan, Nii Allotey Odunton, Anthony T. Jones, C., 1999. Synthesis of environmental impacts of deep seabed mining. *Marine Georesources and Geotechnology*, *17*(4), pp.307-356.

Ligus, M., 2017. Evaluation of Economic, Social and Environmental Effects of Low-Emission Energy Technologies Development in Poland: A Multi-Criteria Analysis with Application of a Fuzzy Analytic Hierarchy Process (FAHP). *Energies*, *10*(10), p.1550.

Lewis, J.I. and Wiser, R.H., 2007. Fostering a renewable energy technology industry: An international comparison of wind industry policy support mechanisms. *Energy policy*, *35*(3), pp.1844-1857.

Mining Weekly, retrieved on July 9th, 2018. http://www.miningweekly.com/article/deep-sea-mining-struggling-to-forge-ahead-amid-investor-and-environmental-concerns-2018-05-24/rep_id:3650.

Majumder, M., 2015. Multi criteria decision making. In *Impact of urbanization on water shortage in face of climatic aberrations* (pp. 35-47). Springer, Singapore.

Ma, W., Schott, D. and Lodewijks, G., 2017a. Continuous line bucket lifting versus pipe lifting. *Journal of Offshore Mechanics and Arctic Engineering*, *139*(5), p.051704.

Ma, W., Schott, D. and Lodewijks, G., 2017b, July. A Research Procedure to Obtain a Green Transport Plan for Deep Sea Mining Systems. *In The 27th International Ocean and Polar Engineering Conference*. International Society of Offshore and Polar Engineers, Jun 25-30, San Francisco, USA, pp. 22-29.

Ma, W., Schott, D. and Lodewijks, G., 2017c. A new procedure for deep sea mining tailings disposal. *Minerals*, *7*(4), p.47.

Ma, W., van Rhee, C. and Schott, D., 2017d. Technological and Profitable Analysis of Airlifting in Deep Sea Mining Systems. *Minerals*, *7*(8), p.143.

Ma, W., van Rhee, C. and Schott, D., 2018a. A numerical calculation method of environmental impacts for the deep sea mining industry–a review. *Environmental Science: Processes & Impacts*, 20, 454-468.

Ma, W., Schott, D., and van Rhee, C., 2018b. Numerical calculations of environmental impacts for deep sea mining activities. Science of the Total Environment, 652, pp. 996-1012.

Mohanty, R.P., Agarwal, R., Choudhury, A.K. and Tiwari, M.K., 2005. A fuzzy ANP-based approach to R&D project selection: a case study. *International Journal of Production Research*, *43*(24), pp.5199-5216.

McDowall, W. and Eames, M., 2007. Towards a sustainable hydrogen economy: A multi-criteria sustainability appraisal of competing hydrogen futures. *International Journal of Hydrogen Energy*, *32*(18), pp.4611-4626.

Mamlook, R., Akash, B.A. and Nijmeh, S., 2001. Fuzzy sets programming to perform evaluation of solar systems in Jordan. *Energy Conversion and Management*, *42*(14), pp.1717-1726.

Mero, J.L., 1965. *The mineral resources of the sea* (Vol. 1). Elsevier.

Miller, K.A., Thompson, K.F., Johnston, P. and Santillo, D., 2018. An Overview of Seabed Mining Including the Current State of Development, Environmental Impacts, and Knowledge Gaps. *Frontiers in Marine Science*, *4*, p.418.

Mero, J.L., 1977. Economic aspects of nodule mining. *Marine manganese deposits*, *15*, p.327.

Morelli, J., 2011. Environmental sustainability: A definition for environmental professionals. *Journal of environmental sustainability*, *1*(1), p.2.

McLellan, B.C., Yamasue, E., Tezuka, T., Corder, G., Golev, A. and Giurco, D., 2016. Critical Minerals and Energy–Impacts and Limitations of Moving to Unconventional Resources. *Resources, 5*(2), p.19.

McKinnon, E., 2002. The environmental effects of mining waste disposal at Lihir Gold Mine, Papua New Guinea. *Journal of Rural and Remote Environmental Health*, *1*(2), pp.40-50.

Miljutin, D.M., Miljutina, M.A., Arbizu, P.M. and Galéron, J., 2011. Deep-sea nematode assemblage has not recovered 26 years after experimental mining of polymetallic nodules (Clarion-Clipperton Fracture Zone, Tropical Eastern Pacific). *Deep Sea Research Part I: Oceanographic Research Papers*, *58*(8), pp.885-897.

McLellan, B.C., Corder, G.D. and Ali, S.H., 2013. Sustainability of rare earths—An overview of the state of knowledge. *Minerals*, *3*(3), pp.304-317.

Masuda, Y., Cruickshank, M.J. and Mero, J.L., 1971, January. Continuous bucket-line dredging at 12,000 feet. In *Offshore Technology Conference*. Offshore Technology Conference, Dallas, Texas, pp. 837-858.

Margaris, D.P.; Papanikas, D.G. A generalized gas-liquid-solid three-phase flow analysis for airlift pump design. *Trans. Am. Soc. Mech. Eng. J. Fluid Eng.* 1997, *119*, 995–1002.

Masuda, Y. and Cruickshank, M.J., 1997, January. Review of Understanding of Continuous Line Bucket System for Deep Seabed Mining. In *Offshore Technology Conference*. Offshore Technology Conference.

Masuda, Y., 1987, September. Cobalt-rich crust mining by continuous line bucket. In *OCEANS'87* (pp. 1021-1026). IEEE.

Masuda, Y. and Cruickshank, M.J., 1994, January. Progress In the Development of the Continuous Line Bucket (CLB) Mining System And a Plan For Crust Mining On the 5th Takayou Sea Mount. In *The Fourth International Offshore and Polar Engineering Conference*. International Society of Offshore and Polar Engineers.

Monin, A.S. and Ozmidov, R.V., 1985. *Turbulence in the Ocean*. D Reidel Publishing Company, vol. 3, pp. 247.

Müller, P.J. and Suess, E., 1979. Productivity, sedimentation rate, and sedimentary organic matter in the oceans—I. Organic carbon preservation. *Deep Sea Research Part A. Oceanographic Research Papers*, *26*(12), pp.1347-1362.

Margalef, R., 1958. Information theory in ecology. *General systems*, *3*, pp.36-71.

Murhammer, D.W. and Goochee, C.F., 1990. Sparged animal cell bioreactors: mechanism of cell damage and Pluronic F-68 protection. *Biotechnology progress*, *6*(5), pp.391-397.

McCave, I.N., 1984. Size spectra and aggregation of suspended particles in the deep ocean. *Deep Sea Research Part A. Oceanographic Research Papers*, *31*(4), pp.329-352.

Mirza, I.A. and Vieru, D., 2017. Fundamental solutions to advection–diffusion equation with time-fractional Caputo–Fabrizio derivative. *Computers & Mathematics with Applications*, *73*(1), pp.1-10.

Miller, D.C., Muir, C.L. and Hauser, O.A., 2002. Detrimental effects of sedimentation on marine benthos: what can be learned from natural processes and rates?. *Ecological Engineering*, *19*(3), pp.211-232.

Morello, E.B., Haywood, M.D., Brewer, D.T., Apte, S.C., Asmund, G., Kwong, Y.J. and Dennis, D., 2016. The ecological impacts of submarine tailings placement. In *Oceanography and Marine Biology* (pp. 323-374). CRC Press.

Nawab, Z.A., 1984. Red Sea mining: a new era. *Deep Sea Research Part A. Oceanographic Research Papers*, *31*(6-8), pp.813-822.

Newell, R.C., Seiderer, L.J. and Hitchcock, D.R., 1998. The impact of dredging works in coastal waters: a review of the sensitivity to disturbance and subsequent recovery of biological resources on the sea bed. *Oceanography and Marine Biology: An Annual Review*, *36*, pp.127-178.

Newell, R.C., Seiderer, L.J., Simpson, N.M. and Robinson, J.E., 2002. Impact of marine aggregate dredging and overboard screening on benthic biological resources in the central North Sea: Production Licence Area 408, Coal Pit. *Coal Pit Marine Ecological Surveys Limited Technical Report*, (1/4), p.02.

Newcombe, C.P. and Jensen, J.O., 1996. Channel suspended sediment and fisheries: a synthesis for quantitative assessment of risk and impact. *North American Journal of Fisheries Management*, *16*(4), pp.693-727.

Nyhart, J.D., Antrim, L., Capstaff, A.E., Kohler, A.D. and Leshaw, D., 1978. A cost model of deep ocean mining and associated regulatory issues.

NAUTILUS Minerals. Nautilus enters into vessel charter. Retrieved on Aug 13th, 2018a. Available at: http://www.nautilusminerals.com/irm/search.aspx?masterpage=3&title=Search.

Nautilus Minerals. Production Support Vessel. Retrieved on July 9th, 2018b. Available at: http://www.nautilusminerals.com/irm/content/production-support-vessel.aspx?RID=264.

Nishi, Y., 2012. Static analysis of axially moving cables applied for mining nodules on the deep sea floor. *Applied Ocean Research*, *34*, pp.45-51.

Nam-Cheol, C., Hwang, I.J., Chae-Moon, L.E.E. and Jung-Won, P.A.R.K., 2009. An experimental study on the airlift pump with air jet nozzle and booster pump. *Journal of Environmental sciences*, *21*, pp.S19-S23.

Norgate, T.E.; Jahanshahi, S.; Rankin, W.J. Assessing the environmental impact of metal production processes. *J. Clean. Prod.* 2007, *15*, 838–848.

Navarro, A.; Begovich, O.; Besançon, G.; Dulhoste, J.F. Real-time leak isolation based on state estimation in a plastic pipeline. *Asian J. Control* 2017, *19*, 255–265.

Nakasone, T. and Akeda, S., 1999, November. The application of deep sea water in Japan. In *Proc 28th UJNR Aquac Panel Symp, UJNR Technical Report*, No. 28, pp. 69-75.

Nakata, K., Kubota, M. and Aoki, S., 1999, January. Environmental Study on the Deep-sea Mining of Manganese Nodules in the Northeastern Tropical Pacific-Modeling the sediment-laden negative buoyant flow. In *Third ISOPE Ocean Mining Symposium*. International Society of Offshore and Polar Engineers.

Oebius, H.U., Becker, H.J., Rolinski, S. and Jankowski, J.A., 2001. Parametrization and evaluation of marine environmental impacts produced by deep-sea manganese nodule mining. *Deep Sea Research Part II: Topical Studies in Oceanography*, *48*(17), pp.3453-3467.

Ohlhorst, C.W., 1981. The use of landsat to monitor deep water dumpsite 106. *Environmental monitoring and assessment*, *1*(2), pp.143-153.

Oebius, H.U., 1997. Deep sea mining and its environmental consequences. *Technische Universität Berlin, Zentraleinrichtung Versuchsanstalt für Wasserbau und Schiffbau, Berlin*, *42*(72), p.52.

O'Neill, F.G., Simmons, S.M., Parsons, D.R., Best, J.L., Copland, P.J., Armstrong, F., Breen, M. and Summerbell, K., 2013. Monitoring the generation and evolution of the sediment plume behind towed fishing gears using a multibeam echosounder. *ICES Journal of Marine Science*, *70*(4), pp.892-903.

Pick, J., Nishida, T. and Zhang, X., 2013. Determinants of China's technology availability and utilization 2006–2009: A spatial analysis. *The Information Society*, *29*(1), pp.26-48.

Promentilla, M.A.B., Furuichi, T., Ishii, K. and Tanikawa, N., 2008. A fuzzy analytic network process for multi-criteria evaluation of contaminated site remedial countermeasures. *Journal of environmental management*, *88*(3), pp.479-495.

Pang, B., 2009, September. A fuzzy ANP approach to supplier selection based on fuzzy preference programming. In *Management and Service Science, 2009. MASS'09. International Conference on* (pp. 1-4). IEEE.

Pilavachi, P.A., Stephanidis, S.D., Pappas, V.A. and Afgan, N.H., 2009. Multi-criteria evaluation of hydrogen and natural gas fuelled power plant technologies. *Applied Thermal Engineering*, *29*(11-12), pp.2228-2234.

Pohekar, S.D. and Ramachandran, M., 2004. Application of multi-criteria decision making to sustainable energy planning—a review. *Renewable and sustainable energy reviews*, *8*(4), pp.365-381.

Portney, K.E., 2013. *Taking sustainable cities seriously: Economic development, the environment, and quality of life in American cities*. MIT Press.

Pougatch, K.; Salcudean, M. Numerical modelling of deep sea air-lift. *Ocean Eng.* 2008, *35*, 1173–1182.

Pulfrich, A., Parkins, C.A. and Branch, G.M., 2003. The effects of shore-based diamond-diving on intertidal and subtidal biological communities and rock lobsters in southern Namibia. *Aquatic Conservation: Marine and Freshwater Ecosystems*, *13*(3), pp.233-255.

Rodrigues, N., Sharma, R. and Nath, B.N., 2001. Impact of benthic disturbance on megafauna in Central Indian Basin. *Deep Sea Research Part II: Topical Studies in Oceanography*, *48*(16), pp.3411-3426.

Raghukumar, C., Bharathi, P.L., Ansari, Z.A., Nair, S., Ingole, B., Sheelu, G., Mohandass, C., Nath, B.N. and Rodrigues, N., 2001. Bacterial standing stock, meiofauna and sediment–nutrient characteristics: indicators of benthic disturbance in the Central Indian Basin. *Deep Sea Research Part II: Topical Studies in Oceanography*, *48*(16), pp.3381-3399.

Rijn, L.C.V., 1984. Sediment transport, part II: suspended load transport. *Journal of hydraulic engineering*, *110*(11), pp.1613-1641.

Reinemann, D.J. A Theoretical and Experimental Study of Airlift Pumping and Aeration with Reference to Aquacultural Applications. Ph.D. Thesis, Cornell University, Ithaca, NY, USA, 1987.

Reed, D. C., Breier, J. A., Jiang, H., Anantharaman, K., Klausmeier, C. A., Toner, B. M., ... & Dick, G. J., 2015. Predicting the response of the deep-ocean microbiome to geochemical perturbations by hydrothermal vents. *The ISME journal*, 9(8), pp: 1857-1869.

Ramirez-Llodra, E., Tyler, P.A., Baker, M.C., Bergstad, O.A., Clark, M.R., Escobar, E., Levin, L.A., Menot, L., Rowden, A.A., Smith, C.R. and Van Dover, C.L., 2011. Man and the last great wilderness: human impact on the deep sea. *PLoS one*, *6*(8), p.e22588.

Rogers, C.S., 1990. Responses of coral reefs and reef organisms to sedimentation. *Marine ecology progress series. Oldendorf*, *62*(1), pp.185-202.

Rodríguez-Murillo, J.C., Zobrist, J. and Filella, M., 2015. Temporal trends in organic carbon content in the main Swiss rivers, 1974–2010. *Science of the Total Environment*, *502*, pp.206-217.

Richmond, R.H., 1993. Coral reefs: present problems and future concerns resulting from anthropogenic disturbance. *American Zoologist*, *33*(6), pp.524-536.

Ramirez-Llodra, E., Trannum, H.C., Evenset, A., Levin, L.A., Andersson, M., Finne, T.E., Hilario, A., Flem, B., Christensen, G., Schaanning, M. and Vanreusel, A., 2015. Submarine and deep-sea mine tailing placements: a review of current practices, environmental issues,

natural analogs and knowledge gaps in Norway and internationally. *Marine pollution bulletin*, *97*(1-2), pp.13-35.

Roche, C. and Bice, S., 2013. Anticipating social and community impacts of deep sea mining. *Deep Sea Minerals and the Green Economy, Secretariat of the Pacific Community, Suva*, pp.59-80.

Shook, C.A. and Bartosik, A.S., 1994. Particle—wall stresses in vertical slurry flows. *Powder Technology*, *81*(2), pp.117-124.

Saaty, T.L., 2005. *Theory and applications of the analytic network process: decision making with benefits, opportunities, costs, and risks*. RWS publications.

Shannon, C.E., 2001. A mathematical theory of communication. *ACM SIGMOBILE Mobile Computing and Communications Review*, *5*(1), pp.3-55.

Simpson, E.H., 1949. Measurement of diversity. *Nature*.

Simpson, S.L. and Spadaro, D.A., 2016. Bioavailability and chronic toxicity of metal sulfide minerals to benthic marine invertebrates: implications for deep sea exploration, mining and tailings disposal. *Environmental science & technology*, *50*(7), pp.4061-4070.

Smit, M.G., Holthaus, K.I., Trannum, H.C., Neff, J.M., Kjeilen-Eilertsen, G., Jak, R.G., Singsaas, I., Huijbregts, M.A. and Hendriks, A.J., 2008. Species sensitivity distributions for suspended clays, sediment burial, and grain size change in the marine environment. *Environmental Toxicology and Chemistry*, *27*(4), pp.1006-1012.

Shi, B., Wang, Y.P., Yang, Y., Li, M., Li, P., Ni, W. and Gao, J., 2015. Determination of critical shear stresses for erosion and deposition based on in situ measurements of currents and waves over an intertidal mudflat. *Journal of Coastal Research*, *31*(6), pp.1344-1356.

Schriever, G., 1995, January. DISCOL-disturbance and recolonization experiment of a manganese nodule area of the southeastern Pacific. In *First ISOPE Ocean Mining Symposium*. International Society of Offshore and Polar Engineers.

Smith, R.W., Bianchi, T.S., Allison, M., Savage, C. and Galy, V., 2015. High rates of organic carbon burial in fjord sediments globally. *Nature Geoscience*, *8*(6), p.ngeo2421.

Saleem, M., Fetzer, I., Harms, H. and Chatzinotas, A., 2016. Trophic complexity in aqueous systems: bacterial species richness and protistan predation regulate dissolved organic carbon and dissolved total nitrogen removal. *Proc. R. Soc. B*, *283*(1825), p.20152724.

Segschneider, J. and Sündermann, J., 1998. Simulating large scale transport of suspended matter. *Journal of marine systems*, *14*(1-2), pp.81-97.

Sharma, R., 2011. Deep-sea mining: Economic, technical, technological, and environmental considerations for sustainable development. *Marine Technology Society Journal*, *45*(5), pp.28-41.

Sharma, R. and Nath, B.N., 1997, January. Benthic disturbance and monitoring experiment in the Central Indian Ocean Basin. In *Second ISOPE Ocean Mining Symposium*. International Society of Offshore and Polar Engineers.

Sharma, R., Nagendernath, B., Valsangkar, A.B., Parthiban, G., Sivakolundu, K.M. and Walker, G., 2000. Benthic disturbance and impact experiments in the Central Indian Ocean Basin. *Marine georesources & geotechnology*, *18*(3), pp.209-221.

Sheng, Y.P., 1983. *Mathematical modeling of three-dimensional coastal currents and sediment dispersion: Model development and application* (No. 83). Office, Chief of Engineers, US Army, *Tech. Rep.* CERC-83-2, pp. 250-287.

Sweeney, R.J., Tollison, R.D. and Willett, T.D., 1974. Market failure, the common-pool problem, and ocean resource exploitation. *The Journal of Law and Economics*, *17*(1), pp.179-192.

Sharma, R., Nath, B.N., Parthiban, G. and Sankar, S.J., 2001. Sediment redistribution during simulated benthic disturbance and its implications on deep seabed mining. *Deep Sea Research Part II: Topical Studies in Oceanography*, *48*(16), pp.3363-3380.

Schriever, C., Ahnert, A., Bluhm, H., Borowski, C. and Thiel, H., 1997, January. Results of the large scale deep-sea environmental impact study DISCOL during eight years of investigation. In *The Seventh International Offshore and Polar Engineering Conference*. International Society of Offshore and Polar Engineers.

Sato, Y.; Yoshinaga, T.; Sadatomi, M. Data and empirical correlation for the mean velocity of coarse particles in a vertical three-phase air-wate~solid particle flow. In Proceedings of the International Conference on Multiphase Flows '91-Tsukuba, Tsukuba, Japan, 24–27 September 1991; Volume 1, pp. 363–366.

Stenning, A.H.; Martin, C.B. An analytical and experimental study of air-lift pump performance. *J. Eng. Power* 1968, *90*, 106–110.

Shi, J.Z., 2010. Tidal resuspension and transport processes of fine sediment within the river plume in the partially-mixed Changjiang River estuary, China: a personal perspective. *Geomorphology*, *121*(3-4), pp.133-151.

Schulte, S.A., 2013. *Vertical Transport Methods in Deep Sea Mining*. Delft University of Technology. Master thesis, pp: 30-132.

Thiel, H. and Tiefsee-Umweltschutz, F., 2001. Evaluation of the environmental consequences of polymetallic nodule mining based on the results of the TUSCH Research Association. *Deep Sea Research Part II: Topical Studies in Oceanography*, *48*(17-18), pp.3433-3452.

Trannum, H.C., Gundersen, H., Escudero-Oñate, C., Johansen, J.T. and Schaanning, M.T., 2018. Effects of submarine mine tailings on macrobenthic community structure and ecosystem processes. *Science of The Total Environment*, *630*, pp.189-202.

Thatje, S., Hillenbrand, C.D. and Larter, R., 2005. On the origin of Antarctic marine benthic community structure. *Trends in Ecology & Evolution*, *20*(10), pp.534-540.

Trueblood, D.D. and Ozturgut, E., 1997, January. The benthic impact experiment: A study of the ecological impacts of deep seabed mining on abyssal benthic communities. In *The Seventh International Offshore and Polar Engineering Conference*. International Society of Offshore and Polar Engineers.

Taguchi, K., Nakata, K., Aoki, S. and Kubota, M., 1995, January. Environmental study on the deep-sea mining of manganese nodules in the Northeastern Tropical Pacific. In *First ISOPE Ocean Mining Symposium*. International Society of Offshore and Polar Engineers.

Tyson, R.V., 2001. Sedimentation rate, dilution, preservation and total organic carbon: some results of a modelling study. *Organic Geochemistry*, *32*(2), pp.333-339.

Thrush, S.F. and Dayton, P.K., 2002. Disturbance to marine benthic habitats by trawling and dredging: implications for marine biodiversity. *Annual Review of Ecology and Systematics*, *33*(1), pp.449-473.

Thiel, H., 1992. Deep-sea environmental disturbance and recovery potential. *Internationale Revue der Gesamten Hydrobiologie und Hydrographie*, *77*(2), pp.331-339.

Taitel, Y.; Bornea, D.; Dukler, A.E. Modelling flow pattern transitions for steady upward gas-liquid flow in vertical tubes. *AIChE J.* 1980, *26*, 345–354.

Turner, A. and Millward, G.E., 2002. Suspended particles: their role in estuarine biogeochemical cycles. *Estuarine, Coastal and Shelf Science*, *55*(6), pp.857-883.

Tivy, J., and G. O'Hare., 1982. Human impact on the ecosystem. Oliver and Boyd, Edinburgh.

UKessays, What Factors of Production can Affect a Construction Project? Retrieved on Oct 1st, 2018. Available at: https://www.ukessays.com/essays/economics/what-factors-of-production-can-affect-a-construction-project-economics-essay.php.

Van Dover, C.L., 2011. Tighten regulations on deep-sea mining. *Nature*, *470*(7332), p.31.

Van Wijk, J.M., Van Rhee, C. and Talmon, A.M., 2014. Axial dispersion of suspended sediments in vertical upward pipe flow. *Ocean Engineering*, *92*, pp.20-30.

Vercruijsse, P., van Muijen, H. and Verichev, S., 2011, January. Dredging technology for deep sea mining operations. In *Offshore Technology Conference*. Offshore Technology Conference.

Vlasák, P., Chára, Z., Krupička, J. and Konfršt, J., 2014. Experimental investigation of coarse particles-water mixture flow in horizontal and inclined pipes. *Journal of Hydrology and Hydromechanics*, *62*(3), pp.241-247.

Van Dover, C.L., 2014. Impacts of anthropogenic disturbances at deep-sea hydrothermal vent ecosystems: a review. *Marine Environmental Research*, *102*, pp.59-72.

Van Dover, C.L., Aronson, J., Pendleton, L., Smith, S., Arnaud-Haond, S., Moreno-Mateos, D., Barbier, E., Billett, D., Bowers, K., Danovaro, R. and Edwards, A., 2014b. Ecological restoration in the deep sea: Desiderata. *Marine Policy*, *44*, pp.98-106.

Van Dover, C.L., Ardron, J.A., Escobar, E., Gianni, M., Gjerde, K.M., Jaeckel, A., Jones, D.O.B., Levin, L.A., Niner, H.J., Pendleton, L. and Smith, C.R., 2017. Biodiversity loss from deep-sea mining. *Nature Geoscience*, *10*(7), p.464.

Vrijenhoek, R.C., 2010. Genetic diversity and connectivity of deep-sea hydrothermal vent metapopulations. *Molecular ecology*, *19*(20), pp.4391-4411.

Van Bloois, J.W. and Frumau, J., 2009, January. SS. Ocean Mining: Deep Sea Mining: A New Horizon for Dredging Technology. In *Offshore Technology Conference*. Offshore Technology Conference.

Williams, M.M.R., 1986. Some topics in nuclear aerosol dynamics. *Progress in Nuclear Energy*, *17*(1), pp.1-52.

Wenger, A.S., Harvey, E., Wilson, S., Rawson, C., Newman, S.J., Clarke, D., Saunders, B.J., Browne, N., Travers, M.J., Mcilwain, J.L. and Erftemeijer, P.L., 2017. A critical analysis of the direct effects of dredging on fish. *Fish and Fisheries*, *18*(5), pp.967-985.

Whitney, S.C., 1977. Environmental Regulation of United States Deep Seabed Mining. *Wm. & Mary L. Rev.*, *19*, p.77.

Wiltshire, J.C., 2017. Sustainable Development and its Application to Mine Tailings of Deep Sea Minerals. In *Deep-Sea Mining* (pp. 423-441). Springer, Cham.

Weaver, P.P., Billett, D.S. and Van Dover, C.L., 2018. Environmental Risks of Deep-sea Mining. In *Handbook on Marine Environment Protection* (pp. 215-245). Springer, Cham.

Wilber, D.H. and Clarke, D.G., 2001. Biological effects of suspended sediments: a review of suspended sediment impacts on fish and shellfish with relation to dredging activities in estuaries. *North American Journal of Fisheries Management*, *21*(4), pp.855-875.

Xia, J., Zoll, L.X.W., Tang, D., Huang, J. and Wang, S., 1997, January. Studies on reasonable hydraulic lifting parameters of manganese nodules. In *Second ISOPE Ocean Mining Symposium*. International Society of Offshore and Polar Engineers.

Xu, L. and Yang, J.B., 2001. *Introduction to multi-criteria decision making and the evidential reasoning approach* (pp. 1-21). Manchester: Manchester School of Management.

Yüksel, İ. and Dagdeviren, M., 2007. Using the analytic network process (ANP) in a SWOT analysis–A case study for a textile firm. *Information Sciences*, *177*(16), pp.3364-3382.

Yoshinaga, T. and Sato, Y., 1996. Performance of an air-lift pump for conveying coarse particles. *International journal of multiphase flow*, *22*(2), pp.223-238.

Yedla, S. and Shrestha, R.M., 2003. Multi-criteria approach for the selection of alternative options for environmentally sustainable transport system in Delhi. *Transportation Research Part A: Policy and Practice*, *37*(8), pp.717-729.

Yoon, C.H., Kwon, K.S., Kwon, O.K., Kwon, S.K., Kim, I.K., Lee, D.K. and Lee, H.S., 2000, January. An experimental study on lab scale air-lift pump flowing solid-liquid-air three-phase mixture. In *The Tenth International Offshore and Polar Engineering Conference*. International Society of Offshore and Polar Engineers.

Zou, W., 2007, January. COMRA's research on lifting motor pump. In *Seventh ISOPE Ocean Mining Symposium*. International Society of Offshore and Polar Engineers.

Zielke, W., Jankowski, J.A., Sündermann, J. and Segschneider, J., 1995, January. Numerical modeling of sediment transport caused by deep-sea mining. In *First ISOPE Ocean Mining Symposium*. International Society of Offshore and Polar Engineers.

Zhou, X., 2012. Fuzzy analytical network process implementation with matlab. In *MATLAB-A Fundamental Tool for Scientific Computing and Engineering Applications-Volume 3*. InTech.

Zionts, S., 1979. MCDM—if not a roman numeral, then what?. *Interfaces*, *9*(4), pp.94-101.

Zadeh, L.A., 1965. Fuzzy set theory and its applications.

Zhang, K., Nieto, A. and Kleit, A.N., 2015. The real option value of mining operations using mean-reverting commodity prices. *Mineral Economics*, *28*(1-2), pp.11-22.

Appendix

Appendix A:

To solve the advection-diffusion model of Eq. 5.7, the current fluid velocity should be solved firstly. Jankowski et al. (1996) claimed that the deep ocean current could be assumed to be composed by free long waves and the geostrophic equilibrium current. The components of the free long waves are shown as follows (Jankowski et al., 1996).

$$
\begin{cases}
u_w = \dfrac{\eta_0}{Hk_h^2}\left(k_1 \omega \cos\psi - k_2 f \sin\psi\right) \\[2mm]
v_w = \dfrac{\eta_0}{Hk_h^2}\left(k_2 \omega \cos\psi + k_1 f \sin\psi\right)
\end{cases}
$$

in which η_0 is the initial value of displacement of vertical free surface [m], ψ is set to represent $k_1 x + k_2 y - \omega t + \phi$, ϕ is the latitude which is set to be negative for the southern hemisphere [rad], $f = 2\Omega \sin\phi$, i.e., Coriolis parameter, which is positive in northern hemisphere and negative in southern hemisphere, Ω is the Earth's angular speed, i.e., $2\pi / 86164$ rad/s, $k_h = (k_1, k_2)$, $k_h = 2\pi / \lambda$ represents wave factor, the values of k_1 and k_2 are the components of k on the axis x and y directions which could be calculated taking into consideration of the angle between the velocity with the latitude θ [rad], λ is the wave length, x and y are the coordinates of species nodes, ω is the angular frequency of the free long wave [s^{-1}], H is the water depth [m].

The free long waves depicted should be superimposed with the geostrophic equilibrium, which are calculated as follows (Jankowski et al., 1996).

$$
\begin{cases}
u_g = -\dfrac{g}{f}\dfrac{\partial \eta}{\partial y} \\[2mm]
v_g = \dfrac{g}{f}\dfrac{\partial \eta}{\partial x}
\end{cases}
$$

in which g is the gravitational acceleration [m^2/s], η is the formula of a plane wave, which could be described as $\eta = \eta_0 \exp\left(i\left(k_1 x + k_2 y - \omega t + \phi\right)\right)$, η_0 could be determined by $\eta_0 = \left(\omega^2 - f^2\right)\cdot|\mathbf{v}| / \omega k_h g$.

Glossary

List of symbols and notations

Below follows a list of the most frequently used symbols and notations in this thesis.

Greek

γ	bucket filling ratio [-]
ρ_b	density of the bucket [kg/m3]
ρ_A	Density of the three phase mixtures [kg/m3]
ρ_s	density of the mineral sediment [kg/m3]
ρ_l	density of the liquid [kg/m3]
ρ_m	density of the slurry mixture [kg/m3]
ρ_{g_0}	initial gas density [ks/m3]
ρ_{g_z}	gas density at position z [kg/m3]
η_c	CLB efficiency [-]
η_h	hydraulic efficiency [-]
η_r	PLS system efficiency [-]
ξ_f	inlet and acceleration coefficient [-]
ξ_H	valve coefficient [-]
λ_l	liquid friction coefficient [-]
λ_p	resuspended particle percentage [-]
λ_s	solid friction coefficient [-]
υ'	kinematic viscosity [m2/s]

τ	shear stress [N/m2]
ε_x	dispersion coefficient [m2/s]

Capital

A_p	transverse area of pipe [m2]
C_d	drag coefficient [-]
C_l	liquid volumetric concentration [-]
C_s	solid volumetric concentration [-]
C_{s0}	concentration of suspension particles [-]
D_i	rigid pipe diameter [m]
E_{c_u}	useful energy consumption of CLB [J/h]
E_{c_t}	total energy consumption of CLB [J/h]
E_{p_u}	useful energy consumption of PLS [J/h]
E_{p_t}	total energy consumption of PLS [J/h]
E_{ton}	energy consumption lifting per tonnage mineral [kWh/ton]
F_b	buoyancy force [N]
F_d	drag force [N]
F_g	gravitational force [N]
F_r	resultant force [N]
F_{wi}	winch force [N]
H	mining depth [m]
J	volumetric flux rate [m/s]
J_{g_atm}	gas flux rate under atmospheric pressure [m/s]

K	maintenance fee [\$/year]
M	cost [\$]
M_c	initial capital cost [\$]
M_p	operation and maintenance cost [\$]
M_{sv}	initial capital cost on the shipping vessels [\$]
M_{res}	erosion rate [kg/m2xs]
M_{m_p}	manufacturing cost of the pipeline system [\$]
N	total number of different kinds of species [-]
N_p	number of pumps [-]
P_r	required pressure [Pa]
P_0	initial gas pressure [Pa]
P_z	gas pressure at position z [Pa]
P_I	pressure at the inlet [Pa]
P_{atm}	atmosphere pressure [Pa]
R	power and energy consumption price [\$/kWh]
Ri	Richardson number [-]
S	species number [-]
SD	integrated species index
Q_s	solid mineral production rate [ton/h] or [kg/s]
W_i	salary for the staff [\$/year]

Non Capital

| a | CLB ascending process [-] |

a_w	work ability factor [-]
c	distribution coefficienct [-]
d	CLB descending process [-]
d_s	particle diameter [m]
l	side lendth of bucket [m]
la	labour expenditure [$]
m	mining system [-]
m_p	particle resuspended rate [kg/s]
ma	maintenance expenditure [$]
$m_{\_CLB}$	mass of CLB system [kg]
n	CLB bucket number [-]
n_s	staff number [-]
n'	index relating with the particle Reynolds number [-]
n_f	lifting bucket surface number [-]
n_{wr}	number of cables [-]
p	mineral processing system [-]
p_i	proposition of different species [-]
pe	power and energy consumption expenditure [$]
r_c	radius of the cable [m]
s	mean working days per year [-]
t	transport system [-]
t_b	thickness of bucket wall [m]
v_c	cable velocity [m/s]
v_l	liquid velocity [m/s]

v_s solid velocity [m/s]

v_m mixture velocity [m/s]

v_{sl} slip velocity [m/s]

v_{st} particle settling velocity [m/s]

v_{sw} wall affected settling velocity [m/s]

Summary

Deep sea mining is an emerging activity which attracts significant attentions from different countries governments and international huge companies around the world. Although its research and development work has been done for roughly half century time, the industrial scale deep sea mining project still has not been implemented yet because of a lot of problems in it, such as the profitability issue and marine environmental impacts.

The research conducted in this thesis aims at designing an assessment system to evaluate the sustainability of DSM transport plans. To evaluate the sustainability of deep sea mining transport plans, three types of vertical lifting mechanisms are considered: continuous line bucket lifting system, pipe lifting with centrifugal pumps, and pipe lifting with air pumps in terms of the energy consumption, profitability and the caused environmental impacts.

The research starts with a systematic literature review on the current research status of deep sea mining activity sustainability development to find out the existing research gaps and the influencing aspects to achieve this goal. Based on the literature review, it is clear that the sustainability of a deep sea mining transport plan could be influenced by its technological performance, e.g., energy consumption and technology maturity, the economic profitability, the environmental impacts and the social impacts.

In chapter 3, the continuous line bucket lifting system and the pipe lifting with centrifugal pumps are modelled and calculated. To analyse the technological performance of different kinds of DSM transport plans, the solid production rate, pipe diameter, energy consumption and mining depth are focused. In chapter 4, the economic performance of DSM transport plans is analysed in terms of the profitability lifting per tonnge mineral focusing on the air pump lifting systems. The environmental impacts generated by DSM activities are researched in chapter 5 utilizing numerical calculation method. In this chapter, we selected the physical disturbances, sediment plume, tailings disposal and species disturbances as our emphasizes. Additionally, the interconnection between the species disturbance and sediment plume is also analysed in terms of the severity of ill effect, turbidity of ocean water, total organic carbon, and sedimentation thickness. The research content in chapter 3, 4, and 5 are based on the sustainability influencing aspects derived in the literature review of chapter 2, which calculation results would be integrated in chapter 6. Numerical calculation is the major research method.

The multi-criteria decision making method is used as the integration method of the technological, economic and environmental impacts of DSM transport plans in chapter 6. Firstly, the evaluating criteria for different kinds of DSM transport plans are selected which consists of both quantitative and qualitative criteria. Secondly, the weights of all evaluating criteria were determined with a questionnaire survery. Thirdly, Fuzzy-ANP method is used to

calculate the comprehensive performance of all DSM transport plans. And the DSM transport plan with the maximum comprehensive performance index is selected as the most sustainable transport plan.

The major contribution of this thesis is the sustainability assessment framework designed for DSM transport plan evaluations, which application might be extended into the whole DSM project evaluation. Additionally, the modelling of economic profitability is also one innovation of this thesis, because most of prior research on this topic was majorly in the stage of conceptualisation making and some basic analyses. Furthermore, the species response to sediment plume in DSM project is firstly discussed and analysed, which is meaningful for the future establishment of environmental impact standard for DSM projects.

Samenvatting

Diepzeemijnbouw is een techniek in opkomst, waarin verschillende overheden en grote internationale bedrijven zeer geïnteresseerd zijn. Hoewel er al ongeveer een halve eeuw onderzoek naar gedaan wordt, zijn er nog geen diepzeemijnbouwprojecten op industriële schaal verwezenlijkt omdat er nog te veel problemen zijn. Het is bijvoorbeeld nog onduidelijk in hoeverre diepzeemijnbouw rendabel is en wat de invloed op het onderwatermilieu is.

Dit proefschrift heeft als doel een systeem te ontwerpen waarmee de duurzaamheid van transportsystemen voor diepzeemijnbouw beoordeeld kan worden. Hierbij worden drie hijsmechanismes beschouwd: een hijssysteem met emmerketting, een pijpsysteem met centrifugaalpompen en een pijpsysteem met luchtpompen. Ze worden vergeleken in termen van energieverbruik, winstgevendheid en milieueffecten.

Het onderzoek begint met een systematische literatuurstudie naar de huidige ontwikkelingen op het gebied van duurzaamheid in de diepzeemijnbouw. Uit het literatuuronderzoek blijkt dat de duurzaamheid van een transportsysteem beïnvloed kan worden door technologische prestaties (zoals energieverbruik en technologische geavanceerdheid), economische winstgevendheid, milieueffecten en sociale effecten.

In hoofdstuk 3 worden het emmersysteem en het pijpsysteem met centrifugaalpomp gemodelleerd en doorgerekend. De technologische kwaliteit van de verschillende transportsystemen wordt geanalyseerd aan de hand van productiesnelheid, pijpdiameter, energieverbruik en mijndiepte. In hoofdstuk 4 wordt een pijpsysteem met luchtpompen beschouwd, en worden de economische resultaten van het transportsysteem geanalyseerd in termen van winst per ton opgehaald mineraal. De milieueffecten van diepzeemijnbouwactiviteiten worden met numerieke methoden onderzocht in hoofdstuk 5. Hiervoor wordt gekeken naar ruimtelijke verstoringen, sedimentwolken, afvalverwerking en de verstoring van organismen. Bovendien wordt de relatie tussen sedimentwolken en de verstoring van organismen geanalyseerd door te kijken naar de invloed op levende organismen, de troebelheid van het zeewater, de hoeveelheid organische koolstof en de sedimentdikte. Het onderzoek van de hoofdstukken 3 tot en met 5 is gebaseerd op de duurzaamheidbeïnvloedende aspecten die in het literatuuronderzoek van hoofdstuk 2 naar voren zijn gekomen. Er is in deze hoofdstukken voornamelijk gebruik gemaakt van numerieke methoden. De resultaten van de berekeningen worden geïntegreerd in hoofdstuk 6.

De technologische en economische resultaten en de invloed op het milieu van transportsystemen voor diepzeemijnbouw worden met een multicriteria-analyse geïntegreerd in hoofdstuk 6. Eerst worden de kwantitatieve en kwalitatieve criteria voor de verschillende transportsystemen geselecteerd. De gewichten van alle criteria worden vervolgens bepaald op basis van een vragenlijst. Ten slotte wordt een Fuzzy-ANP-methode gebruikt om de totale

prestaties van alle transportsystemen te berekenen. Het diepzeemijnbouwtransportsysteem met de maximale prestatie-index wordt geselecteerd als het duurzaamste.

De hoofdbijdrage van dit proefschrift is een systeem waarmee de duurzaamheid van transportsystemen voor diepzeemijnbouw geëvalueerd kan worden. Dit systeem zou uitgebreid kunnen worden om de gehele diepzeemijnbouw te beoordelen. Daarnaast is het modelleren van economische winstgevendheid een nieuw aspect in dit proefschrift; eerder werden er voornamelijk ideeën gevormd en enkele eenvoudige analyses gedaan. Ten slotte is de reactie van organismen op sedimentwolken in diepzeemijnbouwprojecten voor het eerst besproken en geanalyseerd. Dit is belangrijk voor de keuze van een milieustandaard voor diepzeemijnbouwprojecten.

Curriculum viate

Wenbin, Ma was born on Oct 2nd, 1989 in Tengzhou, Shandong, P.R. China. In 2008, he was admitted by Zhejiang Ocean University studying ocean engineering. In 2012, he obtained his bachelor degree in the field of ocean engineering, and at the same year he commenced his master studies at Wuhan University of Technology majoring ship and marine structures design and manufacturing. In 2015, he started his PhD studies at Delft University of Technology supervised by Prof. Cees van Rhee, Dr. Dingena Schott and Prof. Gabriel Lodewijks. His PhD research is sponsored by Chinese Scholarship Council focusing on the sustainability analysis of deep sea mining mineral transport plans.

List of publications

1. Ma, W., Schott, D. and van Rhee, C., 2019. Multi-criteria decision making applied to sustainable deep sea mining vertical transport plans. *Journal of Operations Management* (submitted).

2. Ma, W., Schott, D. and van Rhee, C., 2019. Numerical calculations of environmental impacts for deep sea mining activities. *Science of The Total Environment*, *652*, pp.996-1012.

3. Ma, W., van Rhee, C. and Schott, D., 2018. A numerical calculation method of environmental impacts for the deep sea mining industry–a review. *Environmental Science: Processes & Impacts*, *20*(3), pp.454-468.

4. Ma, W., Schott, D. and Lodewijks, G., 2017. A new procedure for deep sea mining tailings disposal. *Minerals*, *7*(4), p.47.

5. Ma, W., Schott, D. and Lodewijks, G., 2017, July. A Research Procedure to Obtain a Green Transport Plan for Deep Sea Mining Systems. In *The 27th International Ocean and Polar Engineering Conference*. International Society of Offshore and Polar Engineers.

6. Ma, W., Schott, D. and Lodewijks, G., 2017. Continuous line bucket lifting versus pipe lifting. *Journal of Offshore Mechanics and Arctic Engineering*, *139*(5), p.051704.

7. Ma, W., van Rhee, C. and Schott, D., 2017. Technological and Profitable Analysis of Airlifting in Deep Sea Mining Systems. *Minerals*, *7*(8), p.143.

TRAIL Thesis Series

The following list contains the most recent dissertations in the TRAIL Thesis Series. For a complete overview of more than 250 titles see the TRAIL website: www.rsTRAIL.nl.
The TRAIL Thesis Series is a series of the Netherlands TRAIL Research School on transport, infrastructure and logistics.

Ma, W., *Sustainability of Deep Sea Mining Transport Plans,* T2019/7, June 2019, TRAIL Thesis Series, the Netherlands

Alemi, A., *Railway Wheel Defect Identification,* T2019/6, January 2019, TRAIL Thesis Series, the Netherlands

Liao, F., *Consumers, Business Models and Electric Vehicles,* T2019/5, May 2019, TRAIL Thesis Series, the Netherlands

Tamminga, G., *A Novel Design of the Transport Infrastructure for Traffic Simulation Models,* T2019/4, March 2019, TRAIL Thesis Series, the Netherlands

Lin, X., *Controlled Perishable Goods Logistics: Real-time coordination for fresher products*, T2019/3, January 2019, TRAIL Thesis Series, the Netherlands

Dafnomilis, I., *Green Bulk Terminals: A strategic level approach to solid biomass terminal design*, T2019/2, January 2019, TRAIL Thesis Series, the Netherlands

Feng, Fan, *Information Integration and Intelligent Control of Port Logistics System,* T2019/1, January 2019, TRAIL Thesis Series, the Netherlands

Beinum, A.S. van, *Turbulence in Traffic at Motorway Ramps and its Impact on Traffic Operations and Safety,* T2018/12, December 2018, TRAIL Thesis Series, the Netherlands

Bellsolà Olba, X., *Assessment of Capacity and Risk: A Framework for Vessel Traffic in Ports,* T2018/11, December 2018, TRAIL Thesis Series, the Netherlands

Knapper, A.S., *The Effects of using Mobile Phones and Navigation Systems during Driving,* T2018/10, December 2018, TRAIL Thesis Series, the Netherlands

Varotto, S.F., *Driver Behaviour during Control Transitions between Adaptive Cruise Control and Manual Driving: empirics and models,* T2018/9, December 2018, TRAIL Thesis Series, the Netherlands

Stelling-Kończak, A., *Cycling Safe and Sound,* T2018/8, November 2018, TRAIL Thesis Series, the Netherlands

Essen, van M.A., *The Potential of Social Routing Advice,* T2018/7, October 2018, TRAIL Thesis Series, the Netherlands

Su, Zhou, *Maintenance Optimization for Railway Infrastructure Networks*, T2018/6, September 2018, TRAIL Thesis Series, the Netherlands

Cai, J., *Residual Ultimate Strength of Seamless Metallic Pipelines with Structural Damage*, T2018/5, September 2018, TRAIL Thesis Series, the Netherlands

Ghaemi, N., *Short-turning Trains during Full Blockages in Railway Disruption Management,* T2018/4, July 2018, TRAIL Thesis Series, the Netherlands

Gun, van der J.P.T., *Multimodal Transportation Simulation for Emergencies using the Link Transmission Model,* T2018/3, May 2018, TRAIL Thesis Series, the Netherlands

Van Riessen, B., *Optimal Transportation Plans and Portfolios for Synchromodal Container Networks,* T2018/2, March 2018, TRAIL Thesis Series, the Netherlands

Saeedi, H., *Network-Level Analysis of the Market and Performance of Intermodal Freight Transport,* T2018/1, March 2018, TRAIL Thesis Series, the Netherlands

Ypsilantis, P., *The Design, Planning and Execution of Sustainable Intermodal Port-hinterland Transport Networks,* T2017/14, December 2017, TRAIL Thesis Series, the Netherlands

Han, Y, *Fast Model Predictive Control Approaches for Road Traffic Control,* T2017/13, December 2017, TRAIL Thesis Series, the Netherlands

Wang, P., *Train Trajectory Optimization Methods for Energy-Efficient Railway Operations,* T2017/12, December 2017, TRAIL Thesis Series, the Netherlands

Weg, G.S. van de, *Efficient Algorithms for Network-wide Road Traffic Control*, T2017/11, October 2017, TRAIL Thesis Series, the Netherlands

He, D., *Energy Saving for Belt Conveyors by Speed Control,* T2017/10, July 2017, TRAIL Thesis Series, the Netherlands

Bešinović, N., *Integrated Capacity Assessment and Timetabling Models for Dense Railway Networks,* T2017/9, July 2017, TRAIL Thesis Series, the Netherlands

Chen, G., *Surface Wear Reduction of Bulk Solids Handling Equipment Using Bionic Design,* T2017/8, June 2017, TRAIL Thesis Series, the Netherlands

Kurapati, S., *Situation Awareness for Socio Technical Systems: A simulation gaming study in intermodal transport operations,* T2017/7, June 2017, TRAIL Thesis Series, the Netherlands

Jamshidnejad, A., *Efficient Predictive Model-Based and Fuzzy Control for Green Urban Mobility,* T2017/6, June 2017, TRAIL Thesis Series, the Netherlands

Araghi, Y., *Consumer Heterogeneity, Transport and the Environment*, T2017/5, May 2017, TRAIL Thesis Series, the Netherlands

Kasraian Moghaddam, D., *Transport Networks, Land Use and Travel Behaviour: A long term investigation,* T2017/4, May 2017, TRAIL Thesis Series, the Netherlands